

**INSIGHTS INTO CARGO ADAPTOR FUNCTION THROUGH THE STUDY OF
NOVEL INTERACTORS**

by

Bjorn Bean

B.Sc., The University of British Columbia, 2010

A THESIS SUBMITTED IN PARTIAL FULFILLMENT OF
THE REQUIREMENTS FOR THE DEGREE OF

DOCTOR OF PHILOSOPHY

in

THE FACULTY OF GRADUATE AND POSTDOCTORAL STUDIES
(Biochemistry and Molecular Biology)

THE UNIVERSITY OF BRITISH COLUMBIA
(Vancouver)

July 2015

© Bjorn Bean, 2015

Abstract

In Eukaryotes, luminal and transmembrane proteins are moved to their functional locations by conserved membrane trafficking machinery. In this process, cargo adaptors bind motifs present on cargo, indirectly linking the proteins to coats, which deform membranes and form transport vesicles. Here, cargo adaptor recruitment and cargo recognition was studied by characterizing associated factors in the budding yeast *Saccharomyces cerevisiae*. Possible cargo adaptor-associated factors were identified in a proteomics study that grouped protein-protein interactions into 501 putative membrane associated complexes using a Markov clustering algorithm. Two clusters were selected for this work.

The first contained the uncharacterized protein Ssp120 with the endoplasmic reticulum-to-Golgi trafficking complex Emp46/Emp47. Ssp120 stably interacted with the Emp46/Emp47 complex and depended on Emp47 for its punctate localization. The C-terminus of Ssp120 mediated the interaction. Homology with human MCFD2 suggests that Ssp120 may link a subset of cargo to Emp46/Emp47.

The second cluster was comprised of retromer, an endosome-to-Golgi trafficking complex, and the Rab5-family guanine nucleotide exchange factor (GEF) Muk1. Both Muk1 and the other known Rab5-family GEF, Vps9, interacted with retromer and the presence of at least one was required for retromer recruitment to endosomes. Additionally, a new VPS9 domain-containing protein present was identified and shown to complement loss of *MUK1* and *VPS9*. Retromer recruitment was shown to be dependent on putative GEF catalytic residues and the presence of

their target Rabs. Furthermore, loss of GEFs resulted in mislocalization of the potential Rab5-family GTPase effector, Vps34, and its lipid product, phosphatidylinositol 3-phosphate (PI3P), to the vacuolar membrane. As retromer is recruited by PI3P, the data support a positive feedback model whereby retromer interacts with GEFs to indirectly modify the lipid composition of the membrane allowing further localized recruitment.

This study validates the approach of studying novel interactors of cargo recognition complexes to better understand their function. It suggests that Ssp120 may recognize a subset of Emp46-Emp47 cargo, indicating that an associated factor can diversify the proteins recognized by a given cargo adaptor. Furthermore, the work on retromer suggests a novel mechanism for the reinforcement of cargo selective complex recruitment that may be conserved in humans.

Preface

List of publications arising from the research presented in this study:

A version of chapter 2 has been published. Babu M, Vlasblom J, Pu S, Guo X, Graham C, Bean BDM, Burston HE, Vizeacoumar FJ, Snider J, Phanse S *et al.* (2012). Interaction landscape of membrane-protein complexes in *Saccharomyces cerevisiae*. *Nature* 489, 585–589. I conducted the experiments and analyzed the data for Figures 2.3F, 2.3G and 2.4B-H. Furthermore, I wrote the results section associated with Figure 2.4 and edited the manuscript.

A version of chapter 3 has been published. Bean BDM, Davey M, Snider J, Jessulat M, Deineko V, Tinney M, Stagljar I, Babu M, Conibear E (2015). Rab5-family guanine nucleotide exchange factors bind retromer and promote its recruitment to endosomes. *Mol Biol Cell* 26, 1119-1128. I was responsible for writing the manuscript as well as designing, executing and analyzing all experiments with the following exceptions. Figure 2.1A was designed by Mohan Babu and carried out by Matthew Jessulat and Viktor Deineko. While I was responsible for the final version of Figure 2.3B, preliminary iMYTH experiments were designed and carried out by Jamie Snider and Igor Stagljar.

Table of Contents

Abstract.....	ii
Preface.....	iv
Table of Contents	v
List of Tables	ix
List of Figures.....	x
List of Abbreviations	xii
Acknowledgements	xviii
Dedication	xx
Chapter 1: Introduction	1
1.1 Overview of membrane trafficking in yeast	1
1.1.1 Yeast membrane trafficking pathways.....	1
1.1.2 Mechanism of membrane trafficking in yeast	4
1.2 Compartment definition and recognition	6
1.2.1 Lipids	6
1.2.2 Lipid recognition domains	7
1.2.3 Coincidence detection.....	8
1.2.4 SNAREs and tethers	9
1.2.5 Rab GTPases and their regulators.....	10
1.2.6 Compartment maturation	12
1.2.6.1 A focus on endosome maturation in yeast.....	13
1.3 Strategies for cargo recognition	14

1.3.1	Sorting signals.....	14
1.3.2	Accessory adaptors	15
1.4	COPII membrane trafficking	16
1.4.1	Structure and function.....	16
1.4.2	Cargo recognition.....	18
1.4.3	COPII dysfunction in disease.....	19
1.5	Retromer membrane trafficking.....	19
1.5.1	Structure and function.....	19
1.5.2	Cargo recognition.....	22
1.5.3	Retromer dysfunction in disease.....	23
1.6	Research objectives and hypotheses	24
1.6.1	Characterizing novel cargo-adaptor associated factors.....	24

Chapter 2: Interaction landscape of membrane-protein complexes in *Saccharomyces*

<i>cerevisiae</i>	26	
2.1	Synopsis.....	26
2.2	Results and discussion	27
2.3	Methods.....	40
2.3.1	Yeast strains, media and plasmids	40
2.3.2	Tandem affinity purification and mass spectrometry	41
2.3.3	Detergents	42
2.3.4	Colony overlay.....	42
2.3.5	Fluorescence microscopy.....	42
2.3.6	Immunoprecipitation.....	43

2.3.7	Evaluation of Chs3 and Sna2 sorting.....	44
2.3.8	Yeast two-hybrid analysis.....	45
2.3.9	iMYTH assay.....	46
Chapter 3: Rab5-family guanine nucleotide exchange factors bind retromer and promote		
its recruitment to endosomes47		
3.1	Synopsis.....	47
3.2	Introduction.....	48
3.3	Results.....	51
3.3.1	Retromer physically interacts with Rab5-family GEFs.....	51
3.3.2	Identification of Vrl1, a third member of the yeast VPS9-domain family related to mammalian VARP.....	53
3.3.3	Vrl1, Muk1, and Vps9 have partially overlapping functions.....	54
3.3.4	Retromer interacts with the VPS9 domain.....	56
3.3.5	Muk1, Vps9, and Vrl1 can localize to endosomes.....	58
3.3.6	Retromer localization to endosomes is impaired by loss of Rab5 GEFs.....	60
3.3.7	Rab5 GEFs are required for normal PI3P localization.....	62
3.4	Discussion.....	65
3.4.1	Discovery of a new yeast VPS9-domain protein.....	67
3.4.2	The VPS9 family.....	69
3.5	Materials and methods.....	70
3.5.1	Yeast strains and plasmids.....	70
3.5.2	Growth and colony overlay assays.....	73
3.5.3	Western blotting and coimmunoprecipitation.....	73

3.5.4	Integrated membrane yeast two hybrid (iMYTH)	75
3.5.5	Fluorescence microscopy	75
Chapter 4: Discussion and conclusions		76
4.1	Summary of major findings	76
4.2	Functional relevance of Ssp120 in the Emp46/Emp47 complex	77
4.3	Rab regulators in retromer recruitment.....	78
4.4	Vrl1 as a putative Rab5-family GEF	82
4.5	Conclusions and future prospects	84
References		86
Appendices		105
	Appendix A Online supplementary material for chapter 2.....	105
	Appendix B Supplementary material for chapter 3	106

List of Tables

Table B.1 Yeast strains used in chapter 3	106
Table B.2 Plasmids used in chapter 3	107

List of Figures

Figure 1.1 Yeast membrane trafficking pathways.....	2
Figure 1.2 A generalized mechanism for membrane trafficking in yeast.....	4
Figure 1.3 The Rab GTPase cycle.....	11
Figure 2.1 Proteome-wide purification of yeast MPs.....	29
Figure 2.2 Global organization of yeast MP complexes.....	34
Figure 2.3 Functional association of Irc6 with AP1.....	36
Figure 2.4 Ssp120 participates in Golgi to ER recycling.....	38
Figure 3.1 Retromer physically interacts with the Rab5-family GEFs Muk1 and Vps9.....	52
Figure 3.2 Vrl1 is a new yeast VPS9 domain protein.....	55
Figure 3.3 The VPS9 domain of Muk1 is sufficient for interaction with retromer subunits in the iMYTH assay.....	57
Figure 3.4 The yeast VPS9-domain proteins Muk1, Vps9, and Vrl1 localize to endosomes.....	59
Figure 3.5 Rab5-family GEFs and GTPases are required for endosomal recruitment of retromer.	62
Figure 3.6 Rab5-family GEFs are needed for PI3P production at endosomes, and this cannot be bypassed by expressing the constitutively active Rab5-family GTPase Vps21(Q66L).	64
Figure 3.7 Models for the function of the interaction between retromer and Rab5-family GEFs at endosomes.....	67
Figure B.1 There is a deletion present in lab <i>Saccharomyces cerevisiae</i> strains in the gene <i>YML003W</i> that is absent from other <i>S. cerevisiae</i> and truncates the normal gene product.	109

Figure B.2 Conservation of the hVARP N-terminal domain and the VAMP7-interacting domain.
..... 110

Figure B.3 All NubG iMYTH and GFP-*MUK1* vectors were expressed. 111

List of Abbreviations

aa – Amino acid

A-ALP – Alkaline phosphatase-dipeptidyl aminopeptidase A

AD – Activation domain

AD – Alzheimer disease

ADH – Alcohol dehydrogenase

ALS – Amyotrophic lateral sclerosis

AP – Clathrin adaptor protein complex

APL – Clathrin adaptor protein complex large chain

APM – Clathrin adaptor protein complex medium chain

APP – Amyloid precursor protein

a.u. – Arbitrary units

BACE – β APP-cleaving enzyme

BAR – Bin, amphiphysin, Rvs

BD – Binding domain

BioGRID – Biological General Repository for Interaction Datasets

BLOC – Biogenesis of lysosome-related organelles

C12E8 – Octaethylene glycol monododecyl ether

CD41 – Dyserythropoietic anemia type II

CSC – Cargo selective subcomplex

CHS – Chitin synthase-related

CLSD – Cranio-lenticulo-sutural dysplasia

ConA – Concanavalin A

COP – Coat protein complex

CORVET – Class C core vacuole/endosome tethering

CPY – Carboxypeptidase Y

CUB – C-terminal fragment of split ubiquitin

CUE – Coupling of ubiquitin to ER degradation

DIC – Differential interference contrast

DDM – n-dodecyl- b-D-maltopyranoside

DMT – Divalent metal transporter

DSP – Dithiobis(succinimidyl propionate)

DTT – Dithiothreitol

DUB - Deubiquitinase

EMP – Endomembrane protein

ER – Endoplasmic reticulum

ERV – ER vesicle

ESCRT – Endosomal sorting complex required for transport

F5F8D – Combined factor V and factor VIII deficiency

FRET – Fluorescence resonance energy transfer

FYVE – Fab-1, YGL023, Vps27 and EEA1

GAL – Galactose metabolism

GAP – GTPase activating protein

GDF – GDI displacement factor

GDI – Guanine nucleotide dissociation inhibitor

GDP – Guanosine diphosphate

GEF – Guanine nucleotide exchange factor

GFP – Green fluorescent protein

GGA – Golgi-localized, gamma adaptin ear-containing

GLUT – Glucose transporter

GTP – Guanosine triphosphate

HA- Haemagglutinin

HC – High-confidence

HIS – Histidine

HOPS – Homotypic fusion and vacuole protein sorting

HSP – Hereditary spastic paraplegia

IgG – Immunoglobulin G

INP – Inositol polyphosphate 5-phosphatase

IP - Immunoprecipitates

iMYTH – Integrated membrane yeast two-hybrid

IRC – Increased recombination centers

KEX – Killer expression defective

LMAN – Lectin, mannose binding

LC-MS – Liquid chromatography-electrospray ionization-mass spectrometry

MALDI-TOF – Matrix assisted laser desorption/ionization time-of-flight

MBP – Maltose binding protein

MCFD – Multiple coagulation factor deficiency

MIPS – Munich Information Center for Protein Sequences

MP – Membrane proteins

MS – Mass spectrometry

MUK – Computationally-linked to Kap95

MVB – Multivesicular body

NAT – Nourseothricin

NSF – N-ethylmaleimide sensitive factor

NUB – N-terminal fragment of split ubiquitin

OE - Overexpressed

ORF – Open reading frame

PAGE – Polyacrylamide gel electrophoresis

PBS – Phosphate buffered saline

PC – Phosphatidylcholine

PCA – Protein complementation assay

PD – Parkinson disease

PE – Phosphatidylethanolamine

PH – Pleckstrin homology

PI – Phosphatidylinositol

PI3K – Phosphatidylinositol 3-kinase

PI3P – Phosphatidylinositol 3-phosphate

PIP – Phosphatidylinositol phosphate

PIR – Proteins with internal repeat

PPI – Protein-protein interaction

PS – Phosphatidylserine

PX – Phox homology

RABEX – Rabaptin-5-associated exchange factor

RFP – Red fluorescent protein

SAR – Secretion-associated Ras-related

SCS – Suppressor of choline sensitivity

s.d. – Standard deviation

SDS – Sodium dodecyl sulfate

SE – Standard error

SEC – Secretary

SGA – Synthetic genetic array

SILAC – Stable isotope labeling by amino acids in cell culture

SNA – Sensitivity to Na⁺

SNAP – Soluble N-ethylmaleimide sensitive factor attachment protein

SNARE – Soluble NSF attachment protein receptor

SNF – Sucrose nonfermenting

SNX – Sorting nexin

SSP – Saccharomyces secretory protein

TAP – Tandem affinity purification

TMH – Transmembrane helix

TP:FP – True positive:false positive

TRAPP – Transport protein particle

TS – Temperature sensitive

VAMP – Vesicle-associated membrane protein

VARP – VPS9-ankryin repeat protein

VHS – Vps27/Hrs/STAM

VRL – VARP-like

VPS – Vacuolar protein sorting

WASH – Wiskott-Aldrich syndrome protein and scar homolog

WCL – Whole-cell lysates

WT – Wild type

YAP – Yeast assembly polypeptide

YPD – Yeast extract, peptone, dextrose

YPT – Yeast protein two

Acknowledgements

First, and most significantly, I would like to thank my supervisor Elizabeth Conibear for her inspiring positive outlook, willingness to have frank discussion on almost any topic and devoted mentorship. Throughout my degree, her deep wisdom, knowledge of the field and infectious love of science have been there to guide me. I hope to someday acquire her finesse in leadership.

I would also like to thank the Conibear lab members I've had the pleasure of working with in the past five years. They have been good friends who inspire stimulating discussions and frequently create quotable moments. In particular, Cayetana Schluter and Mike Davey were very helpful in my efforts to learn new techniques and plan experiments. Furthermore, Mike Davey and Matt Tinney both contributed key strains and plasmids to my work. David Lin and Helen Burston have both been great companions through the program, contributing extra lively discussions and origami nights. I thank Shawn Whitfield for discussions in the lab and for tolerating me as a roommate. Lauren Dalton has consistently been helpful and I thank her for editing some sections of this thesis. Lastly, Nayomi Gomes has exceeded all my expectations of a volunteer and I thank her for her excellent work.

I have been fortunate to have mentors/collaborators outside of our lab who have greatly contributed to my thesis. In particular, I would like to thank my committee members Phil Hieter and Thibault Mayor for the stimulating discussions and advice they provided over the course of my degree. Additionally, I thank my collaborator Mohan Babu for giving me the opportunity to work with his exciting data set of membrane-associated protein-protein interactions.

Finally, I thank my parents, my brother and my friends who have supported me throughout my program. I appreciate their friendship that has persisted through long days in the lab, ocean explorations, and mountain adventures. I thank them for the energy they have put into understanding my work.

Dedication

To my parents...

who quite literally made me what I am today.

Chapter 1: Introduction

1.1 Overview of membrane trafficking in yeast

1.1.1 Yeast membrane trafficking pathways

Eukaryotic cells contain membrane-bound compartments that enable specialized functions, but necessitate membrane trafficking machinery to localize proteins. As this machinery is well conserved, membrane trafficking studies often use model systems that are more easily genetically manipulated, such as the budding yeast *Saccharomyces cerevisiae*. This section outlines the main trafficking pathways of yeast that transport proteins from the site of protein synthesis at the endoplasmic reticulum (ER), to intermediate locations and finally to the vacuole for degradation (Figure 1.1).

In most cases, during the synthesis of luminal or transmembrane proteins by ribosomes, a short N-terminal signal sequence recognized by the signal recognition particle (SRP), or a N-terminal hydrophobic transmembrane domain, respectively targets the peptides for insertion into the endoplasmic reticulum (ER) through the translocon (Denks *et al.*, 2014). Soluble proteins enter the lumen, whereas integral membrane proteins remain in the membrane by exiting the translocon through a lateral gate. Many proteins are then modified by the covalent addition of sugars (glycosylation) (Helenius and Aebi, 2004; Xu and Ng, 2015) and/or lipids (Lam *et al.*, 2006; Orlean and Menon, 2007), which aid in folding and ER exit. Properly folded proteins are transported to the Golgi by the coat protein complex II (COPII) coat with the aid of cargo adaptors (Jensen and Schekman, 2011).

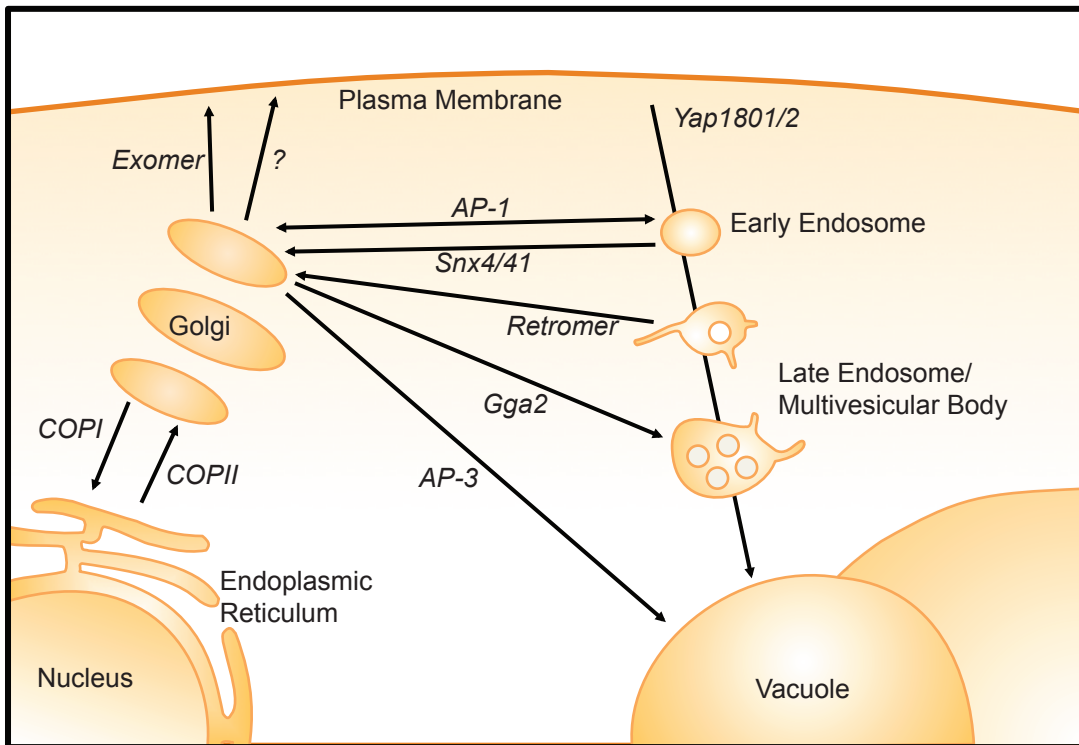


Figure 1.1 Yeast membrane trafficking pathways.

Different complexes or proteins with a key role in a given pathway are identified in italics.

Cargo adaptors are proteins or complexes that bind motifs on cargo and link them to protein coats. Through their interactions with coats, adaptors are often localized to small domains and can therefore sequester cargo, concentrating it prior to transport. Since cargo adaptors are crucial for conferring specificity, many membrane trafficking pathways are referred to by the cargo adaptor they use (Figure 1.1).

At the Golgi further protein modifications such as glycosylation occur (Brigance *et al.*, 2000; Munro, 2001; Stanley, 2011) and mature proteins are distributed to cellular compartments by several trafficking complexes. Some proteins are returned to the ER by COPI (Gaynor *et al.*, 1998; Hsu *et al.*, 2009). Others are transported to the vacuole by adaptor protein complex 3 (AP-

3) (Cowles *et al.*, 1997), to late endosomes by Golgi-localized, gamma adaptin ear-containing, ARF-binding (GGA) proteins (Costaguta *et al.*, 2001; Demmel *et al.*, 2008; De *et al.*, 2012) and to early endosomes by AP-1 (Stepp *et al.*, 1995; Nakatsu and Ohno, 2003). Additionally, proteins are targeted to the plasma membrane by both an exomer-mediated pathway (Wang *et al.*, 2006) and a separate constitutive secretory pathway.

At the plasma membrane luminal proteins are secreted. For the uptake of external nutrients and the down regulation of membrane proteins, the plasma membrane buds into the cell in the process of endocytosis. Endocytosis is mediated by clathrin, actin and cargo adaptors, such as Yap1801/2 (Kaksonen *et al.*, 2005; Burston *et al.*, 2009).

The resultant vesicles fuse with endosomes, which are a major site of cargo sorting. At early endosomes some proteins are recognized and trafficked to the late Golgi by Snx4/41 (Hettema *et al.*, 2003) and AP-1 (Valdivia *et al.*, 2002). As the endosomes mature, retromer further sorts membrane proteins to the late Golgi (Bonifacino and Rojas, 2006). Alternatively, many ubiquitin tagged membrane proteins are internalized into the lumen of endosomes by endosomal sorting complexes required for transport (ESCRT) machinery (Schmidt and Teis, 2012). Eventually these multivesicular bodies (MVBs) fuse with the vacuole and the luminal contents are degraded.

1.1.2 Mechanism of membrane trafficking in yeast

A similar mechanism is used for all yeast membrane trafficking pathways (Figure 1.2). Cargo is recognized by adaptors and incorporated into vesicles, which move through the cell and fuse with a target membrane. Additional factors build specificity into these steps as described below.

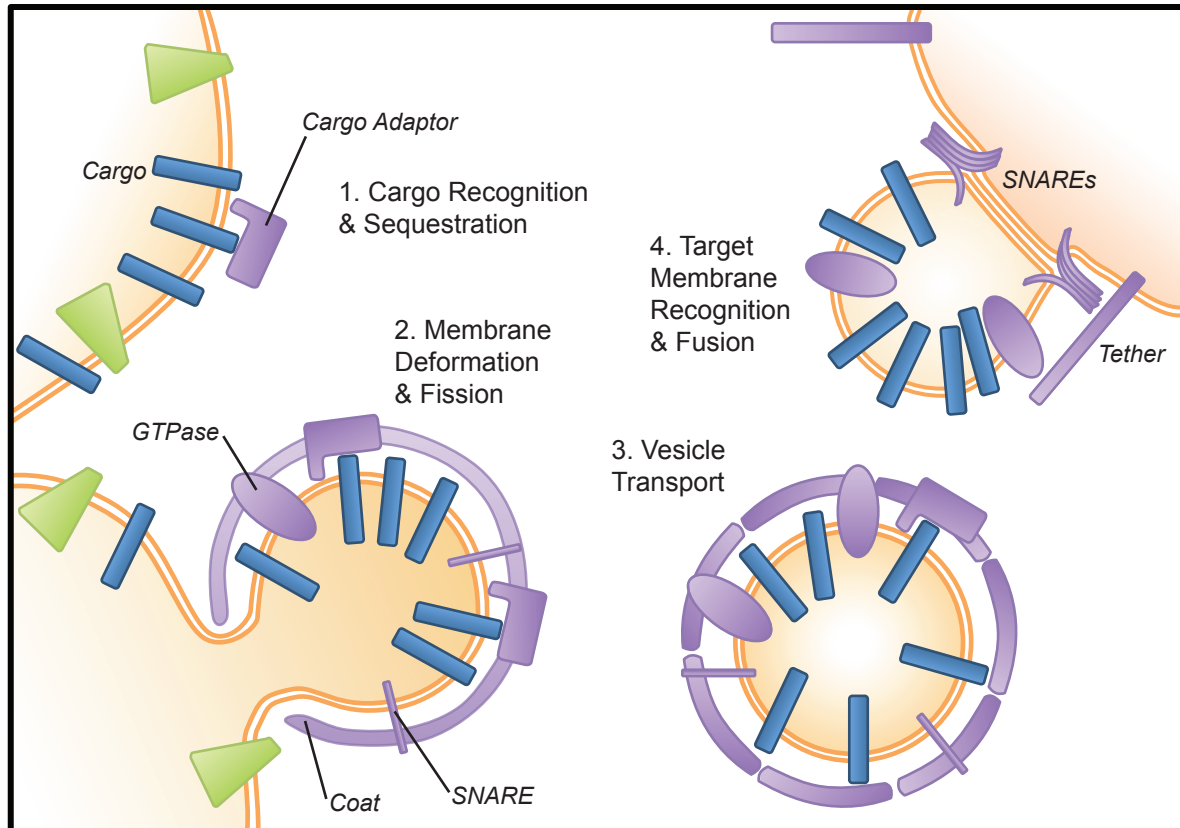


Figure 1.2 A generalized mechanism for membrane trafficking in yeast.

Cargo (dark blue) is transported to a target membrane in a vesicle through four broad steps mediated by trafficking machinery (purple).

Cargo adaptors are recruited to specific membranes by interactions with lipids and proteins such as Rab, Sar and Arf GTPases. There cargo is recognized by short amino acid motifs such as KKxx and KxKxx for COPI sorting (Ma and Goldberg, 2013), or tyrosine and dileucine-based

motifs for AP1 sorting (Rapoport *et al.*, 1998). These cargo adaptors concentrate and link cargo to coat proteins either directly, as in Gga2 sorting (De *et al.*, 2012), or indirectly as in the case of Snx3 adapting Fet3-Ftr1 for retromer trafficking (Strochlic *et al.*, 2007). Coat proteins such as the COPII components Sec13/Sec23/Sec24/Sec31 (Jensen and Schekman, 2011) deform the membrane at sites of cargo enrichment, sometimes with the aid of membrane modifying proteins such as the flippase Drs2 (Liu *et al.*, 2008). Once a bud or a tubule is formed, membrane scission may be mediated by GTPases such as Vps1 (Chi *et al.*, 2014).

The resultant vesicles move through the cell by diffusion or, in many cases, by motor proteins such as Myo2 (Hammer and Sellers, 2012). During transport the vesicle coats disassemble to varying extents. The timing of uncoating is an active area of investigation as vesicles must be uncoated to fuse with a target membrane, but the coats are sometimes involved in the recognition of that membrane (Angers and Merz, 2009; Trahey and Hay, 2010; Lord *et al.*, 2013)

. Target membranes initially recognize vesicles through a group of proteins and protein complexes known as tethers (Sztul and Lupashin, 2009), which anchor the vesicle to the membrane. Once tethered, soluble N-ethylmaleimide sensitive factor attachment protein receptor (SNARE) proteins mediate vesicle fusion (Burri and Lithgow, 2004). One SNARE on the vesicle comes into contact with two or three on the target membrane and bundle together driving their respective membranes into a proximity that makes membrane fusion energetically favourable.

Following fusion, cargo enters the target compartment.

1.2 Compartment definition and recognition

1.2.1 Lipids

Lipids are a diverse class of water insoluble organic molecules that include fatty acids (carbon chains with a terminal carboxyl group) and their derivatives. They are primarily synthesized at the ER, though additional synthesis takes place at the Golgi and mitochondria (van Meer *et al.*, 2008). While lipids are crucial for energy storage and signal transduction this section will focus on their role in forming cellular membranes.

Membranes are formed from a bilayer of polar lipids such that their polar head groups face the surrounding aqueous environment on either side of the bilayer but their hydrophobic tails are protected. Phospholipids, which constitute a major class of these polar lipids, are based on one glycerol molecule esterified to two fatty acids and one phosphate group. These phosphate groups may further serve as attachment points for other molecules such as choline (phosphatidylcholine; PC), ethanolamine (phosphatidylethanolamine; PE), serine (phosphatidylserine; PS) and inositol (phosphatidylinositol; PI) (van Meer *et al.*, 2008). The different sizes and charges of these head groups give the phospholipids different characteristics. For example PS is negatively charged and the small size of the PE headgroup gives it a conical shape, which can induce membrane curvature. The relative abundance of the above four most common phospholipids is part of what defines compartmental identity.

Even though phosphatidylinositol phosphates (PIPs) are not abundant relative to the above phospholipids, they play a key role in compartment identity. Through a series of kinases and

phosphatases the inositol head group may be phosphorylated on up to three sites. A given phosphorylation state is usually enriched at specific compartments, for example phosphatidylinositol 4-phosphate (PI4P) is enriched at the Golgi, and phosphatidylinositol 3-phosphate (PI3P) at the endosome (Di Paolo and De Camilli, 2006). Phosphoinositides help recruit proteins which have domains that recognize specific PIPs.

A final consideration with lipids is how their non-uniform distribution is maintained. Between membranes they can be transported in vesicles or by proteins at organelle-organelle contact sites (van Meer *et al.*, 2008). Within a membrane asymmetries can be generated by P4-type ATPases and ABC transporters, that move specific lipids from one leaflet to the other (Pomorski and Menon, 2006). These processes can both create charged domains and deform membranes, a result exploited for the formation of some vesicles. Scramblases can resolve the lipid asymmetries by moving lipids to the opposing leaflet along their concentration gradients (Pomorski and Menon, 2006).

1.2.2 Lipid recognition domains

Proteins recognize lipid bilayers based on charge, the presence of a specific lipid, lipid packing defects and the curvature of the membrane (Lemmon, 2008). Domains based on charge recognition contain acidic or basic patches that interact with basic or acid phospholipids respectively. Several domains, such as the Annexin domain (Gerke *et al.*, 2005), bind calcium ions that mediate interactions with acidic phospholipids. Other domains bind specific PIPs, as in the cases of PI3P recognition by the Phox homology (PX) domains of Vps5/17 (Burda *et al.*, 2002), PI4P recognition by the Vps27/Hrs/STAM (VHS) domain of Gga2 (Demmel *et al.*, 2008),

and PIP recognition by pleckstrin homology (PH) domains (Lemmon, 2008). Lipid packing defects, which increase accessibility to the hydrophobic core of membranes can be detected and bound by amphipathic lipid packing sensor motifs (Antonny *et al.*, 2015). Finally, proteins can recognize membrane curvature through crescent-shaped domains like the Bin, amphiphysin, Rvs (BAR) domain (Peter *et al.*, 2004).

1.2.3 Coincidence detection

As most protein-lipid interactions are relatively weak, a common strategy for the strong membrane association of peripheral membrane proteins is to simultaneously bind more than one feature of a target membrane. This coincidence detection can include combinations of lipid, membrane curvature and protein recognition (Di Paolo and De Camilli, 2006; Lemmon, 2008). Proteins may also dimerize so that together they have multiple membrane binding domains allowing a higher affinity membrane interaction. Sometimes these strategies are used in parallel. For example, Vps5 and Vps17 each contain PX-BAR domains, which bind PI3P and curvature respectively (Lemmon, 2008; Chi *et al.*, 2014). By dimerizing they have two PI3P binding domains and a curvature-binding domain enabling strong recruitment to curved, PI3P-decorated membranes. Importantly, coincidence detection builds specificity into the recruitment of a protein to a membrane as it means proteins must recognize multiple aspects of a given membrane. Thus, a stray lipid or protein in an incorrect compartment will likely only transiently recruit proteins that are not normally targeted there.

1.2.4 SNAREs and tethers

Soluble N-ethylmaleimide sensitive factor attachment protein receptors (SNAREs) and tethers are particularly important for the recognition of specific membranes for vesicle docking and fusion. SNAREs are defined by a conserved “SNARE motif” that forms coiled coils. For vesicle fusion sets of SNAREs interact, with one SNARE on a vesicle (v-SNARE) and three SNAREs on a target membrane (t-SNAREs) forming an alpha helical bundle (Chen and Scheller, 2001) known as a SNAREpin. SNAREpin formation is driven by interactions between the four SNARE motifs, which pull the two membranes together, providing the energy required for vesicle fusion (Chen and Scheller, 2001; Jahn and Scheller, 2006). After fusion, the *cis*-SNARE complex is disassembled by N-ethylmaleimide sensitive factor (NSF/Sec18) in conjunction with soluble NSF attachment protein (SNAP/Sec17) (Chen and Scheller, 2001). The SNAREs can then be recycled and reused.

In yeast 24 SNAREs have been identified and humans contain at least 35 (Burri and Lithgow, 2004). These can be grouped based on a central polar residue in their SNARE motif, which is either a glutamine (Q-SNAREs) or an arginine (R-SNAREs). Interactions between SNAREs are specific because a SNAREpin can only contain one R-SNARE and a given SNARE only interacts with a small subset of possible SNAREs as outlined by Burri and Lithgow (Burri and Lithgow, 2004). Since SNAREs are carefully localized and their interactions are specific (Lewis *et al.*, 2000; Burri and Lithgow, 2004), they facilitate the compartmental targeting of a vesicle.

Tethers, a group of peripherally associated proteins and complexes also recognize specific vesicles (Sztul and Lupashin, 2009). Tethers associate with well-defined target membranes often

through coincidence detection of t-SNAREs and Rab GTPases (Sztul and Lupashin, 2009). On those membranes they interact with proteins on incoming vesicles, in some cases the coat proteins themselves (Lord *et al.*, 2011), tethering the vesicles to the target membrane. By spatially restricting the vesicles, tethers increase the likelihood of SNAREs forming a SNAREpin and mediating membrane fusion. Interestingly, some tethers have Rab guanine nucleotide exchange factor (GEF) activity, which allows them to activate the compartment-defining Rab GTPases discussed in the following section (Sztul and Lupashin, 2009).

1.2.5 Rab GTPases and their regulators

Rab GTPases are small enzymes that inefficiently hydrolyze guanosine triphosphate (GTP) into guanosine diphosphate (GDP) and are integral to defining compartments through the recruitment of downstream effector proteins. After synthesis Rabs are prenylated at two C-terminal cysteines by geranylgeranyl transferases such as Bet2/4 (Witter and Poulter, 1996), which allows Rab membrane association. In the cytosol GDP-bound Rabs interact with guanine nucleotide dissociation inhibitors (GDIs), Gdi1 in yeast (Garrett *et al.*, 1994), which protect the hydrophobic prenyl chains and maintain solubility (Pfeffer and Aivazian, 2004).

Rabs cycle between the soluble GDI-bound state and an active membrane-bound state as shown in Figure 1.3. In order to enter a membrane GDI-bound Rabs may need to interact with GDI displacement factors (GDFs), which dislodge the GDI and facilitate insertion of the prenyl groups into a membrane (Pfeffer and Aivazian, 2004). However, there are some indications that GDFs are not always required in yeast (Cabrera and Ungermann, 2013). On the membrane, guanine nucleotide exchange factors (GEFs) facilitate the exchange of the Rab-bound GDP with

GTP. Rabs undergo a conformational change upon binding GTP, particularly in two “switch” regions (Stroupe and Brunger, 2000). In this state they are considered active and are able to interact with their effector proteins. When a Rab comes into contact with a GTPase activating protein (GAP) its catalytic activity increases and GTP is rapidly hydrolyzed into GDP resulting in a conformational reversion. This GDP-bound form can be recognized by GDIs, which can then remove the Rab from the membrane, allowing it to be cycled back to its functional site.

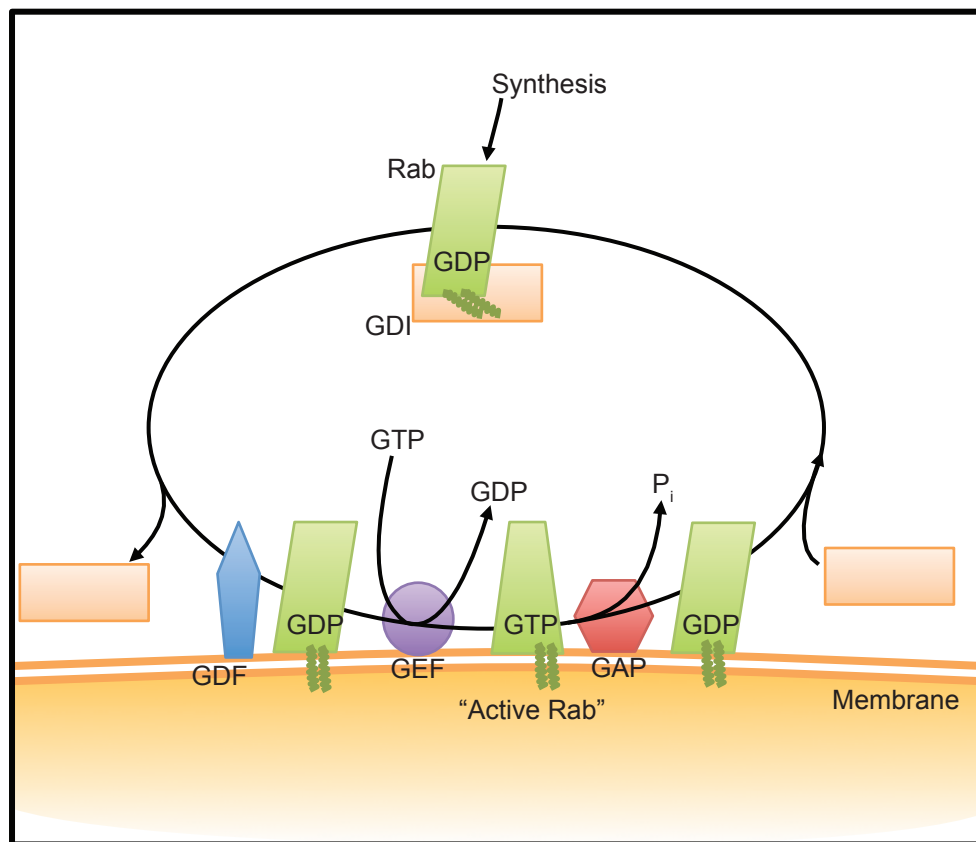


Figure 1.3 The Rab GTPase cycle.

Rabs cycle between an inactive GDP-bound state and an active GTP-bound state with the aid of accessory proteins. These include guanine nucleotide dissociation inhibitors (GDIs), GDI displacement factors (GDFs), guanine nucleotide exchange factors (GEFs) and GTPase activating proteins (GAPs). Rab prenylation is indicated by the dark green chains.

By dynamically cycling on and off membranes Rabs are able to maintain a steady state localization to the membrane of a specific compartment. This makes them ideal regulators of compartment-specific membrane trafficking events, where they are involved in the recruitment of factors that drive membrane fission and fusion events (Stenmark and Olkkonen, 2001; Stenmark, 2009). In this role Rabs interact with tethers, lipid modifying enzymes and possibly SNAREs (Hutagalung and Novick, 2011). Rabs are central to the maturation of compartments because of their ability to alter the lipid and protein composition of membranes.

1.2.6 Compartment maturation

Cellular compartments change composition over time as proteins and lipids are processed and transported to or from the compartment. In particular, the compartments in the secretory (Losev *et al.*, 2006) and endocytic (Huotari and Helenius, 2011) pathways mature over time. As the compartments mature, proteins central to their identity, such as Rabs and tethers, are displaced as new ones are recruited. In the secretory pathway, Rabs have been found to facilitate this exchange by recruiting the GEF for a downstream Rab (Hutagalung and Novick, 2011). This ordered conversion of Rabs was first observed by the Novick group, who found that the Rab Ypt32 recruits Sec2, the GEF for the downstream Rab Sec4 (Ortiz *et al.*, 2002). Furthermore, the downstream Rab can recruit a GAP, leading to the extraction of the upstream Rab and a full Rab conversion (Hutagalung and Novick, 2011). These conversions are an appealing model for compartment maturation.

1.2.6.1 A focus on endosome maturation in yeast

After their formation, yeast endosomes are bound by Rab5-family GEFs, which include Muk1 and Vps9 (Paulsel *et al.*, 2013). Vps9 is likely recruited through interactions between ubiquitinated cargo and its ubiquitin-binding CUE domain (Shideler *et al.*, 2015) while the domain responsible for Muk1 recruitment has not been determined. Rab5-family GEFs recruit and activate the Rab5-family GTPases Vps21, Ypt52 and Ypt53 (Nickerson *et al.*, 2012; Cabrera and Ungermann, 2013). Once active, the Rab5-family GTPases can recruit effectors such as the tether class C core vacuole/endosome tethering (CORVET), a complex composed of Vps3/8/11/16/18/33 (Peplowska *et al.*, 2007). Together the Rab5-family GTPases, CORVET and other effectors mediate clustering and fusion of endosomes (Markgraf *et al.*, 2009). Furthermore, the synaptojanin-like proteins, Inp52 and Inp53, hydrolyze the plasma membrane marker PI(4,5)P₂ to PI (Odorizzi *et al.*, 2000). PI is also phosphorylated by the PI 3-kinase (PI3K) Vps34 to produce the endosomal lipid PI3P (Backer, 2008). As endosomes fuse and lipid composition changes, endosomal sorting complex required for transport (ESCRT) machinery drives ubiquitin-tagged transmembrane proteins into luminal vesicles (Schmidt and Teis, 2012).

Rab5-family GTPases have also been proposed to recruit the Ypt7 GEF Mon1/Ccz1 in a model put forward by Nordmann *et al.* (Nordmann *et al.*, 2010). This would trigger a Rab conversion where the Rab7-family GTPase Ypt7 is recruited to endosomes and activated. Once Ypt7 is present, the Rab5-family GTP hydrolysis activity is triggered by the GAP Msb3 (Lachmann *et al.*, 2012; Nickerson *et al.*, 2012) and the GDP-bound forms are extracted from the membrane by Gdi1 (Garrett *et al.*, 1994). Interestingly, a Rab5-family effector, the biogenesis of lysosome-related organelles 1 (BLOC-1) complex can recruit Msb3 to endosomes in a Ypt7-dependent

manner, providing a mechanism for the activation and extraction of Rab5-family GTPases (John Peter *et al.*, 2013; Rana *et al.*, 2015). During this Rab conversion, the CORVET complex is exchanged for a different tethering complex known as homotypic fusion and vacuole protein sorting (HOPS) (Wurmser *et al.*, 2000; Nordmann *et al.*, 2010; Bröcker *et al.*, 2012). HOPS interacts with Ypt7, PIPs and SNAREs such as Vam7 and, together with Ypt7, coordinates late endosome tethering and fusion with the vacuole (Stroupe *et al.*, 2006). HOPS is also able to tether the δ -ear domain of the AP-3 subunit Apl5, mediating Golgi to vacuole trafficking (Angers and Merz, 2009). Additionally, on these membranes the PI3P 5-kinase Fab1 converts the endosomal marker PI3P into the vacuolar lipid PI(3,5)P₂ (Gary *et al.*, 1998). Finally, the GAP Gyp7 activates Ypt7 GTP hydrolysis, resulting in Ypt7 extraction (Brett *et al.*, 2008).

Endosome maturation demonstrates how the different forms of membrane identity are interconnected. Rabs recruit effectors such as tethers and likely regulate which signaling lipids are present. Further, the tethers can bind SNAREs and help coordinate fusion with the compartment. Given the multitude of factors present, it is not surprising that coincidence detection is a common strategy among peripheral membrane proteins for association with specific membranes.

1.3 Strategies for cargo recognition

1.3.1 Sorting signals

In order to incorporate the correct cargo into vesicles, trafficking machinery recognizes proteins with specific traits or short motifs that serve as sorting signals. For example, in AP-2 driven

endocytosis the sorting signals $Yxx\Phi$ (where Φ is a bulky hydrophobic residue) (Owen and Evans, 1998) and $[DE]xxxL[LIM]$ (Traub, 2009) are recognized by pockets on the AP-2 $\mu 2$ subunit and $\alpha/\sigma 2$ subunits respectively (Owen and Evans, 1998). Here, multiple binding sites allow for differential regulation of cargo recognition. Other proteins are recognized independently of short motifs as in the case of the COPII cargo adaptor Erv14 interacting with long transmembrane domains (Powers and Barlowe, 2002). Furthermore, protein modifications can act as sorting signals, allowing additional regulation of cargo recognition. A well-studied example is ubiquitination signaling the internalization of plasma membrane proteins (Rotin *et al.*, 2000; Traub, 2009).

1.3.2 Accessory adaptors

While most cargo is recognized by adaptors that directly link cargo to coat proteins, other proteins can associate with the core adaptors, expanding their repertoire of cargo. These accessory adaptors bind additional cargo through different motifs and link it to the core trafficking machinery. As most trafficking machinery peripherally associates with membranes, accessory adaptors, which may be integral proteins, play a key role in recognizing and binding luminal cargo. Examples include Emp46/47 for COPII trafficking (Sato and Nakano, 2002) and Snx3 for retromer trafficking (Strohlic *et al.*, 2007). Though accessory adaptors have been identified, their abundance and regulation is not fully understood.

1.4 COPII membrane trafficking

1.4.1 Structure and function

The coat protein complex II (COPII) membrane trafficking machinery has a well-defined role in the transport of proteins from the endoplasmic reticulum (ER) to the Golgi (Lord & Miller 2013). The discovery of COPII (Barlowe *et al.*, 1994) stemmed from an impressive series of studies that identified (Novick *et al.*, 1980) and ordered (Novick *et al.*, 1981) temperature sensitive secretory mutants. In this section the mechanism of COPII trafficking in yeast will be reviewed, followed by a brief comparison with the more complex metazoan COPII.

Assembly of the COPII coat on the ER is triggered by the GEF Sec12, which activates the Arf family GTPase Sar1 (Barlowe and Schekman, 1993; Barlowe *et al.*, 1993). GTP-bound Sar1 can then bind the ER membrane through an amphipathic helix, likely inducing curvature (Lee *et al.*, 2005). Sar1 recruits the Sec23/24 dimer that forms the inner coat of COPII (Bi *et al.*, 2002). Sec23 has Sar1 GAP activity (Bi *et al.*, 2002) and Sec24 recognizes cargo for inclusion in COPII-derived vesicles (Miller *et al.*, 2003). Furthermore, Sec23/24 recruits the outer coat, a 2:2 Sec13/31 heterotetramer (Jensen and Schekman, 2011). Sec13/31 can form a lattice that stabilizes Sec23/24, drives bud formation (Stagg *et al.*, 2006), and further activates the Sar1 GTPase (Bi *et al.*, 2007). The activation of Sar1 GTPase activity within the coat may restrict GTP-bound Sar1 to the vesicle bud neck, consistent with its role in driving the scission of buds with assembled COPII coats (Pucadyil and Schmid, 2009; Kung *et al.*, 2012).

The yeast COPII vesicle then diffuses towards the Golgi. On the vesicle, Sec23 recruits the transport protein particle (TRAPP) complex, which acts as a GEF for the Rab Ypt1 (Cai *et al.*, 2008). Active Ypt1 can recruit its effector Uso1, a long coiled coil protein that tethers the COPII vesicle to the Golgi (Lord *et al.*, 2011). The tether is hypothesized to bend, bringing the vesicle closer to the Golgi membrane and allowing the SNAREs Sec22, Sed5, Bos1 and Bet1 to form a trans-SNARE complex and mediate membrane fusion (Newman *et al.*, 1990). Phosphorylation of Sec23/24 by the Hrr25 kinase is required for efficient fusion and may trigger uncoating of the vesicle (Lord *et al.*, 2011). After fusion, the cis-SNARE complex is disassembled by Sec17 and Sec18 allowing the SNAREs to act in further rounds of fusion (Mayer *et al.*, 1996). Furthermore, transmembrane proteins involved in COPII trafficking, such as cargo-selective adaptors, may contain KKxx or KxKxx motifs that enable their recycling to the ER by COPI coat machinery (Ma and Goldberg, 2013).

COPII-based trafficking is largely conserved in metazoans (Lord & Miller 2013). One notable difference is that metazoans contain multiple isoforms of all core COPII proteins except Sec13 (Jensen and Schekman, 2011). It is plausible that this allows metazoan COPII to recognize further sorting signals (with the four Sec24 paralogs) or form coats of different sizes. The ability to form different size coats is critical for the secretion of large proteins such as collagen, a process that appears to require the ubiquitination of Sec31 (Jin *et al.*, 2012). Other differences include the targeting of COPII vesicles to an ER-Golgi intermediate compartment (ERGIC) and the use of motor proteins for vesicle transport (Lord *et al.*, 2013). Even with these differences, yeast remains the premier model for understanding many aspects of COPII function such as regulation, uncoating and cargo recognition.

1.4.2 Cargo recognition

COPII recognizes cargo through multiple binding sites associated with the coat, consistent with the need to transport a wide range of cargo. The inner coat protein Sec24, and its two homologs Sfb2 and Sfb3, are central to cargo recognition (Miller *et al.*, 2003). Each of these proteins contains at least three different cargo-binding sites (sites A, B and C), which recognize different signals. For example the Sec24 A-site recognizes YxxxNPF while the B-site binds (DE)_x(DE) and Lxx(LM)E motifs (Miller *et al.*, 2003; Sato and Nakano, 2007). Adding to the diversity of signals recognized, Sec24 homologs can bind unique cargo, as is the case in Sfb3 recruiting a plasma membrane ATPase to COPII vesicles (Roberg *et al.*, 1999). Furthermore the GTPase associated with Sec23/24, Sar1, may directly bind some COPII cargo with dibasic motifs (Giraud and Maccioni, 2003).

Beyond cargo recognition sites on core COPII machinery, other COPII cargo selective adaptors have been identified. As the COPII coat is peripherally associated with the ER, proteins must link luminal proteins to the coat for efficient sorting. Two proteins responsible for this function are Emp47 (Sato and Nakano, 2002, 2003) and Erv29 (Belden and Barlowe, 2001). As GPI-anchored proteins also may not have any amino acids in the membrane, they too require an adaptor. Muniz *et al.* have shown that Emp24 links some GPI-anchored proteins to the COPII coat (Muñiz *et al.*, 2000). Finally, transmembrane proteins can interact with COPII through adaptors such as Erv14, Erv29 and Gsf2 (Powers and Barlowe, 2002). COPII function is clearly dependent on multiple cargo recognition sites, but the reason why so many are required remains an open question. One possibility is that they offer ways to regulate the ER exit of subsets of cargo, although the regulation of COPII accessory adaptors is poorly understood.

1.4.3 COPII dysfunction in disease

Likely owing to the central role of COPII trafficking in the secretory pathway, mutations in COPII subunits and associated factors result in a wide range of diseases in humans. Mutations in Sar1B GTPase have been associated with diseases of fat malabsorption such as chylomicron retention disease and Anderson disease (Jones *et al.*, 2003). These mutations cluster in the GTP-binding pocket of Sar1B and affect nucleotide binding. On the COPII inner coat, the two Sec23 paralogs (Sec23A and Sec23B) have been linked to diseases. The Sec23A(F382L) mutant can lead to the recessive craniofacial disease cranio-lenticulo-sutural dysplasia (CLSD) (Boyadjiev *et al.*, 2006; Fromme *et al.*, 2007), where as many mutations in Sec23B have been tied to congenital dyserythropoietic anemia type II (CDAII) (Schwarz *et al.*, 2009). This indicates that the Sec23 paralogs likely have some unique functions in humans. Finally, mutations in the Emp47 homolog LMAN1 and its binding partner MCFD2, which together function as a cargo selective adaptor for COPII, can cause combined blood coagulation factor V and VIII deficiency (F5F8D) (Zhang, 2009).

1.5 Retromer membrane trafficking

1.5.1 Structure and function

Retromer was first identified in the yeast *Saccharomyces cerevisiae* as a pentameric complex that drives endosome to Golgi retrograde trafficking (Seaman *et al.*, 1998). The complex could be separated into a structural complex (Vps5/Vps17) capable of membrane deformation and an elongated cargo selective complex (CSC; Vps26/Vps29/Vps35) (Hierro *et al.*, 2007). The original cargo identified were the acid hydrolase receptor Vps10 and the furin protease Kex2

(Seaman *et al.*, 1998). Since its discovery, it has been shown that retromer is widely conserved (Koumandou *et al.*, 2011), and is responsible for sorting a multitude of proteins in yeast and humans (Seaman, 2012). This section will overview our understanding of retromer function in yeast and then highlight differences in humans.

In yeast retromer is recruited to endosomes through two distinct sets of interactions. The structural subcomplex, composed of the sorting nexins (SNXs) Vps5/Vps17, binds the endosomal lipid PI3P through each protein's PX domain. The structural subcomplex can then recruit the CSC (Burda *et al.*, 2002). The CSC is also recruited through direct interactions with the late endosomal Rab7-family GTPase Ypt7 (Liu *et al.*, 2012). As retromer recruitment involves both an early endosomal lipid and a late endosomal Rab, it has been proposed that recruitment is highest at the transition between early (Rab5-bound) and late (Rab7-bound) endosomes (Cullen and Korswagen, 2012; van Weering *et al.*, 2012b).

Once the structural complex is recruited to an endosome it deforms the membrane, forming a tubule roughly 50 nm in diameter (van Weering *et al.*, 2012a). As the CSC is recruited it interacts with cargo directly through Vps35 (Nothwehr *et al.*, 1999) and the adaptor Snx3 (Strochlic *et al.*, 2007), sequestering cargo in the forming tubules. Interestingly, as the retromer tubule forms, retromer is essentially competing with other processes occurring on the endosome. It is blocking fusion events at the vacuole by interacting with Ypt7 (Liu *et al.*, 2012) and competing for transmembrane domain proteins that would otherwise be sorted into luminal vesicles by ESCRT (Strochlic *et al.*, 2008). Once a tubule has formed, the dynamin-related GTPase Vps1, in association with the SNX Mvp1, drives scission of the tubule, which can occur

at multiple locations (Chi *et al.*, 2014). The resultant vesicles are recognized and tethered at the Golgi by the Golgi associated retrograde protein (GARP) complex prior to membrane fusion (Conibear and Stevens, 2000; Bonifacino and Rojas, 2006). It is worth noting that efficient vesicle formation may require a retromer-Ypt7 interaction (Liu *et al.*, 2012). Indeed consistent with tubule formation in the late endocytic pathway, retromer activity on the vacuole was recently observed (Arlt *et al.*, 2015)

In humans retromer refers to a complex made up of the homologs of the yeast CSC. Retromer differs in the array of sorting nexins used, the sorting destinations, the association with actin and the use of motor proteins. It uses combinations of the Vps5/17 homologs SNX1/2 and SNX5/6 respectively for tubule formation (Wassmer *et al.*, 2009). Furthermore, SNX3 directs retromer to a morphologically distinct early endosome sorting pathway (Harterink *et al.*, 2011). SNX27 can act as a cargo selective adaptor for retromer (Temkin *et al.*, 2011; Steinberg *et al.*, 2013) and a SNX27-retromer sorts cargo, such as plasma membrane receptors, in a direct endosome to Golgi pathway not observed in yeast (Temkin *et al.*, 2011). This pathway requires a direct interaction between VPS9-ankryin repeat protein (VARP) and the retromer subunit VPS29, as well as the R-SNARE vesicle-associated membrane protein 7 (VAMP7) (Hesketh *et al.*, 2014). The actin nucleating Wiskott-Aldrich syndrome homolog (WASH) complex also interacts with retromer and appears to be involved in tubule elongation and scission (Gomez and Billadeau, 2009; Harbour *et al.*, 2012), as well as linking different retromer complexes together (Jia *et al.*, 2012; Burd and Cullen, 2014). Linking retromer complexes is proposed to play a role in efficient cargo recruitment to tubules (Burd and Cullen, 2014). Finally, SNX5/6 interact with p150-glued which

binds the motor protein dynein, which may drive both tubule extension and the transport of budded vesicles to the Golgi via microtubules (Wassmer *et al.*, 2009).

1.5.2 Cargo recognition

As briefly mentioned in the previous section, retromer identifies cargo both directly, through Vps35, and indirectly through adaptors in both yeast and humans. It was first demonstrated in yeast that there are multiple sites on Vps35 that can recognize cargo by the discovery of mutants that disrupted Vps10 trafficking, but not that of the Ste13-based cargo A-ALP (Nothwehr *et al.*, 1999, 2000). Those residues that affect Vps10 binding correspond with a groove between two alpha helices near the C-terminus in the crystal structure of human VPS35, which represents a plausible binding site (Hierro *et al.*, 2007). A-ALP on the other hand was later shown to interact with retromer through the adaptor Snx3, as does Fet3-Ftr1 (Strochlic *et al.*, 2007). Since then, additional cargo selective adaptors have been identified including yeast Ere1/Ere2 for the arginine transporter Can1 (Shi *et al.*, 2011) and human SNX27, which recognizes cargo for sorting to the plasma membrane (Temkin *et al.*, 2011).

Recent progress has been made in determining cargo and adaptor binding sites, though some binding sites and sorting signals remain to be identified. Perhaps the best understood signals are the large hydrophobic aromatic signals found on CIM6PR (WLM), sortilin (FLV) and the mammalian iron transporter DMT1-II (YLL) (Seaman, 2007; Tabuchi *et al.*, 2010). Based on homology between CIM6PR and Vps10 it seems likely that these proteins interact with the Vps10 binding pocket on Vps35 and DMT1-II has been shown to do so (Harrison *et al.*, 2014). In contrast, human SNX3 interacts with VPS35 near the N-terminus, adjacent to the Ypt7

binding site (Harrison *et al.*, 2014). SNX27 doesn't bind VPS35, instead it selects cargo (Temkin *et al.*, 2011) and interacts with VPS26 through its PDZ domain (Steinberg *et al.*, 2013). Given the extended 21 nm structure of the CSC (Hierro *et al.*, 2007) it is quite plausible that there are other binding pockets on the CSC. Thus, it will be interesting to identify retromer sorting motifs to see if they all fit known pockets on the CSC or adaptors and determine if some have been missed.

1.5.3 Retromer dysfunction in disease

Disruption of retromer has been linked to several diseases, but it is most strongly associated with Alzheimer disease (AD) and Parkinson disease (PD) (Small and Petsko, 2015). The first study to associate retromer with AD found that in the region where neurons are most affected in AD patients, the entorhinal cortex, the levels of retromer subunits VPS26 and VPS35 are significantly lower than in a control group (Small *et al.*, 2005). Subsequent studies confirmed this association and linked mutations in many other retromer-associated factors to the disease (Small and Petsko, 2015). The primary mechanism proposed to link retromer to AD is that disruptions in retromer lead to decreased sorting of its cargo SorL1 (Fjorback *et al.*, 2012). SorL1 normally binds the amyloid precursor protein (APP), removing APP from endosomes where it is most likely to be processed by β APP-cleaving enzyme 1 (BACE1), the first step towards APP processing into the AD pathogenesis-linked β -amyloid (Fjorback *et al.*, 2012). Thus, disruption of retromer is linked to an increase in β -amyloid production. Additionally, a decrease in retromer sorting of phagocytic receptors to the plasma membrane of microglia is associated with microglial abnormalities in AD patients (Lucin *et al.*, 2013).

The association between retromer and PD originates from an exome sequencing study that found a VPS35(D620N) point mutant is associated with late onset PD (Vilariño-Güell *et al.*, 2011). Subsequent studies have confirmed the association between VPS35 and PD and functionally linked VPS35 with the PD susceptibility genes LRRK2 and PARK16 (Macleod *et al.*, 2013). One plausible hypothesis for the PD association of VPS35 is that the mutation reduces retromer binding of the actin nucleating WASH complex (Zavodszky *et al.*, 2014), which may disrupt retrograde trafficking of CI-M6PR (Follett *et al.*, 2014). In turn, this results in lower levels of the protease Cathepsin D (Follett *et al.*, 2014), which is responsible for the normal processing of α -synuclein, a protein found in aggregates in PD (Miura *et al.*, 2014).

As retromer dysfunction or down regulation has been implicated in AD, PD, Down syndrome (Wang *et al.*, 2013), hereditary spastic paraplegia (Valdmanis *et al.*, 2007) and neuronal ceroid lipofuscinosis (Mamo *et al.*, 2012) a drug that could stabilize the complex would have a high therapeutic potential. Remarkably, a compound that stabilizes retromer has been found and it reduces APP processing (Mecozzi *et al.*, 2014). The multitude of diseases associated with retromer motivates further work on understanding its sorting mechanism and associations in the hope of uncovering further drug targets.

1.6 Research objectives and hypotheses

1.6.1 Characterizing novel cargo-adaptor associated factors

Cargo adaptors occupy a key position in membrane trafficking as they recognize cargo and link it to nascent coats. Other proteins can associate with them as well, altering or extending the

function of a cargo adaptor in unexpected ways. Therefore, to completely understand a cargo adaptor and the roles its dysfunction may play in diseases, these associated factors must be identified and characterized. Fortunately, many new membrane-associated protein-protein interactions have recently been identified by a proteomics study employing a mass spectrometry based approach, modified with the use of various detergents in the preparations (Chapter 2). The central hypothesis of this study is that novel interactors of known cargo adaptors have functions associated with cargo selection. To this end, two sets of novel interactions involving known cargo adaptors were verified and characterized.

The first set involved the interaction of Ssp120 with the cargo receptor complex Emp46/47 (Chapter 2). Emp46 and Emp47 form a multimeric protein complex involved in recognizing a subset of COPII cargo and adapting it to the coat for ER to Golgi transport (Sato and Nakano, 2002, 2003). The experiments described in chapter two test our hypothesis that Ssp120 is a core component of this trafficking complex and that it plays a role in cargo selection.

The second set of interactions studied is that of the Rab5-family guanine nucleotide exchange factor (GEF) Muk1 with subunits of retromer (Chapter 3). Muk1 is one of two known yeast GEFs that activate Rab5-family GTPases, which are involved in recruiting proteins that define the endosomal compartment. This link to an endosomal membrane modifying protein led us to hypothesize that the interaction plays a role in retromer recruitment. Experiments outlined in chapter three confirm the interaction and suggest a role for retromer-GEF interactions. Together, chapters two and three provide insights into cargo adaptor function through the study of associated factors.

Chapter 2: Interaction landscape of membrane-protein complexes in

*Saccharomyces cerevisiae*¹

2.1 Synopsis

This chapter describes the identification of membrane-associated complexes through a mass spectrometry-based approach and the characterization of the novel interactions of two proteins with different cargo adaptors. As the functions of many proteins can be understood through their interactions, a fundamental goal of biology is to identify the protein interactome. Determining the interactions of membrane-associated proteins by mass spectrometry is particularly challenging, as the membranes must be solubilized. Here, we engaged in a collaborative study to address this by using various detergents in sample preparations, which resulted in the identification of 501 putative membrane-associated complexes. A subset of these were subsequently characterized in detail.

Several putative complexes contained the proteins of a known cargo adaptor with at least one novel interactor. We pursued these interactors as an opportunity to further understand cargo adaptor function. First, an interaction between AP-1 and the uncharacterized protein Irc6 was demonstrated by co-immunoprecipitation and yeast two hybrid experiments. Irc6 was found to be required for normal trafficking of some AP-1 cargo suggesting a functional role in the complex. The second cluster studied in this chapter contained the uncharacterized Ssp120 with

¹ A version of chapter 2 has been published. Babu M, Vlasblom J, Pu S, Guo X, Graham C, Bean BDM, Burston HE, Vizeacoumar FJ, Snider J, Phanse S *et al.* (2012). Interaction landscape of membrane-protein complexes in *Saccharomyces cerevisiae*. *Nature* 489, 585–589

Emp46/Emp47. Emp46/Emp47 act as a cargo selective adaptor for the COPII coat. Our experiments show that Ssp120 is a stable component of the complex and suggest that it may interact with a subset of Emp46/Emp47 cargo, similar to a mammalian homolog. Collectively, this work successfully identifies many putative membrane-associated complexes and focuses on a subset of these to validate the complexes and gain insight into cargo adaptor function.

2.2 Results and discussion

Macromolecular assemblies involving membrane proteins (MPs) serve vital biological roles and are prime drug targets in a variety of diseases (Bao *et al.*, 2009). Large-scale affinity purification studies of soluble-protein complexes have been accomplished for diverse model organisms, but no global characterization of MP-complex membership has been described so far. Various experimental methods have been used to examine protein–protein interactions (PPIs) among MPs (Miller *et al.*, 2005; Tarassov *et al.*, 2008; Costanzo *et al.*, 2010), but integral and lipid-anchored MPs are still notably under-represented in public interaction databases (Turner *et al.*, 2010). In contrast to the success of tandem affinity purification (TAP) procedures for characterizing soluble-protein complexes in yeast (Gavin *et al.*, 2006; Krogan *et al.*, 2006), native MP complexes are more difficult to purify owing to their hydrophobic nature (Bao *et al.*, 2009). Therefore, alternative TAP extraction and affinity isolation procedures were developed, using buffers containing one of three different mild, non-denaturing detergents optimized for MP solubilization. Based on pilot studies, Triton X-100, DDM (n-dodecyl- b-D-maltopyranoside), and C12E8 (octaethylene glycol monododecyl ether) were selected, as these were most effective and extracted complementary sets of yeast MPs (Appendix A Figure 1A–C and Text). For proteome-wide analysis, yeast strains bearing MP fusions with a carboxy-terminal chromosomal

TAP tag expressed at endogenous levels from native promoters were used (Ghaemmaghami *et al.*, 2003). The tagged MPs and stably associated proteins were purified essentially as described previously (Babu *et al.*, 2009), except that all steps were carried out in the presence of one of the three detergents.

Based on existing database annotations, transmembrane helix (TMH) predictions, subcellular localization, literature curation and other information sources (Appendix A Figure 1D and Table 1), a target list was compiled that encompassed 2,141 annotated or predicted MPs (Figure 2.1A and Appendix A Table 2), of which 1,590 were tagged and processed (Appendix A Figure 2A). These included 1,144 putative integral, 400 peripheral and 46 lipid-anchored MPs. Detection coverage ranged from approximately 81% for low abundance MPs ($<10^3$ molecules per cell) to approximately 94% for high abundance proteins ($>10^4$ molecules per cell) (Appendix A Figure 2B) (Ghaemmaghami *et al.*, 2003). No attempt was made to purify 551 open reading frames (ORFs) because they were not detectably expressed (Ghaemmaghami *et al.*, 2003) or the growth of the tagged strains was impaired (Appendix A Table 2), although a substantial fraction (~66%; 362 of 551) were subsequently detected as interacting ‘preys’ in successful bait purifications.

The overall target recovery rates were comparable for each detergent (~50%), and 77% (1,228 out of 1,590) of the tagged MPs were successfully purified (Figure 2.1B). In addition to bait abundance, success varied based on the cellular compartment (Figure 2.1C) and TMH number of each MP (Figure 2.1D). The highest coverage was obtained for those MPs associated with the Golgi, endoplasmic reticulum or mitochondria with fewer than four TMH (~80%), whereas MPs associated with the bud neck or possessing ≥ 10 TMH had lower success (~70%). Nevertheless,

we were successful in purifying baits harbouring characteristic membrane-associated Pfam domains such as the ABC transporter, SNARE (soluble NSF attachment protein receptor) and PX domains (>90% success; Appendix A Figure 2C and Table 3).

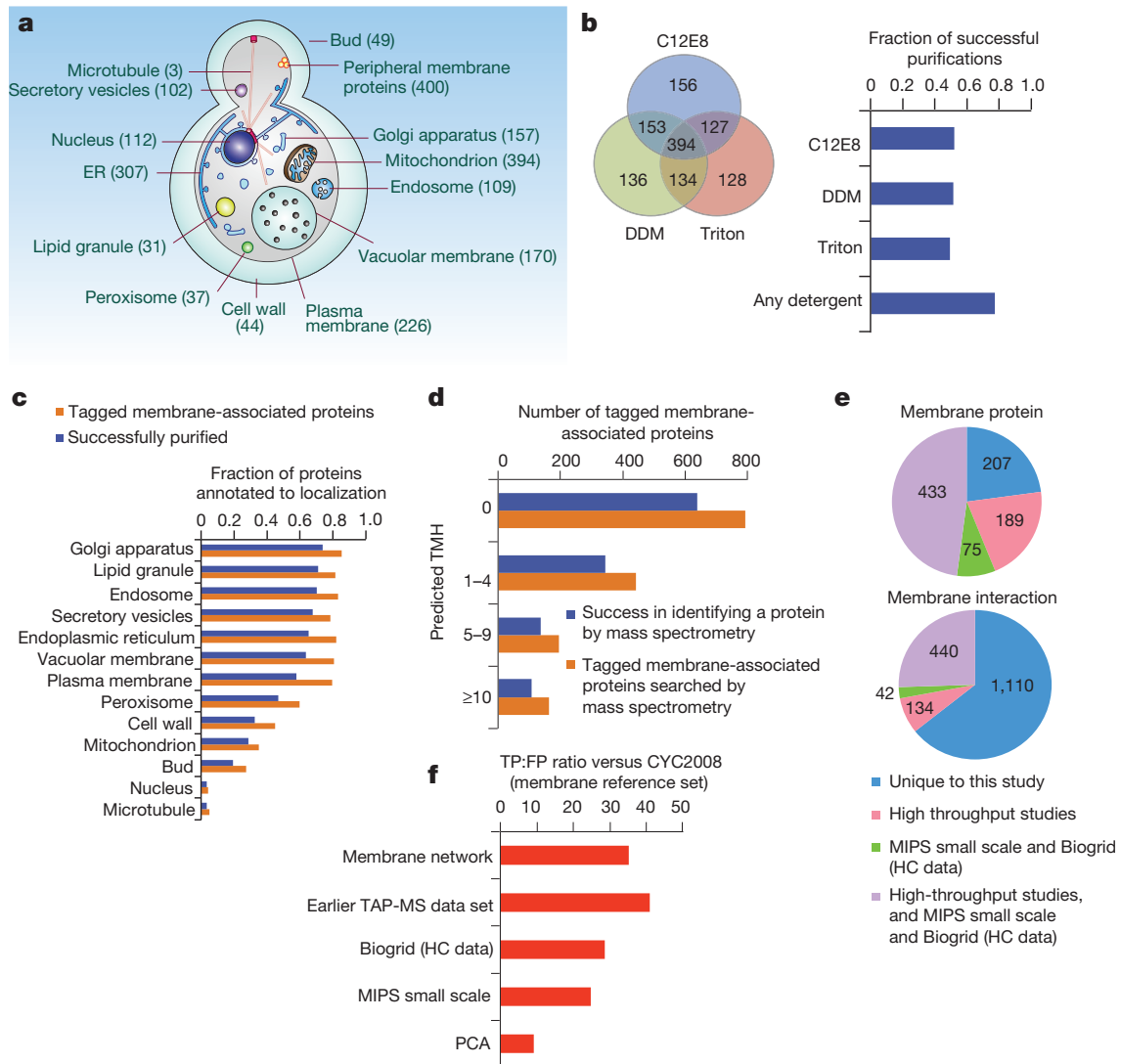


Figure 2.1 Proteome-wide purification of yeast MPs.

(A) Yeast membrane compartments. Numbers indicate annotated or predicted MPs (listed in Appendix A Table 2). (B) Overlap of tagged bait proteins identified by mass spectrometry after purification in three

different detergents (left panel), and the proportion of successful bait recovery (right panel). (C) Fraction of tagged and successfully purified MPs according to simplified Gene Ontology consortium cellular-component annotations. (D) Number of tagged and purified yeast MPs according to TMH number. (E) Overlap of MPs (top panel) and their interactions (bottom panel) in the MP sub-network, compared to previous high-throughput studies (Miller *et al.*, 2005; Pu *et al.*, 2007; Tarassov *et al.*, 2008; Yu *et al.*, 2008) and high-confidence (HC) literature PPI from the MIPS (Munich Information Center for Protein Sequences) and BioGRID (Biological General Repository for Interaction Datasets) databases (Mewes *et al.*, 2006; Reguly *et al.*, 2006). (F) Average true positive:false positive (TP:FP) ratio of this study (MP sub-network) versus an earlier TAP-MS-derived soluble yeast protein data set (Pu *et al.*, 2007), literature curated interactions (Mewes *et al.*, 2006; Reguly *et al.*, 2006), and a PCA yeast interactome study (Tarassov *et al.*, 2008), as measured against a random reference membrane PPI set (CYC2008 complex catalogue) (Pu *et al.*, 2009). Note that the actual TP:FP ratio depends on the definition of the reference set and is given here only to compare data sets. ER, endoplasmic reticulum.

To assign confidence scores, the observed physical associations, including non-MPs, were first ranked using the purification enrichment score (Collins *et al.*, 2007b), and then integrated with purification enrichment scores computed from published yeast TAP mass spectrometry (TAP-MS) surveys of soluble proteins (Gavin *et al.*, 2006; Krogan *et al.*, 2006) to describe the cytoplasmic interface of membrane systems better. To optimize accuracy and coverage (Appendix A Text), a high-confidence ‘integrated network’ was built with the same precision (that is, a reference benchmark true positive to false positive ratio of approximately 22:1) as that of a highly accurate yeast soluble-protein interaction map (Appendix A Figure 2A) (Pu *et al.*, 2009).

The integrated network consists of 13,343 high-confidence associations among 2,875 proteins (Appendix A Table 4), representing two-thirds of the yeast proteome detectable by mass spectrometry (de Godoy *et al.*, 2008). Notably, 6,082 of these PPIs are directly supported by the purification data described here and, for 1,726 PPIs involving at least one of 905 putative MPs (Appendix A Table 4), two-thirds (64%; 1,110 out of 1,726) have not been reported previously (Figure 2.1E and Appendix A Figure 2D). For example, putative binding partners for 20 plasma membrane proteins with previously unreported interactions were identified, including orthologues (Ostlund *et al.*, 2010) of 8 human therapeutic targets (Appendix A Table 5).

On average, the MPs have approximately half the number of identified interaction partners as yeast soluble proteins (geometric mean ~ 2.1 versus ~ 4.7 ; Appendix A Figure 2E, F), possibly owing in part to partial detergent-induced dissociation. As with soluble proteins (Krogan *et al.*, 2006), essential, highly expressed and evolutionarily conserved MPs exhibit greater connectivity (Appendix A Figure 2G, H), particularly components of the bud, cortex and Golgi (mean connectivity of ≥ 2.8).

Independent criteria support the reliability of the integrated and MP interaction networks, and the quality of the underpinning data. First, benchmarking against a reference set of PPIs derived from MPs in the CYC2008 catalogue of manually curated protein complexes (Pu *et al.*, 2009) showed that the accuracy of the MP interactions was comparable to, or higher than, published small-scale experiments (Mewes *et al.*, 2006; Reguly *et al.*, 2006), protein-fragment complementation assay (PCA) (Tarassov *et al.*, 2008) and large-scale yeast PPI networks derived for soluble proteins in past TAP surveys (Gavin *et al.*, 2006; Krogan *et al.*, 2006) (Fig. 2.1F).

Second, we observed significant enrichment ($P < 0.05$) for interactions between MPs in the same, or related, subcellular compartments (Appendix A Figure 3A and Table 6). Third, the average semantic similarity of the Gene Ontology consortium annotations of the interacting proteins in the MP network (Appendix A Figure 3B) was comparable to or higher than that obtained for several previous high-confidence PPI networks (Miller *et al.*, 2005; Tarassov *et al.*, 2008; Yu *et al.*, 2008), although slightly lower than that obtained for soluble protein TAP (Pu *et al.*, 2007) or literature curation (Mewes *et al.*, 2006; Reguly *et al.*, 2006), probably reflecting the less complete annotations of MPs in general. Finally, the integrated network was compared with genetic interaction data derived for yeast membrane (Schuldiner *et al.*, 2005; Aguilar *et al.*, 2010) and non-membrane (Collins *et al.*, 2007a; Costanzo *et al.*, 2010) biological systems (Appendix A Text). Highly correlated genetic interaction profiles between pairs of physically interacting proteins were significantly enriched ($P < 10^{-9}$) compared to random pairs (Appendix A Figure 3C). Collectively, these results suggest that our high-confidence PPI are of similarly high quality as the most reliable soluble yeast interactome data sets published so far (Gavin *et al.*, 2006; Krogan *et al.*, 2006; Collins *et al.*, 2007b; Pu *et al.*, 2007).

To deduce the membership of MP complexes, the Markov clustering algorithm (Enright *et al.*, 2002) was used to partition the integrated network into densely connected subgroups of interacting proteins, allowing for component sharing between clusters (Pu *et al.*, 2007) (Appendix A Text). In total, 720 clusters representing putative multi-protein complexes were identified (Appendix A Table 7 and Figure 3D), of which most (501) contain at least one MP (Figure 2.2 and Appendix A Table 7). Many (99) of the 264 predicted heterodimeric MP-containing complexes consisted of only uncharacterized proteins or one uncharacterized factor

with an annotated MP (Appendix A Table 7), which most commonly contained Pfam domains related to the cell wall or intracellular signaling (Appendix A Table 8).

Overlap between these clusters and the CYC2008 complex catalogue showed that of the curated yeast complexes containing an MP, 40% (67 out of 167) had 90% or more subunits matching a cluster, whereas only approximately 7% (12 out of 167) of known MP complexes were missed in this study, presumably indicating limitations of our isolation procedures (Appendix A Figure 3E). Conversely, 280 of the predicted MP clusters had limited overlap (<5% of the components) with CYC2008 complexes (Appendix A Figure 3F), representing a rich resource for biological discovery. Unexpected connections were uncovered that suggest new roles even for well-characterized MPs, such as the association between Tor2 and Vps8 (Appendix A Figure 4J) that may mediate TOR signaling at endosomes (Flinn and Backer, 2010). Likewise, this study provides additional support for proteasome engagement with organelles through the membrane fusion factor Sec18 (Appendix A Text and Figure 5A–C).

Independently, 21 interactions involving MP components were evaluated by co-immunoprecipitation and/or iMYTH (Paumi *et al.*, 2007) (integrated membrane yeast two-hybrid) assays and confirmed >90% (19 out of 21) (Figure 2.2 and Appendix A Figure 4A–K). These included the validation of an interaction between the PIR (proteins with internal repeat) domain-containing envelope proteins Pir3 and Pir4 (Appendix A Figure 4I), and the association of Sct1, an integral membrane acyltransferase involved in glycerolipid biosynthesis, with the uncharacterized integral MP Ypr091c, which localizes to the endoplasmic reticulum (Appendix A Figure 4H).

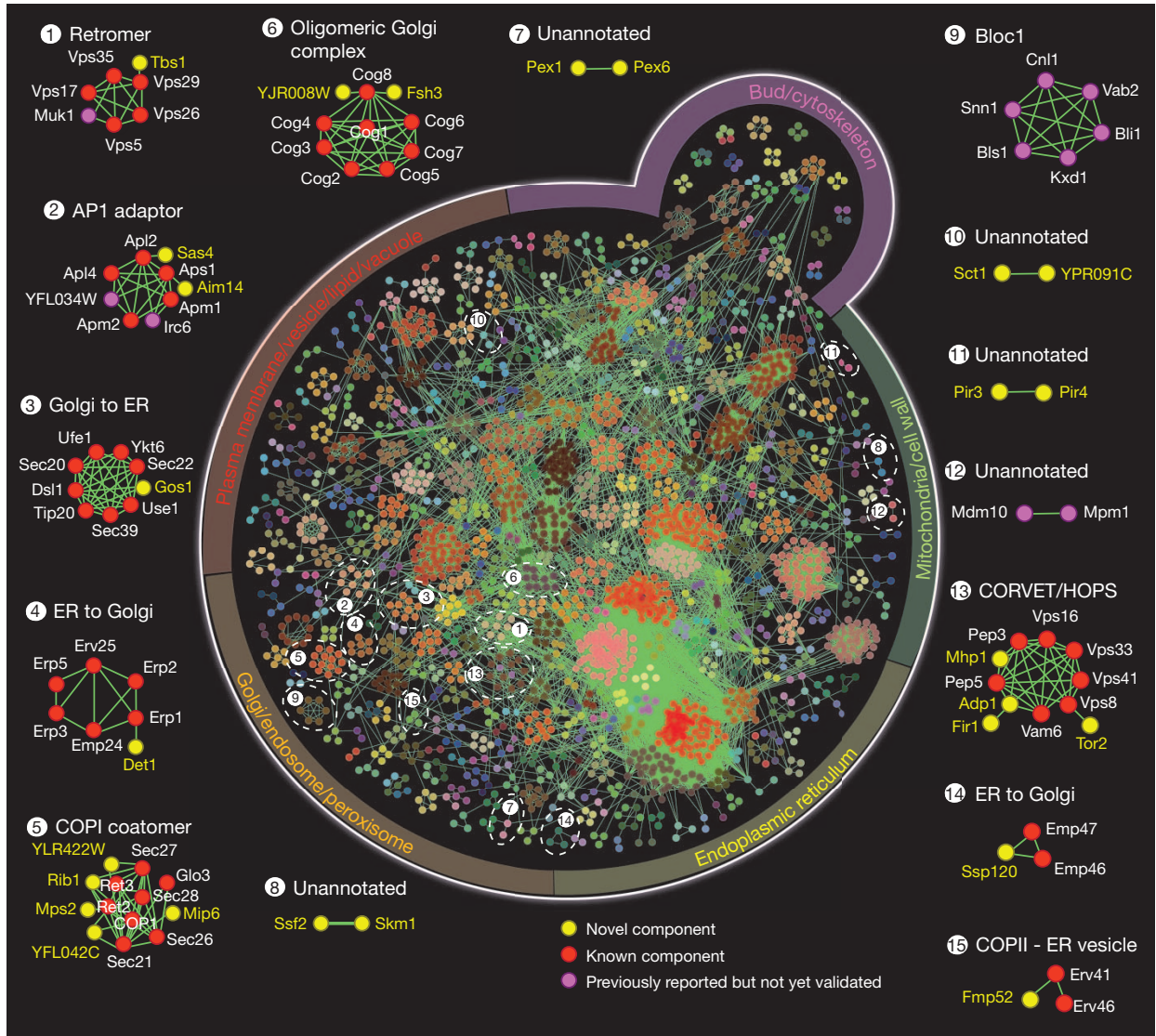


Figure 2.2 Global organization of yeast MP complexes

Global organization of yeast MP complexes. Predicted MP clusters (subunits shown as similarly coloured nodes) inferred from the integrated network of high-confidence PPI (edges), demarcated according to primary compartment annotations. Representative complexes at the periphery highlight some of the findings of this study, including novel complexes and known complexes with new components. Purifications were most successful for MPs localized to the Golgi and endoplasmic reticulum, a bias reflected in the highlighted examples. For each complex, previously reported components (red nodes), novel subunits (yellow nodes) and previously reported but not yet validated interactors (pink nodes) are displayed.

As subunits of the same complex typically have a common biological role, high-content fluorescence screening of mutant strains was used to systematically investigate the phenotypic consequences of deleting individual components of 26 different MP complexes (Appendix A Fig. 6A and Table 9). Based on the patterns of compartment-specific fluorescent markers, subunit loss typically resulted in a discernible and consistent phenotype for most (20 out of 26) of the predicted complexes tested (representative data shown in Appendix A Figure 6; see Appendix A Table 9 and Text).

The association of 321 functionally uncharacterized proteins with putative MP complexes provides insight into their possible cellular roles (Appendix A Table 10), demonstrated by the identification of Irc6 as a binding partner of the heterotetrameric AP1 clathrin adaptor complex (Figure 2.3A). AP1 is peripherally associated with Golgi and endosomal membranes, where it incorporates cargo proteins like Sna2 and chitin synthase Chs3 into clathrin-coated vesicles (Renard *et al.*, 2010). As with loss of the AP1 subunit Apm1, we found that loss of Irc6 increased cell-surface missorting of Chs3 and Sna2 (Figure 2.3B–E). Irc6 is homologous to mammalian p34, which associates with soluble AP1 adaptors in human cells but has not been characterized in detail (Page *et al.*, 1999). Consistent with this, an Irc6–GFP (green fluorescent protein) fusion localizes to the cytosol (data not shown) and shows sub-stoichiometric binding to AP1 by co-immunoprecipitation (Figure 2.3F). Although many AP1 regulators recognize the c-adaptin (Apl4) ear (appendage) domain, yeast two-hybrid assays indicated that Irc6 interacts with the core domain of Apl4 and with a subunit of the AP2 complex (Figure 2.3G), suggesting a wider role in regulating clathrin adaptors. Interestingly, the amino-terminal conserved domain of Irc6 (Figure 2.3H), which is necessary and sufficient for the interaction with AP1 (Figure 2.3I),

has a predicted fold similar to that of regulatory Rab-like GTPases (Pieper *et al.*, 2011). These data suggest Irc6 is a conserved, functionally important AP1 interacting protein.

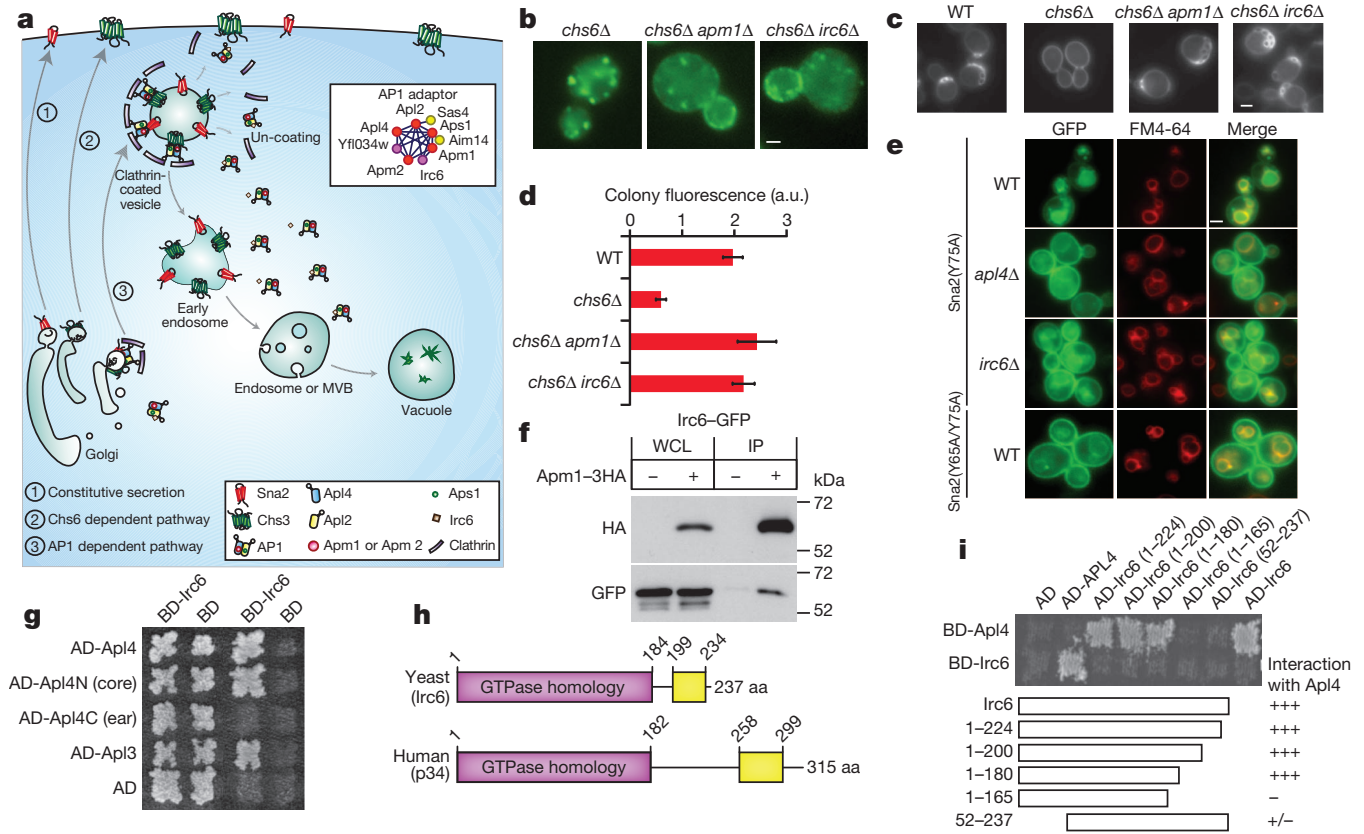


Figure 2.3 Functional association of Irc6 with AP1

(A) Model illustrating AP1 dependent incorporation of Chs3 and Sna2 into clathrin-coated vesicles at Golgi and endosomal compartments. Inset indicates subunit associations of the AP1 complex. MVB, multivesicular body. (B) Fluorescence microscopy of Chs3–GFP. Mutation of AP1 (Apm1) or Irc6 restores Chs3–GFP cell-surface delivery in *chs6* mutants (see Methods). (C) Loss of AP1 or Irc6 in *chs6* mutants restores Chs3-dependent chitin ring formation as detected by calcofluor white. (D) Quantification of chitin production. The graph shows the average colony fluorescence (arbitrary units, a.u.) ± s.d. of at least six replicates. (E) A Sna2(Y75A)–GFP mutant lacking an AP3 sorting motif mislocalizes to the cell surface in strains lacking AP1 (Apl2) or Irc6, similar to a Sna2(Y65A/Y75A)–GFP mutant lacking both AP1 and AP3 motifs. (F)

Immunoblot analyses of epitope-tagged proteins in whole-cell lysates (WCL) and anti-haemagglutinin (HA) immunoprecipitates (IP). Molecular masses are indicated on the right. (G) Two-hybrid assay of the indicated Gal4-activation domain (AD) and DNA-binding domain (BD) fusion proteins; cells were grown on medium containing histidine (left panel) or tested for activation of a HIS3 reporter on medium lacking histidine (right panel). (H) Sequence conservation between Irc6 and human p34. (I) Two-hybrid analysis of interactions between AP1 subunit Apl4 and truncated forms of Irc6. aa, amino acid; WT, wild type.

A second example is the interaction of the uncharacterized protein Ssp120 with the annotated MPs Emp46 and Emp47, which facilitate secretion by sorting cargo proteins into endoplasmic-reticulum-derived COPII-coated vesicles (Sato and Nakano, 2002) (Figure 2.4A). Ssp120 lacks a transmembrane domain but contains a signal sequence mediating endoplasmic reticulum translocation (Sidhu *et al.*, 1991) and, like Emp47, localizes to early Golgi in wild-type yeast (Huh *et al.*, 2003). Ssp120 is missorted to the vacuole in *emp47* (but not *emp46*) mutants (Figure 2.4B) and is secreted after additional deletion of *VPS10*, a receptor that carries luminal cargos from the late Golgi to the endosome and vacuole (Figure 2.4C). Ssp120 has a domain structure similar to human MCFD2 (Figure 2.4D), which binds the mammalian Emp46 and Emp47 homologue LMAN1 and is a cargo-specific adaptor for secretion of the blood coagulation factors V and VIII. Mutations in LMAN1 or MCFD2 cause the bleeding disorder F5F8D, or combined factor V and factor VIII deficiency (Zhang, 2009). Intriguingly, the C-terminal region but not the EF-hand motifs of Ssp120 (Fig. 2.4D) are important both for Golgi localization (Figure 2.4E) and interaction with Emp47 (Figure 2.4F). Consistent with a shared role, both *ssp120* and *emp47* single mutants show calcium-sensitive growth, whereas *ssp120 emp47* double mutants do not display increased sensitivity (Figure 2.4G) (Sato and Nakano, 2002). Consistent with a conserved role for Ssp120 as a cargo-specific adaptor, Emp47 retained its ability to escort

Emp46 from the endoplasmic reticulum in *ssp120* mutants (Figure 4H). Further elucidation of this and other novel predicted interactions should yield mechanistic insights into membrane system function, many of which are likely to be conserved.

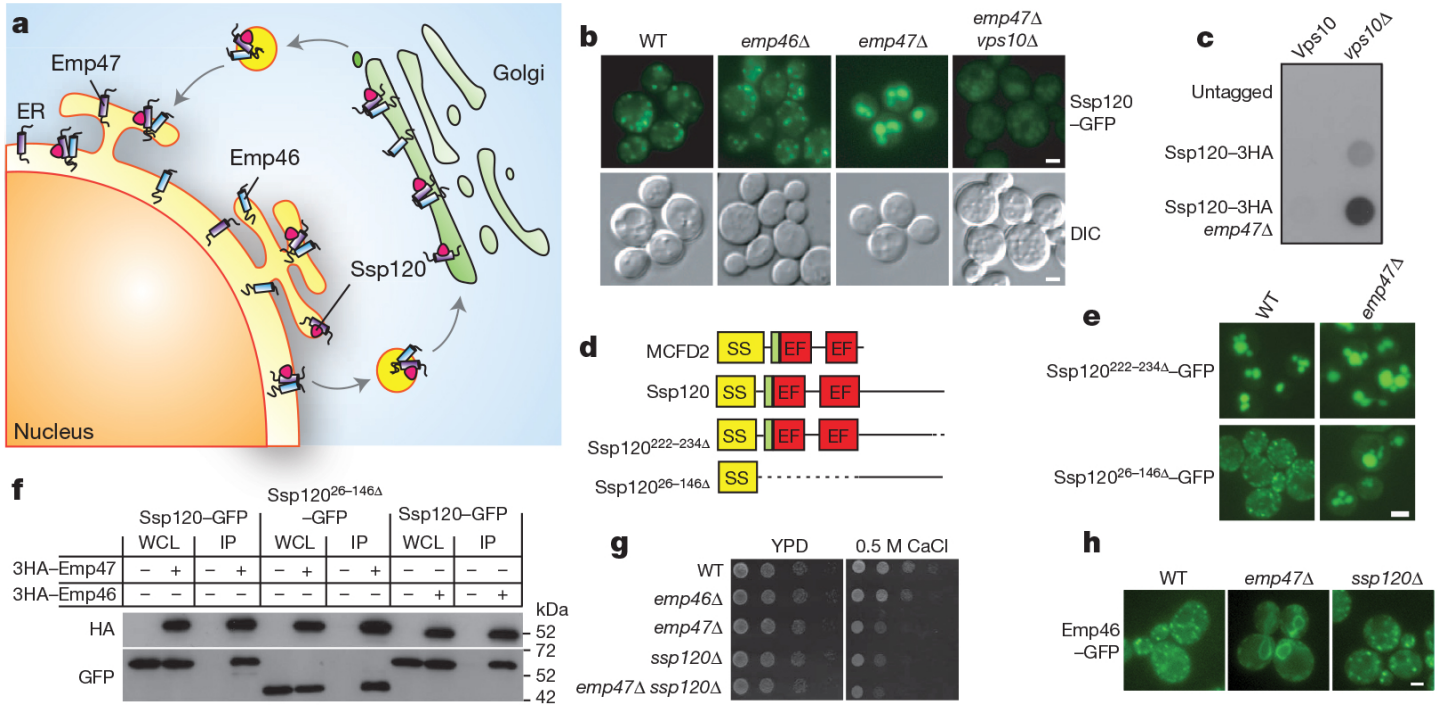


Figure 2.4 Ssp120 participates in Golgi to ER recycling

(A) Model showing recycling of the Emp46–Emp47–Ssp120 complex between endoplasmic reticulum and early Golgi. (B) Fluorescence microscopy of GFP-tagged Ssp120 in wild-type and mutant strains. DIC, differential interference contrast. (C) Immunoblot showing secretion of tagged Ssp120 constructs from indicated strains. (D) Domain organization of human MCFD2 and yeast Ssp120 constructs. Signal sequences (SS) and EF-hand domains highlighted; green boxes indicate additional homology, dotted lines mark deleted regions. (E) Localization of Ssp120–GFP constructs in wild-type cells and *emp47* mutants. (F) Immunoblot analyses of epitope-tagged proteins in whole cell lysates (WCL) and anti-HA immunoprecipitates (IP). (G) Strain growth on YPD media containing 0.5 M CaCl₂. (H) Fluorescence microscopy of GFP-tagged Emp46 in wild-type and mutant strains. Scale bars, 2 μm.

To investigate the broader evolutionary conservation of MP complexes, homology relationships across 71 sequenced eukaryotic genomes were mapped using InParanoid and Compara (Appendix A Table 11). Among our 501 MP-containing complexes, one-third (132) of the constituent proteins were present among >90% of organisms considered, whereas <10% (48) were restricted to fungi (Appendix A Table 12). Most MP complexes had at least half of their subunits conserved in worm (363), fly (374) and/or human (389) (Appendix A Figure 7A), including 90 complexes whose components were fully conserved (Appendix A Figure 7B).

The MP interactions reported here reveal the global modular architecture of the membrane systems of a model eukaryote. A key element was the parallel purification of endogenous MP complexes in the presence of three different detergents. Although TAP-MS offers exceptional coverage and accuracy, this approach has potential caveats. The affinity tag may interfere with protein localization or interactions, transient associations may be lost and the detergents may disrupt associations, potentially contributing to the smaller average size of MP complexes compared to non-membrane assemblies. The data presented here may also be impacted by missing, incomplete or conflicting information on functional annotations, genome sequences and subcellular localization information (Appendix A Figure 1D), as well as the occurrence of spurious interactions. Nevertheless, the rate of false positive PPIs in the integrated network, as estimated from the reference benchmark precision (true positive:false positive ratio of 22:1), is just 4.3% (corresponding to 573 non-specific interactions), comparable to that for previous TAP studies of the soluble yeast interactome (Gavin *et al.*, 2006; Krogan *et al.*, 2006).

Although limitations exist, the systematic elaboration of a high-confidence MP interactome provides many opportunities for functional inference. The results of this study identify associations between un-annotated yeast MPs and functionally cohesive complexes involved in diverse biological processes. The conservation of many of these complexes provides insights into the membrane biology of eukaryotes, including humans. Just as genetic studies in yeast have led to the characterization of conserved human disease pathways, the network of MP complexes reported here predicts orthologous relationships that may be relevant to human disorders.

All of the experimental data, interactions and predicted complexes of this study are publicly accessible through a dedicated database (<http://wodaklab.org/membrane/>), complementing previous maps of the yeast soluble proteome as valuable community resources.

2.3 Methods

2.3.1 Yeast strains, media and plasmids

The yeast strains and plasmids used in this study are listed in Appendix A Table 13. For the large-scale purifications, the yeast strains were obtained from the Yeast-TAP-fusion library deposited in Open Biosystems (Ghaemmaghami *et al.*, 2003). Standard rich (YPD), synthetic medium plus dextrose lacking histidine, and synthetic complete medium containing 2% glucose as a carbon source were used for cell growth. Standard methods were used for the introduction of DNA into yeast (Gutsche, 1991).

2.3.2 Tandem affinity purification and mass spectrometry

Each tagged protein was purified from 4L yeast cultures grown in rich media (YPD) under native conditions and prepared for mass spectrometry essentially as described previously (Babu *et al.*, 2009), except with some modifications of our standard procedures. With the addition of non-ionic detergents to our buffers, the majority of the yeast MPs could be solubilized and purified. For most of the MPs, three purifications were carried out in parallel using three different non-ionic detergents, and two complementary mass-spectrometry techniques, MALDI–TOF (matrix assisted laser desorption/ionization time-of-flight) mass spectrometry and tandem LC–MS (liquid chromatography–electrospray ionization–mass spectrometry), were used to detect physically interacting proteins.

These detergents not only have different abilities to solubilize affinity-tagged proteins (Appendix A Text) but may differ in the extent to which they disrupt PPI. The detergents were removed from the purified protein samples before mass-spectrometric identification of co-purifying polypeptides using tandem LC–MS instruments that are more sensitive than those used previously to characterize soluble yeast protein complexes (Krogan *et al.*, 2006). Gel images and confidence scores for protein identification by MALDI-TOF MS are made available in the database (<http://wodaklab.org/membrane/>). Confidence scores for protein identification by MALDI–TOF and tandem LC–MS were calculated essentially as described previously (Babu *et al.*, 2009). A tagged protein is considered successfully purified if either it or an annotated or putative MP with ≥ 2 TMH is identified by mass spectrometry (probability score $\geq 90\%$ for tandem LC–MS; Z score ≥ 1 for MALDI–TOF mass spectrometry). Details on the derivation of the PPI network and prediction of protein complexes are described in Appendix A Text.

2.3.3 Detergents

The following eleven detergents were used at a final concentration of 1% in the affinity purification of the initial test set of yeast MPs: Triton X-100, DDM (n-dodecyl-β-D-maltopyranoside), C12E8 (octaethylene glycol monododecyl ether), LDAO (lauryldimethylamine-oxide), CHAPS, (3-[(3-cholamidopropyl) dimethylammonio]-1-propanesulfonate), OG (octaethylene glycol monododecyl ether), DM (n-dodecyl-β-D-maltoside CHAPSO (3-[(3-cholamidopropyl) dimethylammonio]-2-hydroxy-1-propanesulfonate), FC-12 (fos-choline-12), Nonidet P-40 (NP-40) and deoxycholate.

2.3.4 Colony overlay

The immunoblotting assay for secretion of haemagglutinin- tagged proteins was carried out essentially as described previously (Conibear and Stevens, 2002) with antisera against haemagglutinin.

2.3.5 Fluorescence microscopy

The plasmids encoding fluorescent markers for actin, spindle and mitochondria (Appendix A Table 13) were constructed essentially as described previously (Li *et al.*, 2011). The endoplasmic reticulum fluorescent plasmid, pScs2-RFP, was a gift from T. Levine. The Golgi Sec7-RFP fluorescent plasmid was constructed using a SEC7 gene from the MORF (moveable ORF) library (Gelperin *et al.*, 2005) through the Gateway recombineering system. For the morphological study, each compartment-specific fluorescent plasmid was transformed into the Y7072 MATa can1D::STE2pr-spHIS5 lyp1D; his3D1 leu2D0 ura3D0 met15D0 LYS21 strain

background. The resulting query strain with the expressed fluorescent plasmid was then mated to an array of MATa mutant strains through synthetic genetic array (SGA) technology (Costanzo *et al.*, 2010). After the subsequent standard SGA selections (Costanzo *et al.*, 2010), the mutants containing compartment-specific markers were visualized using high-content confocal fluorescent microscopy.

For vacuolar staining, cells were pulsed with 32 mM of endocytic dye FM4-64 (Life Technologies) for 20 min in the dark at 30 °C, after which cells were resuspended in YPD and incubated for 30 min at 30 °C. Cells were subsequently washed twice in phosphate buffered saline (PBS) before visualization. When required, images were captured using a spinning disc confocal system (WaveFX; Quorum) with an ultra-cooled 512 back-tinned electron-multiplying charge-coupled device camera, or a microscope (E-600FN; Nikon) with an OrcaII camera (Hamamatsu). Alternatively, in Figures 2.3 and 2.4 strains expressing GFP fusion proteins were viewed using an Axioplan 2 fluorescence microscope (Carl Zeiss). Images were captured with a CoolSNAP camera (Roper Scientific) using MetaMorph software (Molecular Devices) and adjusted using Adobe Photoshop (Adobe Systems).

2.3.6 Immunoprecipitation

The endogenously non-overproduced TAP-tagged proteins expressed in BY4741 by targeted homologous recombination (Babu *et al.*, 2009) were confirmed by western blot analysis using anti-TAP antibody that recognizes the protein A epitope of the TAP tag. TAP-tagged strains were transformed with plasmids expressing a galactose inducible overproduced haemagglutinin-tagged full-length protein. The transformants were selected on synthetic-defined media lacking

uracil. These strains were grown at 30 °C in synthetic-defined media lacking uracil with 2% sucrose as a carbon source. The cells were then sub-cultured and induced for 4 h at 30 °C in yeast peptone medium with 2% galactose. The cells were pelleted by centrifugation at 1,900g for 20 min and then resuspended in lysis buffer essentially as described previously (Babu *et al.*, 2009). The lysed yeast cells were incubated for 3 h in the presence of 1% Triton X-100 at 4 °C with immunoglobulin G (IgG) Sepharose 6 Fast Flow beads. The immunoprecipitation procedure was then carried out essentially as described previously (Babu *et al.*, 2009), except that in each purification step we added 1% Triton X-100. Alternatively, for the immunoprecipitation experiments in Figures 2.3 and 2.4, cell extracts were prepared from spheroplasts resuspended in lysis buffers (50 mM Tris-Cl pH 8.0; 50 mM NaCl; 0.1% Triton X-100; 1mM DTT (dithiothreitol) and 1/100 EDTA-free protease inhibitor (Thermo) (Figure 2.3); as well as 50mM HEPES pH7.9, 150mM KCl, 1% Triton X-100, 1 mM DTT and 1/100 EDTA-free protease inhibitor (Thermo) (Figure 2.4) and incubated with rabbit anti-HA.11 (Santa Cruz) and protein A Sepharose beads. Western blot analysis of immunoprecipitated proteins was carried out using mouse anti-GFP (Roche) and mouse anti-HA.11 monoclonal antibodies (Covance).

In the case of co-immunoprecipitation with untagged proteins, the standard protocol was adapted with protein A resins (Pierce). The mouse Pre4 and rabbit Rpt1 polyclonal antibodies were obtained from Abcam, and the Sec18 rabbit polyclonal antibody was a gift from C. Ungermann.

2.3.7 Evaluation of Chs3 and Sna2 sorting

Assays to measure the function of the AP1 pathway were based on the localization of AP1 cargo proteins Sna2 and Chs3. Sna2–GFP is sorted to the vacuole by the binding of either AP1 or AP3

adaptors to distinct Sna2 motifs (Renard *et al.*, 2010). The Sna2(Y75A)–GFP mutant, which lacks the AP3 motif, depends on AP1 for its vacuolar targeting and is mis-sorted to the cell surface in strains lacking AP1, similar to a Sna2 mutant (Sna2(Y65A/Y75A)–GFP) lacking both AP1 and AP3 motifs, thus providing a visual indication of AP1 function.

The chitin synthase Chs3, which requires Chs6 for transport to the cell surface, is retained in the cell by the AP1-dependent recycling pathway in *chs6* mutants (Valdivia and Schekman, 2003), preventing chitin ring formation. Disruption of the AP1 complex restores Chs3 cell surface delivery through a bypass pathway and restores chitin ring formation in *chs6* mutants. Thus, chitin levels in *chs6* mutants provide a quantitative measure of AP1 function. Chitin levels were quantified by measuring the fluorescence of colonies grown on YPD plates containing 50 mg/ml (Enright *et al.*, 2002) calcofluor white at 30 °C for 3 days. Fluorescent-light images were captured with a Fluor S Max MultiImager (Bio-Rad Laboratories) using the 530DF60 filter and Quantity One software (version 4.2.1; Bio-Rad Laboratories), and image densitometry was performed as described previously (Lam *et al.*, 2006). Alternatively, chitin rings were visualized by fluorescence microscopy of cells fixed with 3.7% formaldehyde, incubated in 100 mg/ml calcofluor white in 0.5 M Tris pH 9.6 for 30 min at 30 °C, and washed twice before analysis (Enright *et al.*, 2002).

2.3.8 Yeast two-hybrid analysis

All plasmids for yeast two-hybrid analysis were generated by homologous recombination in pGAD-C2 and pGBDUC-2, essentially as described previously (James *et al.*, 1996). Haploid strains expressing GAL4-AD fusion proteins were mated with strains expressing GAL4-BD

fusion proteins. Diploid cells were tested for activation of the HIS3 reporter by growth on selective media lacking histidine.

2.3.9 iMYTH assay

SCT1 prey generation in the pPR3N vector, endogenous tagging of YPR091C with the Cub-LexA-VP16 MYTH tag and subsequent iMYTH screening were carried out as previously described (Snider *et al.*, 2010). In brief, bait and artificial bait expressing variants of the *Saccharomyces cerevisiae* NMY51 or L40 MYTH reporter strains were generated and transformed with prey plasmid expressing either control construct or NubG-SCT1p construct. Control plasmids, expressing NubI-tagged ('positive') and NubG-tagged ('negative') forms of the unrelated, plasma membrane-localized Fur4 uracil permease, were obtained from Dualsystems Biotech (<http://www.dsbiotech.ch/>). Transformed cells were picked from solid media, diluted into 150 ml of sterile ddH₂O and spotted directly onto selective media. Plates were grown at 30 °C for 3–6 days and growth was scored.

Chapter 3: Rab5-family guanine nucleotide exchange factors bind retromer and promote its recruitment to endosomes²

3.1 Synopsis

This chapter explores another set of interactions identified by the proteomics study in chapter two, that of retromer with the Rab5-family GEF Muk1. As active Rab5-family GTPases help define the early endosomal membrane, we hypothesized the interaction may recruit retromer to early endosomes. We confirmed the interaction with Muk1 and found that Vps9, the other yeast Rab5-family GEF, also interacts with retromer. Furthermore, the presence of at least one Rab5-family GEF is required for recruitment of retromer to endosomes. Recruitment appears to depend on Rab activation and the endosomal localization of Vps34, which produces PI3P. The data support a model where the retromer-GEF interaction works in a positive feedback loop to reinforce retromer recruitment on endosomes.

While exploring the retromer-GEF interactions, the function of an ORF that appeared to encode a protein with a partial VPS9 GEF domain was probed. In other strains the ORF included an adjacent ORF and encoded a protein with a complete VPS9 domain and several ankryin repeats. While an interaction between retromer and the complete VPS9 domain-containing protein could not be detected, the protein could complement some functions of the Rab5-family GEFs including retromer localization. Given homology with human VARP, which acts in retromer-

² A version of chapter 3 has been published. Bean BDM, Davey M, Snider J, Jessulat M, Deineko V, Tinney M, Stagljar I, Babu M, Conibear E (2015). Rab5-family guanine nucleotide exchange factors bind retromer and promote its recruitment to endosomes. *Mol Biol Cell* 26.

mediated endosome-to-plasma membrane sorting, we named the full gene VARP-Like 1 (VRL1) and speculate that it may act in a novel pathway in yeast. The experiments in this chapter identify a new putative Rab5-family GEF and characterize Rab5-family GEFs as novel retromer recruitment factors.

3.2 Introduction

Retromer is a retrograde endosomal trafficking complex that facilitates recycling of integral membrane proteins to the late Golgi and the plasma membrane (Seaman, 2005, 2012; Bonifacino and Hurley, 2008; Attar and Cullen, 2010). It was first identified in yeast as a complex required to recycle the acid hydrolase receptor, Vps10, and maintain the Golgi localization of Kex2 (Seaman *et al.*, 1998). Since then it has been linked to many processes in higher organisms including the endosome-to-Golgi recycling of the cation-independent mannose 6-phosphate receptor and the iron transporter DMT1, and the direct endosome-to-plasma membrane trafficking of the β 2 adrenergic receptor (Seaman, 2004; Tabuchi *et al.*, 2010; Temkin *et al.*, 2011). In addition, deficiencies in the retromer complex and its associated factors have been linked to Parkinson's (Vilariño-Güell *et al.*, 2011; Zavodszky *et al.*, 2014) and Alzheimer's diseases (Fjorback *et al.*, 2012).

Yeast retromer is composed of a structural subcomplex containing the sorting nexins Vps5/Vps17, and a cargo selective subcomplex (CSC) comprised of Vps26/Vps29/Vps35 (Seaman *et al.*, 1998). The sorting nexins bind phosphatidylinositol 3-phosphate (PI3P) at endosomes, and deform the membrane (Burda *et al.*, 2002), whereas the CSC recruits cargo into the retromer tubule (Nothwehr *et al.*, 1999; Seaman, 2005). While these two subcomplexes form

a stable pentamer in yeast, the CSC and sorting nexins are not tightly associated in mammalian cells (Mcgough and Cullen, 2011). The mammalian CSC assembles with Vps5/Vps17 homologs and with other sorting nexins to form spatially distinct classes of retromer tubules that engage different cargo (Harterink *et al.*, 2011). While the sorting nexin SNX3 is enriched at early endosomes, retromer tubules formed by the Vps5 and Vps17 homologs SNX1/2 and SNX5/6 respectively (Wassmer *et al.*, 2009) are most abundant on endosomes undergoing the early-to-late transition (Rojas *et al.*, 2008; Cullen and Korswagen, 2012; van Weering *et al.*, 2012b).

Rab GTPases are important for membrane identity, vesicle budding and membrane fusion (Stenmark, 2009). Rabs are converted to their active, membrane-bound form by guanine nucleotide exchange factors (GEFs) that catalyze the exchange of GDP for GTP, and are inactivated by GTPase-activating proteins, which increase the rate of GTP hydrolysis by the Rabs. As early endosomes mature into late endosomes, they undergo a Rab conversion where active Rab7-family GTPases are recruited and Rab5-family GTPases are inactivated and extracted from the membrane (Rink *et al.*, 2005).

Both Rab5- and Rab7-family GTPases are implicated in the recruitment of retromer to endosomes in mammalian cells (Rojas *et al.*, 2008; Liu *et al.*, 2012). GTP-bound Rab5 does not bind retromer directly, but instead recruits a complex containing VPS34, a phosphatidylinositol 3-kinase (PI3K) (Christoforidis *et al.*, 1999). This catalyzes the production of PI3P, which is recognized by the Phox homology (PX) domains of the sorting nexins (Xu *et al.*, 2001; Yu and Lemmon, 2001; Cozier *et al.*, 2002). In contrast, direct binding of Rab7 to Vps35 is essential for the endosomal recruitment of mammalian CSC (Harrison *et al.*, 2014). The CSC also interacts

with a number of regulatory factors, including the putative Rab7 GTPase activating protein TBC1D5 (Seaman *et al.*, 2009; Harbour *et al.*, 2010) and retromer tubule formation is reported to be maximal at the time of Rab5-to-Rab7 conversion (Cullen and Korswagen, 2012; van Weering *et al.*, 2012b). Thus, retromer assembly at endosomes may be tightly coupled to the regulation of Rab activation.

In yeast, the regulation of retromer function by Rab proteins is less well understood. Vps35 binds to the yeast Rab7 homolog Ypt7, but while this interaction directs it to the vacuole it is not required for recruitment to endosomes (Balderhaar *et al.*, 2010; Liu *et al.*, 2012). Moreover, many of the retromer-associated regulatory proteins identified in mammalian cells are not conserved in yeast. Thus the extent to which retromer assembly at endosomes is subject to Rab-dependent regulation is still unknown.

Here, we show that retromer physically interacts with the VPS9 domain GEFs Muk1 and Vps9, and that at least one of these must normally be present for retromer recruitment at endosomes. We further identify a new yeast VPS9 domain-containing protein related to human VARP that is present in wild but not laboratory strains of *S. cerevisiae*. All three proteins can act through Rab5-family GTPases and the phosphatidylinositol 3-kinase Vps34 to localize retromer to endosomal membranes. This suggests that association with Rab5 family GEFs could provide a mechanism to regulate the location or extent of retromer assembly.

3.3 Results

3.3.1 Retromer physically interacts with Rab5-family GEFs

Previous high throughput mass spectrometry studies of yeast protein complexes suggested an interaction between several subunits of the retromer complex and the VPS9 domain GEF Muk1 (Krogan *et al.*, 2006; Babu *et al.*, 2012). This interaction was surprising as VPS9 domain GEFs activate Rab5-family GTPases, whereas yeast retromer has been shown to interact only with the Rab7-like GTPase, Ypt7.

To validate the retromer-Muk1 interaction, Muk1-HA was expressed from a *GAL1* promoter in strains containing different TAP-tagged retromer subunits, and pulldowns were carried out using calmodulin resin under batch purification conditions similar to those used for mass spectrometry. This showed that all five retromer subunits were able to co-purify Muk1 (Figure 3.1A).

To estimate the fraction of interacting proteins, small-scale co-immunoprecipitations were subsequently carried out in strains where HA-Muk1 was expressed from the weaker *ADHI* promoter and the retromer subunit Vps35 was GFP-tagged at its endogenous locus. Interactions between Muk1 and retromer were reproducibly detected in the presence of the crosslinker DSP. However, purification of roughly 30% of cellular Muk1 co-precipitated less than 1% of the total pool of Vps35 (Figure 3.1B). The fact that interactions were detected only in the presence of the crosslinker and represented a minor fraction of the total Vps35 protein suggests that Vps35-Muk1 interactions are weak or disrupted on lysis, and are likely to be sub-stoichiometric. Furthermore, as retromer is a stable pentameric complex, we cannot exclude the possibility that Muk1 binds another subunit or that it interacts with retromer through a bridging protein.

Yeast express two known Rab5-family GEFs, Vps9 and Muk1, which share a catalytic VPS9 domain but have divergent C-termini (Carney *et al.*, 2006; Balderhaar *et al.*, 2010; Paulsel *et al.*, 2013). Retromer-Vps9 interactions were not previously identified by large-scale mass spectrometry. Nevertheless, we found that HA-Vps9, when expressed from the *ADHI* promoter, reproducibly co-purified with Vps35-GFP from DSP-treated cell lysates (Figure 3.1C). These results indicate that retromer binds more than one VPS9 domain GEF.

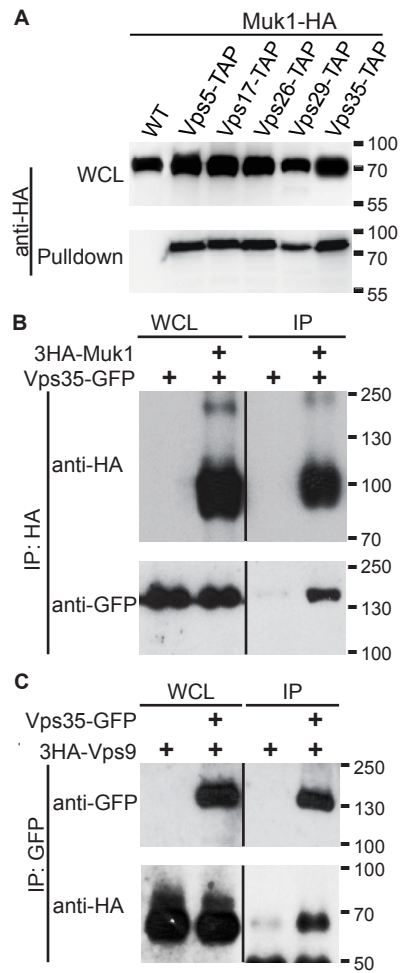


Figure 3.1 Retromer physically interacts with the Rab5-family GEFs Muk1 and Vps9.

(A) TAP-tagged retromer subunits were pulled down using calmodulin beads from GAL1pr-MUK1-HA strains. Samples were resolved by 12% SDS-PAGE and detected by immunoblotting. Loading of lysates

relative to the pulldown was 1:25. (B) Endogenously tagged Vps35-GFP and ADH1pr-3HA-Muk1 were cross-linked with 1.6 mg/mL DSP, 3HA-Muk1 was immunoprecipitated and co-purifying Vps35-GFP was probed by immunoblotting. Loading of lysates relative to IP was 1:1.6 (anti-HA) and 1:388 (anti-GFP). (C) Cells expressing Vps35-GFP and ADH1pr-3HA-Vps9 were cross-linked and immunoprecipitated with anti-GFP. Co-purification of 3HA-Vps9 was detected with anti-HA. Loading of lysates relative to IP was 1:1.6 (anti-GFP) and 1:388 (anti-HA).

3.3.2 Identification of Vrl1, a third member of the yeast VPS9-domain family related to mammalian VARP

Muk1 and Vps9 are the only two VPS9 domain GEFs described in yeast to date. Interestingly, the Superfamily database (Gough *et al.*, 2001), which identifies domains using hidden Markov models, reported a partial VPS9 domain at the N-terminus of the uncharacterized open reading frame (ORF) YML002w. In wild strains of *S. cerevisiae*, YML002w is continuous with an upstream ORF (YML003w), and is predicted to encode a single protein of 1090 amino acids with a full-length VPS9 domain. Comparison of sequences from wild and laboratory strains of *S. cerevisiae* suggest that a single thymine residue at chrXIII:264337 is deleted in commonly studied strains, causing a frameshift and premature stop codon (Figure B.1A). Re-sequencing of the corresponding region in the BY4741 parental strain confirmed the presence of the mutation. Integration of a 3HA tag at the 5' end of the upstream ORF, YML003w, under control of the *ADH1* promoter, showed the frameshift produces a truncated protein of the predicted size (Figure B.1B). Thus, it appears that wild yeast strains encode a third VPS9 domain protein that has been mutated in laboratory strains of *S. cerevisiae*.

Sequence comparisons suggest this new VPS9 domain protein is conserved in most species and is related to human VARP (hVARP), a Rab21 GEF (Zhang *et al.*, 2006). Accordingly, we have named this ORF *VRL1*, for VaRp-Like1. hVARP is a multi-functional protein that binds the R-SNARE VAMP7 and is a key regulator of endosome-to-cell surface transport (Burgo *et al.*, 2009, 2012; Ohbayashi *et al.*, 2012). While VARP GEF activity is essential for recycling to the cell surface in neurites, VARP has a separate role as a Rab32/38 effector in the trafficking of tyrosinase-related protein 1 to melanosomes, which does not require its GEF activity (Tamura *et al.*, 2011; Ohbayashi *et al.*, 2012). VARP and Vrl1 share extensive regions of conservation, including an N-terminal region not found in other GEFs, followed by the VPS9 domain and several Ankyrin repeats (Figure 3.2A and Figure B.2). However, the yeast protein lacks the second of two sets of Ankyrin repeats present in hVARP. Other hVARP features, including the Rab32/38 binding site and the VAMP7 interacting domain (Burgo *et al.*, 2009; Ohbayashi *et al.*, 2012; Schäfer *et al.*, 2012) are only partially conserved, suggesting the proteins may not be functionally identical (Figure B.2C).

3.3.3 Vrl1, Muk1, and Vps9 have partially overlapping functions

Muk1 and Vps9 were previously shown to have redundant yet distinct functions. Muk1 overexpression rescues the temperature sensitive growth phenotype of *vps9* cells, but cannot replace Vps9's role in the late endosomal sorting of carboxypeptidase Y (CPY) (Paulsel *et al.*, 2013). To determine if Vrl1 can functionally substitute for Muk1 or Vps9, the genomic region that includes both YML003w and YML002w was cloned into a single copy plasmid, and a nucleotide (T856) was inserted into *YML003W* to re-create the full length ORF. We use *VRL1* to refer to the full-length gene that results from the correction of the frame shift mutation; it is

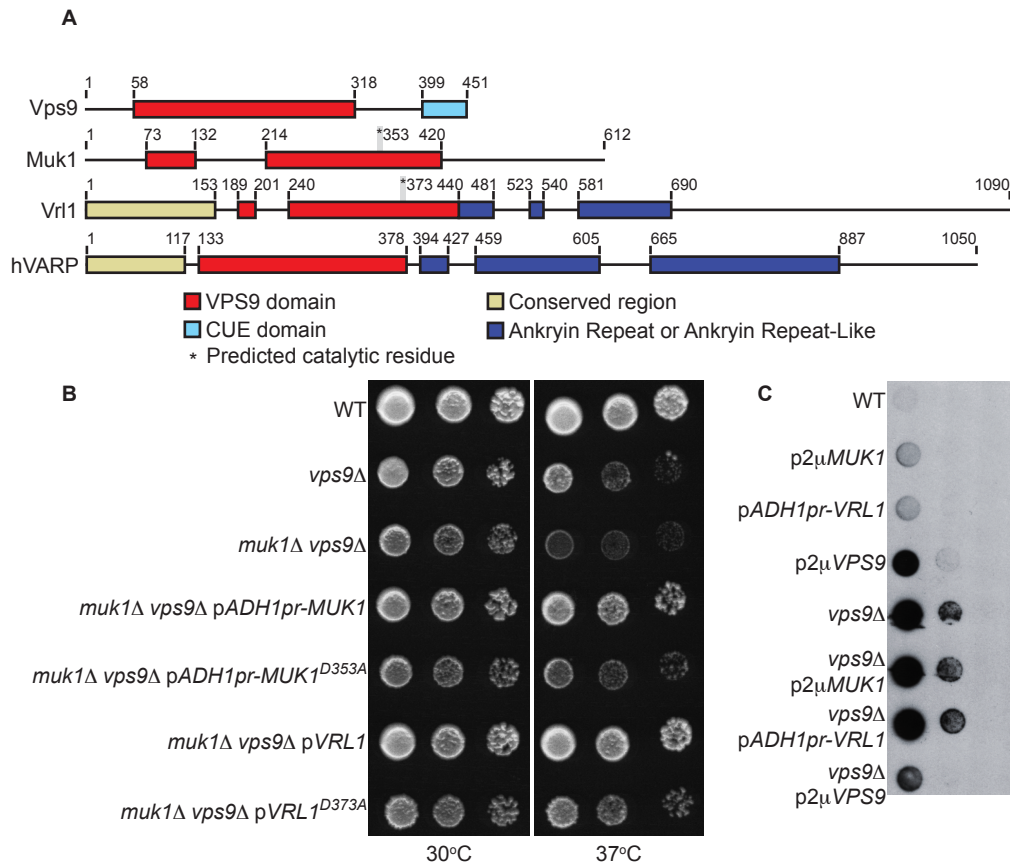


Figure 3.2 Vrl1 is a new yeast VPS9 domain protein.

(A) Schematic of yeast VPS9 domain-containing proteins and human VARP based on Superfamily (Gough *et al.*, 2001) and ClustalW alignments. (B) Yeast were spotted in 10x dilution series and grown two days at 37°C to assess temperature sensitivity of the indicated strains. *VRL1* was expressed from its endogenous promoter. (C) A colony overlay assay was used to assess carboxypeptidase Y (CPY) secretion. Cells spotted in 10x dilution series were overlaid with nitrocellulose and incubated 16 hours. The nitrocellulose was then immunoblotted with anti-CPY antibodies.

important to note that the laboratory yeast strains used in this paper do not express functional *VRL1*. Introduction of a plasmid expressing *VRL1* from its endogenous promoter fully restored growth of *muk1 vps9* strains at high temperatures, suggesting it can replace some function of Muk1 and/or Vps9 (Figure 3.2B).

The VPS9 domain of Rabex-5 contains a single invariant residue, D313, which is required for catalytic activity (Delprato and Lambright, 2007). We mutated the corresponding aspartate residues in Muk1 and Vrl1, and found that expression of Muk1^{D353A} or Vrl1^{D373A} failed to rescue the *muk1 vps9* ts growth defect, suggesting the suppression requires an active VPS9 domain (Figure 3.2B). However, overexpression of Vrl1 did not rescue the CPY secretion of a *vps9Δ* strain. In addition, high levels of Vrl1 induced mild CPY secretion in a wild type strain similar to overexpression of Muk1 (Paulsel et al., 2013; Figure 3.2C). These data suggest that while Vrl1, Muk1 and Vps9 show some degree of redundancy, they are not functionally equivalent.

As both known VPS9 domain GEFs interact with retromer, we tested Vrl1-retromer binding by co-immunoprecipitation. No physical interaction between *ADHIpr*-driven HA-Vrl1 and the retromer subunit Vps35-GFP was observed, although HA-Vrl1 was expressed at a significantly lower level than Muk1 or Vps9 (~5% of HA-Muk1 level, data not shown), and thus any interaction may be below the detection threshold. Taken together, our data suggest that Vrl1 can partially substitute for Muk1/Vps9, but cannot replace all functions of these GEFs.

3.3.4 Retromer interacts with the VPS9 domain

Retromer physically interacts with both Muk1 and Vps9, yet their sequence similarity outside the VPS9 domain is limited. To map the site of interaction, we used the integrated membrane yeast two hybrid (iMYTH) system, which detects interactions of membrane-associated proteins at their normal organellar localization (Snider *et al.*, 2010). The N-terminal half of ubiquitin (NubG) was fused to full length and truncated versions of Muk1 and co-expressed with retromer subunits fused to a ubiquitin C-terminus-transcription factor cassette (Figure 3.3A). Interactions that

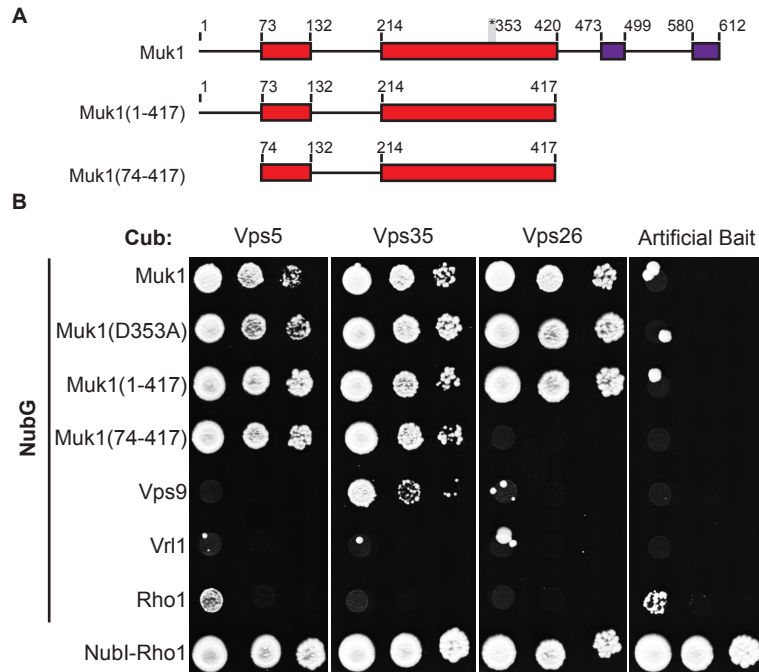


Figure 3.3 The VPS9 domain of Muk1 is sufficient for interaction with retromer subunits in the iMYTH assay.

(A) Schematic of Muk1 truncations. The position of the invariant aspartate residue required for GEF activity, and conserved C-terminal motifs, are indicated. (B) Strains containing Cub-tagged retromer subunits and plasmids encoding Rab5-family GEFs tagged N-terminally with NubG were tested for activation of the *HIS3* reporter on selective media lacking tryptophan, adenine and histidine. NubG-tagged Rho1 acted as a negative control, whereas the Nubl tag, which binds tightly to Cub independently of other interactions, confirmed the expression of Cub fusions. iMYTH, integrated membrane yeast two-hybrid; Cub, C-terminal fragment of split ubiquitin; Nub, N-terminal fragment of split ubiquitin.

reconstitute ubiquitin result in the DUB-dependent release of the transcription factor and the activation of reporter genes. Full length Muk1 and a truncated version (aa1-417) corresponding to the VPS9 domain interacted with three of the five retromer subunits, and this interaction was not affected by the D353A mutation predicted to block Muk1's GEF activity (Figure 3.3B). Vps9 also interacted with Vps35-Cub in this assay, though no interaction was observed with the

remaining tested retromer subunits. We were unable to detect an interaction between Vrl1-Nub and any of the retromer Cubs; however, Vrl1-Nub was expressed at relatively low levels compared to the other Nub fusions (Figure B.3A). Moreover, interactions will not be detected if the Nub and Cub fusions are not positioned in close proximity in the complex. Our results suggest that retromer interacts, directly or indirectly, with the Muk1 VPS9 domain. This is the only domain shared by Muk1 and Vps9, suggesting that retromer might recognize a conserved feature of this domain.

3.3.5 Muk1, Vps9, and Vrl1 can localize to endosomes

Both Muk1 and Vps9 have a predominantly cytosolic distribution in wild type cells (Paulsel *et al.*, 2013). Vps9 is believed to be recruited to ubiquitinated cargo via its C-terminal CUE domain (Carney *et al.*, 2006), which is not present in Muk1. Accordingly, Vps9, but not Muk1, localizes to the aberrant endosome of ESCRT mutants (Paulsel *et al.*, 2013), where ubiquitinated proteins accumulate. Overexpression of the tagged ESCRT-III subunit Snf7-RFP disrupts ESCRT function and causes an endosomal maturation defect (Froissard *et al.*, 2007). We confirmed that GFP-Vps9 co-localizes with Snf7-RFP at endosomes (21% of cells, SE = 6.5%; 3 experiments, N \geq 77 cells) (Figure 3.4A). Interestingly, when expressed from a plasmid under its endogenous promoter, GFP-Muk1 could be detected at Snf7-RFP marked endosomes in some cells (5%, SE = 1.5%; 3 experiments, N \geq 130 cells) in the absence of Vps9 (Figure 4A). Furthermore, GFP-Vrl1 formed puncta that co-localized with Snf7-RFP puncta in 16% (SE = 3.7%; 3 experiments, N \geq 178 cells) of cells (Figure 3.4A). Taken together, this suggests that all three VPS9 domain proteins are able to associate with endosomes to some extent.

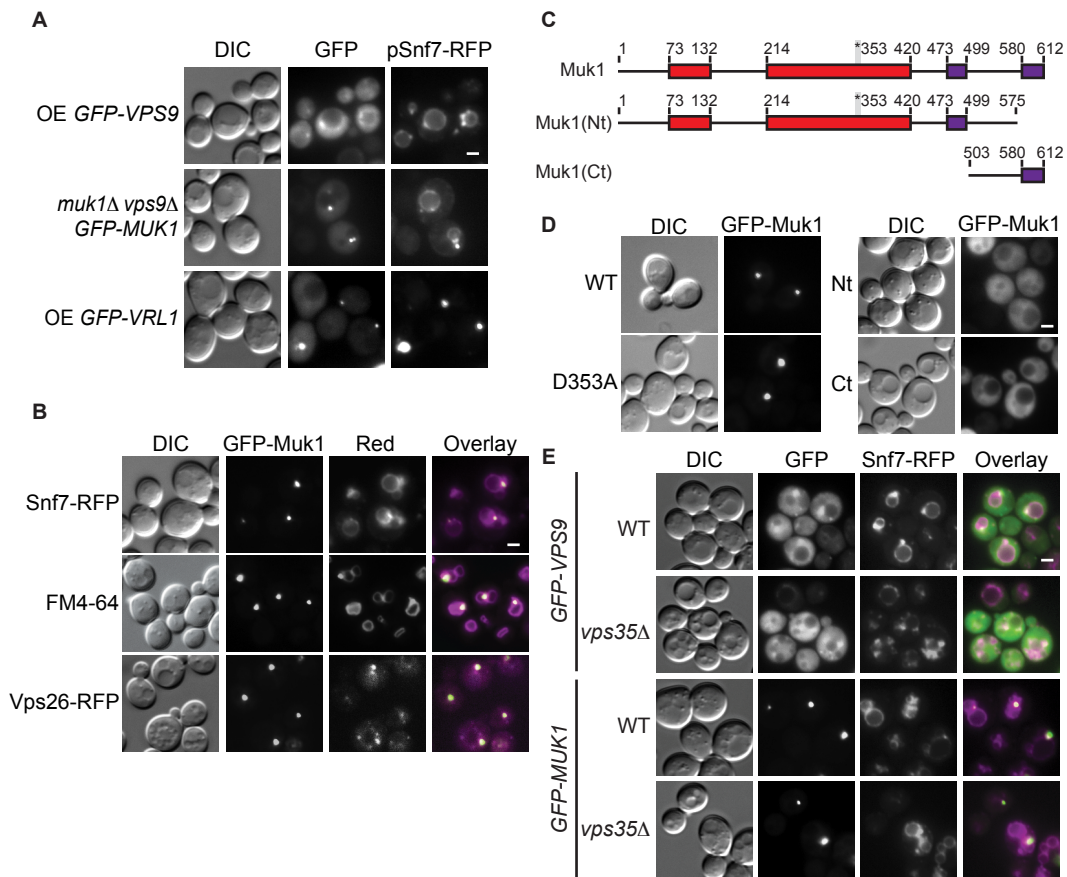


Figure 3.4 The yeast VPS9-domain proteins Muk1, Vps9, and Vrl1 localize to endosomes

(A) *MUK1pr*-GFP-Muk1, *ADHIpr*-GFP-Vps9 and *ADHIpr*-GFP-Vrl1 localize to Snf7-RFP marked late endosomes by fluorescence microscopy. (B) Fluorescence microscopy of *ADHIpr*-GFP-Muk1 with Snf7-RFP, the lipophilic dye FM4-64 and the tagged retromer subunit RFP-Vps26. (C) Schematic of Muk1 truncations used in (D) showing conserved C-terminal motifs identified by alignments (purple). (D) Fluorescence microscopy of full length or mutated *ADHIpr*-GFP-Muk1. (E) Deletion of *VPS35* does not disrupt the endosomal localization of overexpressed GFP-Vps9 or GFP-Muk1. Scale bars = 2 μ m; OE, overexpressed.

When GFP-Muk1 was expressed from the stronger *ADHI* promoter, bright puncta were seen in 37% (SE = 4.8%) of cells, and these overlapped with the endosomal markers FM4-64 and Snf7-RFP, and with the retromer subunit Vps26-RFP (Figure 3.4B). Two regions in the Muk1 C-terminal domain, corresponding to residues 473-499 and 580-612, are highly conserved in

different fungal species (Figure 3.4C). A truncation that removes the last 37 aa of Muk1 (GFP-Nt-Muk1) did not alter protein stability (Figure B.2B), yet abolished puncta formation (Figure 3.4D), suggesting this region contributes to Muk1's localization. However, the Muk1 C-terminus alone (aa 503-612), while expressed at similar levels to the full length GFP-Muk1, did not form puncta, indicating the Muk1 C-terminal domain is necessary but not sufficient for endosomal localization (Figure 3.4D). The localization determinant may not be correctly folded in the truncated protein. Alternatively, membrane localization of Muk1 may require multiple interacting domains.

To test if retromer is involved in recruiting the Rab5 GEFs to endosomes we deleted retromer subunits *VPS26* or *VPS35* from the strains expressing *ADH1pr*-driven GFP-Muk1 or GFP-Vps9. Both GEFs were found in puncta that co-localized with Snf7-RFP in the retromer deletion strains (Figure 3.4E, data not shown), suggesting Muk1 and Vps9 localize to endosomes independent of their interactions with retromer.

3.3.6 Retromer localization to endosomes is impaired by loss of Rab5 GEFs

We have shown that retromer interacts with two different VPS9 domain GEFs, and that these GEFs can localize to endosomes. To test if the GEFs are required for retromer recruitment we deleted them singly and in combination (Figure 3.5A). Vps26-GFP localized to puncta in wild type cells and in *muk1* and *vps9* single mutants, though punctate localization was reduced in the *vps9* strain. Strikingly, deletion of both *MUK1* and *VPS9* greatly reduced localization of Vps26-GFP and Vps5-GFP to endosomes. This was complemented by expression of either *VPS9* or *MUK1* from single copy plasmids (Fig. 3.5A,B). Strikingly, the *MUK1*^{D353A} GEF mutant failed to

restore Vps26-GFP localization, demonstrating the importance of Muk1 GEF activity *in vivo*. Similarly, expression of Vrl1, but not Vrl1^{D373A}, from its endogenous promoter also restored retromer localization to *muk1 vps9* mutant cells. Thus, any of the three active VPS9 domain proteins is sufficient to recruit retromer to endosomes.

The need for an intact VPS9 domain suggests that active Rabs are required for efficient retromer recruitment to endosomes. There are three Rab5-family GTPases in yeast: Vps21, Ypt52 and Ypt53. Ypt53 is normally expressed at very low levels and is only activated under conditions of stress (Nickerson *et al.*, 2012). We found that loss of *VPS21* alone caused a slight reduction in retromer recruitment (Figure 3.5A), consistent with observations of others (Balderhaar *et al.*, 2010), but deletion of both *VPS21* and *YPT52* strongly reduced retromer recruitment. This was not complemented by expression of *VRL1*, suggesting that Vrl1 acts upstream of the Rab5 GTPases, consistent with its role as a putative GEF. Together, this suggests the GEFs redundantly activate different Rab5 GTPases, and this in turn is needed for retromer's localization to endosomes.

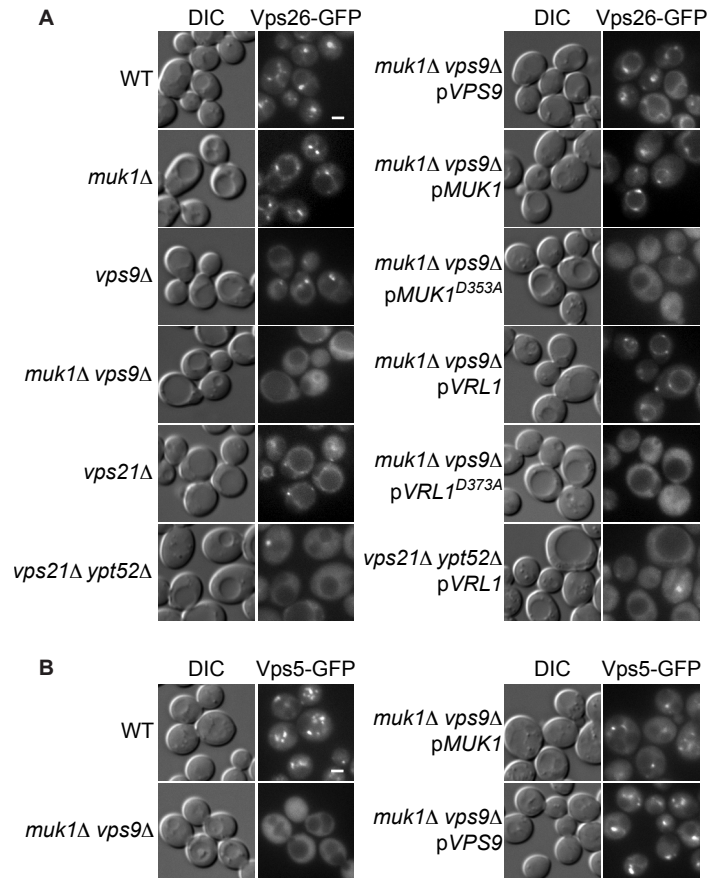


Figure 3.5 Rab5-family GEFs and GTPases are required for endosomal recruitment of retromer.

(A) Fluorescence microscopy of Vps26-GFP in strains lacking Rab5-family GEFs and Rab5-family GTPases. Muk1 and Vrl1 are expressed from endogenous promoters. Muk1^{D353A} and Vrl1^{D373A} are predicted to be catalytically inactive. (B) Microscopy of Vps5-GFP in strains with deletions of Rab5-family GEFs. Scale bars = 2 μm.

3.3.7 Rab5 GEFs are required for normal PI3P localization

Overexpression of active Rabs can often overcome loss of their respective GEFs (Siniosoglou *et al.*, 2000; Lynch-Day *et al.*, 2010). Therefore, we expressed different forms of Vps21 from high copy plasmids to see if this would rescue retromer recruitment (Figure 3.6A, B). Expression of the constitutively active Vps21Q66L in WT and *muk1 vps9* strains stimulated recruitment of retromer to the vacuolar membrane, but not to endosomes.

Because retromer recruitment to early endosomes requires PI3P, its vacuolar localization might result from loss of endosomal PI3P, or from elevated levels of PI3P at the vacuole in these mutant strains. Indeed, the PI3P-binding biosensor GFP-FYVE showed endosomal localization in wild type strains, but prominent vacuole rim staining in a *muk1 vps9* strain (Figure 3.6C), similar to that of a *vps21 ypt52* strain (Nickerson *et al.*, 2012). This vacuolar pool of PI3P could originate at endosomes and accumulate at the vacuole due to a disruption in its turnover or metabolism. Alternatively, PI3P could be produced at the vacuolar membrane by a vacuole-localized pool of the PI 3-Kinase Vps34 (Burda *et al.*, 2002). We examined Vps34-GFP localization in each of the mutants, and found it was strongly mislocalized to the vacuole in *muk1 vps9* mutants and partially mislocalized in a *vps9* mutant (Figure 3.6D). VPS34 is recruited by Rab5 GTPases in mammals (Christoforidis *et al.*, 1999), and others have shown that, in yeast, constitutively active forms of Vps21, which cannot be extracted from membranes by Rab guanine dissociation inhibitors, are transported to the vacuolar membrane (Markgraf *et al.*, 2009). Thus, overexpressed Vps21Q66L may activate Vps34 at the vacuole of *muk1 vps9* strains, resulting in high levels of PI3P that drive retromer recruitment to the vacuolar membrane.

These results suggest that VPS9 domain GEFs are critical for maintaining an endosomal pool of Rab5-family GTPases that in turn recruit and activate the PI3K Vps34. The partial mislocalization of Vps34 in *vps9* but not *muk1* mutants suggests that the three VPS9 domain proteins do not contribute equally to this process. Nevertheless, expression of Vrl1, but not the VPS9 domain mutant Vrl1^{D373A}, was found to rescue Vps34 localization (Figure 3.6D) and restore endosomal pools of PI3P in *muk1 vps9* strains (Figure 3.6C). Taken together, this

suggests that Vps9 domain GEFs play a key role in promoting the enrichment of PI3P at endosomes.

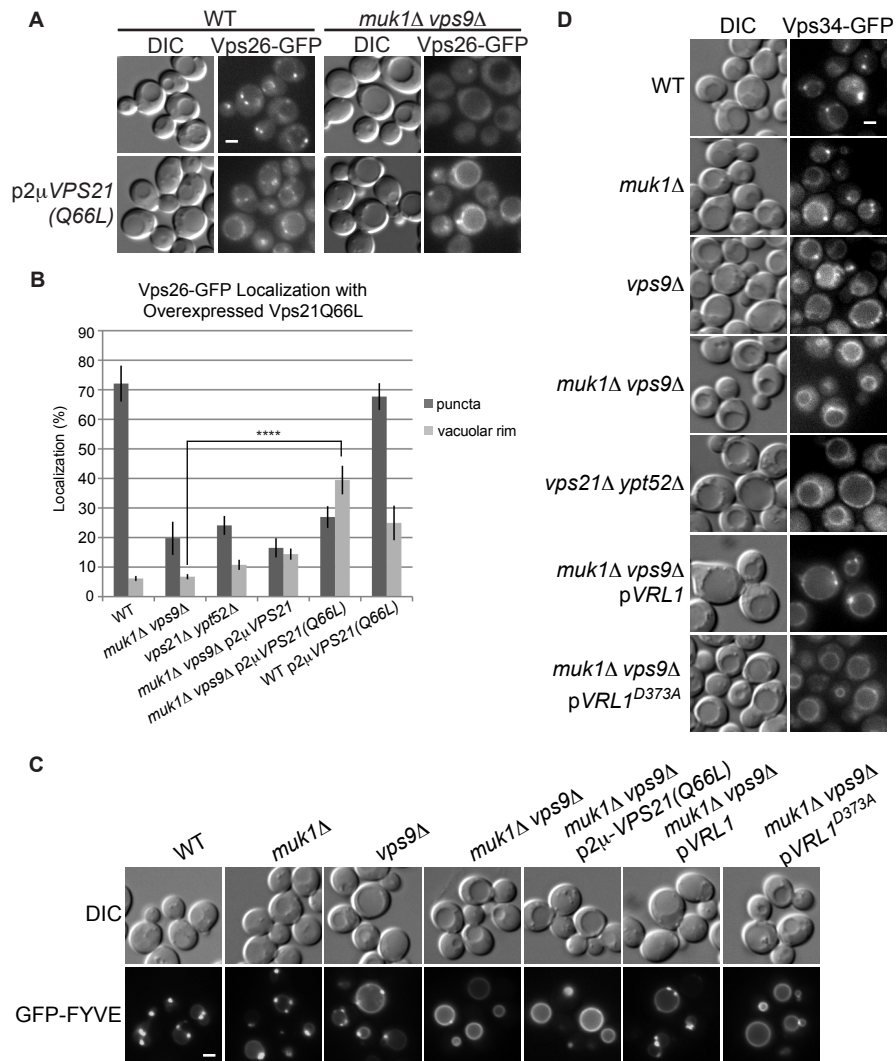


Figure 3.6 Rab5-family GEFs are needed for PI3P production at endosomes, and this cannot be bypassed by expressing the constitutively active Rab5-family GTPase Vps21(Q66L).

(A) Fluorescence microscopy shows that Vps26-GFP is mislocalized to the vacuolar rim when Vps21(Q66L) is expressed, even in the absence of Rab5-family GEFs. (B) Quantification of Vps26-GFP fluorescence microscopy. Images of Vps26-GFP localization from four independent experiments were manually scored for localization to the vacuolar rim or puncta ($N \geq 140$ /strain/experiment). Error bars represent SE. Unpaired one-way ANOVA: $p < 0.0001$ overall; ****, $p < 0.0001$. (C) Fluorescence microscopy of GFP-FYVE, a biomarker for PI3P, in strains with deletions of Rab5-family GEFs. (D) Vps34-GFP localization to puncta is

dependent on expression of Rab5-family GEFs and GTPases. Vrl1 is expressed from the endogenous promoter in C,D. Scale bars = 2 μ m

3.4 Discussion

Here we identify two VPS9 domain Rab5-family GEFs as new retromer-associated proteins and show their activity is important for the recruitment of retromer to endosomal membranes.

Whereas many of the retromer accessory factors that have been identified in higher cells are absent in yeast (Harbour *et al.*, 2010; Seaman, 2012), VPS9 domain proteins constitute a broadly conserved family, and may contribute to fundamental aspects of retromer assembly or function present in all eukaryotic cells.

Our co-immunoprecipitation experiments showed clear interactions between retromer and two different VPS9 domain GEFs, Muk1 and Vps9. Interestingly, the interaction was mapped to the VPS9 domain of Muk1, suggesting that the binding of retromer to the VPS9 domain might regulate its GEF activity. Indeed, the human homolog of Vps9, Rabex-5, is autoinhibited by a conserved helix C-terminal to the VPS9 domain, and this is overcome by Rabex-5 binding the Rab5 effector Rabaptin-5 (Delprato and Lambright, 2007). Because Rabaptin-5 helps recruit Rabex-5 to endosomes, this creates a positive feedback loop that results in robust Rab5 activation (Horiuchi *et al.*, 1997; Zhang *et al.*, 2014). It is not known if Muk1 is subject to autoinhibition, or if retromer binding could similarly affect GEF activity. However, the interaction with retromer is expected to increase the local concentration of the GEF, which would thus serve to enhance Rab5 activation at sites of retromer tubule formation.

Yeast retromer does not bind directly to Rab5-family GTPases (Liu *et al.*, 2012). Instead, we found that Rab5-family GTPases and an active VPS9 domain GEF are required for the correct localization of the phosphatidylinositol 3-kinase Vps34 at endosomes, and for the production of the endosomal pool of PI3P. While Rab5 directly recruits the human homolog of Vps34, hVPS34, a similar relationship between yeast Rab5-family GTPases and Vps34 has not previously been reported (Christoforidis *et al.*, 1999). Because the structural subcomplex of retromer binds PI3P through the PX domains of Vps5/17 (Burda *et al.*, 2002), the loss of endosomal PI3P provides a likely explanation for the retromer localization defect in strains lacking active VPS9 domain GEFs.

The endosomal localization of yeast VPS9 domain GEFs does not depend on retromer, and thus a physical interaction between retromer and the GEF may not be absolutely required for endosomal PI3P production and retromer recruitment. Instead, we propose that retromer-GEF binding enhances the rate or extent of retromer assembly through a positive feedback loop like that described for Rabaptin-5 (Horiuchi *et al.*, 1997); Figure 3.7A). In this model, the initial recruitment of retromer to PI3P-labeled endosomes allows it to bind and concentrate Muk1 and/or Vps9, which then recruit and activate Rab5-like GTPases in the vicinity of the forming retromer tubule. This, in turn, stimulates the recruitment and activation of PI3K, increasing local PI3P production and promoting further retromer assembly. Interactions with distinct VPS9 domain GEFs could conceivably enhance retromer assembly at different endosomal compartments, or in response to different stimuli. A similar model has been proposed to explain the action of the Salmonella effector protein SopB, which causes the over activation of Rab5,

promoting PI3P production that drives the formation of extensive Snx3 and Snx1-coated tubules at *Salmonella*-containing vacuoles (Braun *et al.*, 2010).

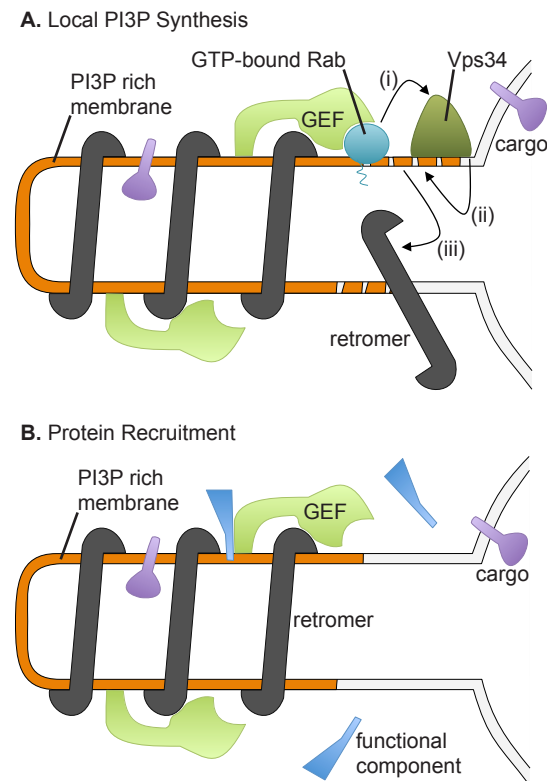


Figure 3.7 Models for the function of the interaction between retromer and Rab5-family GEFs at endosomes.

(A) In the first model, the GEFs concentrate Rab5-family GTPases at the retromer tubules. The GTPases recruit the PI3K Vps34 (i), which locally increases the concentration of PI3P (ii), leading to further retromer recruitment (iii). **(B)** In the second model, GEFs physically recruit specific factors to the tubules.

3.4.1 Discovery of a new yeast VPS9-domain protein

As this manuscript was being prepared, it was reported that the human VPS9 domain GEF hVARP interacts with retromer, and that this interaction is responsible for the normal trafficking of GLUT1 from endosomes to the plasma membrane (Hesketh *et al.*, 2014). This, together with the work presented here, raises the possibility that retromer interacts with a variety of VPS9

domain GEFs, and that retromer-GEF interactions may contribute to protein trafficking in yeast and mammals. The VARP-Like protein Vrl1, which is present in wild strains of *S. cerevisiae* but mutated in common lab strains, has many similarities to hVARP, yet exhibits key differences. hVARP binds the retromer subunit VPS29 through two conserved cysteine-rich motifs, and this interaction recruits hVARP to endosomal tubules. These cysteine-rich motifs are not present in Vrl1, and we found Vrl1 was not fully dependent on retromer for localization to endosomes. Although our co-immunoprecipitation and iMYTH experiments did not identify an interaction between retromer and Vrl1, such an interaction may be undetectable by these methods due to the relatively low level of Vrl1 expression.

A key role of hVARP in the trafficking of GLUT1 is to recruit the R-SNARE VAMP7 into retromer-derived vesicles, and thus enable their fusion with the plasma membrane (Hesketh *et al.*, 2014). hVARP has a VAMP7 interacting domain (Burgo *et al.*, 2009; Ohbayashi *et al.*, 2012; Schäfer *et al.*, 2012) which is conserved in Vrl1 homologs from many fungal species, though is less well conserved in *S. cerevisiae*. A retromer-mediated recycling pathway from endosomes to the plasma membrane has not been reported in yeast, but the laboratory strains used in most trafficking studies lack functional Vrl1. Thus it is intriguing to speculate that Vrl1, like hVARP, repurposes an R-SNARE to regulate an as-yet-undiscovered recycling pathway that is missing in lab strains but present in other yeast species.

The role of hVARP in VAMP7 transport suggests an alternative model for the function of retromer-GEF interactions: that GEFs bind retromer to recruit specific cargo proteins or accessory factors to forming retromer tubules (Figure 3.7B). In fact, Vps9 has a ubiquitin-

binding CUE domain that is important for the normal progression of ubiquitinated cargo through endosomes (Davies *et al.*, 2003; Donaldson *et al.*, 2003). While Muk1 lacks a CUE domain or other recognizable motifs, it has conserved regions that could mediate interactions with additional factors that influence the composition or targeting of endosome-derived vesicles.

It is important to note that the two models presented in Figure 3.7 are not mutually exclusive.

The retromer-GEF interaction could enhance retromer assembly by promoting local Rab5 activation and PI3P production, while at the same time recruiting specific cargo or accessory factors. By providing a means of reinforcing local recruitment, this could explain why retromer coats subdomains of endosomes (Seaman *et al.*, 1998; Temkin *et al.*, 2011). Moreover, the positive feedback model could address puzzling aspects of retromer biology in higher cells. Because the mammalian cargo-selective complex (CSC) does not bind tightly to the PI3P-binding sorting nexins, it is unclear what prevents the sorting nexins from driving the formation of empty tubules devoid of cargo (Cullen and Korswagen, 2012). If recruitment of hVAMP by the VPS29 subunit of the CSC also increases local PI3P production, this could enhance co-assembly with the sorting nexin subcomplex, and link membrane deformation to cargo recruitment.

3.4.2 The VPS9 family

There are three VPS9 domain proteins in yeast and at least nine in humans (Carney *et al.*, 2006).

While the yeast VPS9 domain proteins share some overlapping functions, our results suggest they have unique functions that are as yet uncharacterized. Some mammalian Vps9 domain GEFs can preferentially activate a subset of Rab5-family GTPases (Delprato and Lambright,

2007), or contain domains that confer distinct localizations (Balaji *et al.*, 2012). While in vitro activity assays suggest the yeast VPS9 domain GEFs do not have differential specificity for Rab GTPases (Singer-Krüger *et al.*, 1994; Cabrera *et al.*, 2013; Paulsel *et al.*, 2013), we and others have found they show differential recruitment to endosomes. Further studies will be needed to determine if the yeast GEFs localize to distinct endosome subpopulations, or associate with membranes only in response to specific regulatory inputs. It will also be important to determine if the retromer binding is a general feature of VPS9 domain GEFs in humans and to what extent the interaction serves to reinforce retromer recruitment or select other cargo.

3.5 Materials and methods

3.5.1 Yeast strains and plasmids

Yeast strains and plasmids used are listed in Table B.1 and Table B.2 respectively. With the exception of the strains described below all strains from this study were made by homologous recombination as described (Longtine *et al.*, 1998; Janke *et al.*, 2004; Sheff and Thorn, 2004). The iMYTH strains were made via integration of the L2 Cub cassette as previously described (Snider *et al.*, 2010). *VPS34* and *VPS5* were tagged with a bright GFP variant, GFP+ (Scholz *et al.*, 2000), by amplifying and transforming GFP+::NAT from pLC1318, a gift from R.

Rachubinsky.

Plasmids were made by homologous recombination in yeast (Scholz *et al.*, 2000), rescued in *E. coli* and confirmed by sequencing. To make *pGFP-FYVE(EEA1)::LEU2* (pBB21), *pGFP-FYVE(EEA1)::TRP1* (Addgene #36096) was cut with Bsu36I and cotransformed with a *LEU2* PCR fragment containing flanking homology to *TRP1* 5' and 3' regions. *pNubG-HA-MUK1 FL*

(*pAO470*), *pNubG-HA-MUK1 1-417* (*pAO538*) and *pNubG-HA-MUK1 74-417* (*pAO542*) were made by co-transforming *MUK1* gene regions amplified from yeast genomic DNA, together with *SmaI* digested pPR3-N MYTH prey vector, as described previously (Snider *et al.*, 2010). The Muk1 D353A mutant (*pA0531*) was made via site directed mutagenesis of *pNubG-HA-MUK1 FL* (*pAO470*) construct following the QuikChange II protocol (Agilent). *pNubG-HA-VPS9* (*pBB9*) and *pNubG-HA-VRL1* (*pBB24*) were made by *EcoRI*-HF/*ClaI* digesting pPR3-N and cotransforming it with the respective genes as previously described (Snider *et al.*, 2010).

Other *MUK1* plasmids made in this study were based on pRS416 (*URA3* CEN) as follows. 972 bp of the 5'UTR of *MUK1*, referred to as *MUK1pr*, was amplified using primers with homology to pRS416 and two thirds of a 3HA tag. A second product containing *MUK1* was generated using primers with homology to two thirds of the 3HA tag and a downstream pRS416 sequence. The two products were cotransformed with *KpnI*/*SacII* digested pRS416 to generate *pMUK1pr-3HA-MUK1* (*pMD120*). *pMD120* was *AatII*/*BamHI* digested and cotransformed with a GFP PCR product with ends homologous to 5' and 3' of the 3HA tag to make *pMUK1pr-GFP-MUK1* (*pMD121*). The *pMD121 Muk1* promoter was *KpnI*/*BamHI* digested and the cut plasmid was cotransformed with an *ADHI* promoter PCR product that had homology outside of the cut region, forming *pADHpr-GFP-MUK1* (*pMT1*). Both *pMD120* and *pMT1* were cut with *HindIII*/*NruI* and cotransformed with PCR products containing *MUK1-D353A* with terminal homology outside the cut sites to generate *pMUK1pr-3HA-MUK1-D353A* (*pBB12*) and *pADH1pr-GFP-MUK1-D353A* (*pBB14*). *pMD120* and *pBB12* were cut with *KpnI* and transformed with an *ADHI* PCR product with flanking *MUK1* homology to form *pADH1pr-3HA-MUK1* (*pBB33*) and *pADH1pr-3HA-MUK1-D353A* (*pBB34*). *pADH1pr-GFP-MUK1(1-*

575) (pBB15) was made by cutting out bp 544-1800 of *MUK1* from pMT1 using BglIII and cotransforming the cut plasmid with a PCR product containing bp 1-1725 of *MUK1* with flanking homology to the plasmid. *pADH1pr-GFP-MUK1(503-612)* (pMT2) was made by excising the N-terminus of *MUK1* in pMT1 with ClaI/HindIII and cotransforming the plasmid with a hybridized oligo with homology to GFP and *MUK1* after bp 1506.

VRL1 plasmids were based on *pADH1pr-GFP-MUK1* (pMT1). Genomic DNA was used as a template for *VRL1* and primers were used to correct the thymine deletion in *YML003W* of the parental yeast strain. The DNA upstream of the deletion was amplified with the reverse oligo (5' ATATTTATATTTTTCAGTGTCTACTTCGTGGCCT TTGAAATGTGTAGTAAGCCTAGACCA) and the region downstream was amplified with (5' TGGTCTAGGCTTACTACACATTTCAAAGGCCACGAAGTAGACACTGAAAAATA TAAATAT). The reverse oligo was used to amplify upstream *YML003W* with homology to either the *ADH1* promoter or GFP of pMT1 and the forward oligo was used to amplify downstream *YML003W* and *YML002W* with homology to pMT1 after *MUK1*. The two sets of PCR products were cotransformed with HindIII cut pMT1, to make plasmids *pADH1pr-VRL1* (pBB23) or *pADH1pr-GFP-VRL1* (pBB22). The GFP tag of pBB22 was cut with HpaI and cotransformed with an oligo containing 3HA and flanking homology to make *pADH1pr-3HA-VRL1* (pBB25). Expression of N-terminally HA or GFP-tagged forms of *VRL1* resulted in a protein of the expected size. The *VRL1* promoter was substituted for the *ADH1* promoter by cutting pBB25 with SphI and cotransforming with a PCR product containing 366bp upstream of *YML003w* and flanking homology to form *pVRL1pr-3HA-VRL1* (pBB25). pBB25 was cut with

MscI and BglII and cotransformed with two overlapping PCR products containing *VRL1* with the D373A mutation, forming *pVRL1pr-3HA-VRL1D373A* (*pBB32*).

3.5.2 Growth and colony overlay assays

For the concentration limiting growth assays, 4 μ L of 1 OD₆₀₀/mL log phase yeast were spotted onto Yeast Extract-Peptone-Dextrose (YPD) media in 10x serial dilutions, and imaged using a CanoScan 4400F scanner after two days growth at the indicated temperatures. A colony overlay assay was used to assess CPY secretion. In the assay yeast (containing pRS415 and pRS416 as required) were spotted onto synthetic amino acid dropout media lacking histidine and uracil and overlaid with a nitrocellulose membrane. After 16 hours the membrane was removed, washed and blotted with mouse anti-carboxypeptidase Y (Molecular Probes A6428) and then goat anti-mouse conjugated to horseradish peroxidase (Jackson ImmunoResearch 115035146). The blot was developed with the enhanced chemiluminescent West Pico (Pierce 34077) and exposed to Amersham Hyperfilm (GE Healthcare 28906839).

3.5.3 Western blotting and coimmunoprecipitation

For co-immunoprecipitation from batch cultures, 50ml samples of the appropriate strains were grown in YPD media to mid-log phase, washed and transferred to galactose media for 1 h. Cells were harvested, resuspended in an equal volume of IPLB buffer (20 mM Hepes KOH, pH 7.4, 150 mM KOAc, 2 mM Mg(Ac)₂, 1 mM EGTA, 10% glycerol, Protease inhibitor cocktail and 1% triton X-100), and disrupted by glass beads for 5 min. Cell lysates were then cleared by centrifugation at 1,500 \times g for 3 min. One-half of the cleared lysate was incubated with 50ul calmodulin beads for 2 h and washed with ten volumes of fresh IPLB. 10 μ l loading buffer (5%

SDS, 50mM Tris pH 6.8, 0.4 mg/mL bromophenol blue and 1% β -mercaptoethanol) was added to 20 μ l of beads and eluates resolved on 12% SDS-PAGE gels. Gels were then transferred to nitrocellulose membrane using the iBlot transfer system following the manufacturer's instructions (Life technologies). Membranes were probed using anti-HA (Santa Cruz Biotechnologies sc-805) or anti-TAP (GeneScript #A01435) rabbit primary antibodies and HRP-tagged goat anti-rabbit secondary antibody (Pierce #31462) and visualized using a Kodak image station 4000.

Western lysates were prepared from log phase cells by bead bashing, freezing and resuspension in Thorner buffer (8M Urea, 5% SDS, 50mM Tris pH 6.8, 0.4 mg/mL bromophenol blue and 1% β -mercaptoethanol). Lysates were heated to 70°C and the equivalent of 0.5 OD₆₀₀ of cells was loaded into 10% SDS PAGE gels. In cross-linking co-immunoprecipitation experiments, fresh spheroplasts were prepared by digesting cell walls with zymolyase (MJS BioLynx SK1204911). 20 OD₆₀₀ of spheroplasts were crosslinked with 1.6 mg/mL dithiobis(succinimidyl propionate) (DSP) and lysed as described (Čopič *et al.*, 2007), except that 1% n-Dodecyl- β -D-maltoside (DDM) was used in the lysis buffer instead of TX-100. The lysates were incubated at 4°C with rabbit anti-HA (Santa Cruz Biotechnologies sc-805) or rabbit anti-GFP (Molecular Probes A6455) followed by Protein A sepharose beads (GE Healthcare 17-5280-04). The beads were washed and proteins were eluted by heating at 95°C for 5 minutes. Samples were loaded into 10% SDS PAGE gels. For both Westerns and co-immunoprecipitations proteins were transferred overnight to nitrocellulose membranes and blotted with either mouse anti-GFP (Roche 11814460001) or mouse anti-HA (Covance MMS-101R). Probing with secondary antibodies and exposure was done as in the colony overlay assay.

3.5.4 Integrated membrane yeast two hybrid (iMYTH)

Log phase yeast were serially diluted by a factor of 10 from 1 OD₆₀₀ and 4 µL was spotted onto synthetic dextrose dropout plates lacking tryptophan, adenine and histidine (SD-WAH).

Tryptophan selected for N-terminal ubiquitin (Nub) plasmids and adenine and histidine selected for an interaction between the C-terminal ubiquitin (Cub) bait and Nub prey constructs (Snider *et al.*, 2010). Yeast were grown at 37°C for 4 days and then imaged using a CanoScan 4400F scanner.

3.5.5 Fluorescence microscopy

Log phase yeast were imaged in minimal selective media at room temperature with a Plan-Apochromat 100× 1.40 NA oil immersion objective lens on an Axioplan 2 fluorescence microscope (Carl Zeiss Inc.). Images were taken with a CoolSNAP camera (Roper Scientific) using MetaMorph 7.7 software (MDS Analytical Technologies) and adjusted using MetaMorph and Photoshop CS5 (Adobe). Exposure times varied from 100ms to 3s based on the protein tagged with GFP or RFP, but were kept the same within a given experiment. Where the FM4-64 (Life Technologies T-3166) lipophilic dye was used, cells were incubated with the dye for one hour in minimal media, washed once and then grown another hour in minimal media prior to imaging. Cellular features were quantified by manually scoring images.

Chapter 4: Discussion and conclusions

4.1 Summary of major findings

By characterizing proteins associated with cargo adaptors, this study provides insights into cargo adaptor assembly and recruitment to target membranes. We found Ssp120 is a stable component of the Emp46/Emp47 complex, which may adapt cargo including glycoproteins to the COPII coat for ER exit (Sato and Nakano, 2002). Ssp120 has a similar domain structure to human MCFD2, a protein that links a subset of glycoproteins to the human Emp47 homolog LMAN1, suggesting a similar function (Nyfeler *et al.*, 2006). However, the regions of Ssp120 and MCFD2 required for Emp47 or LMAN1 binding were different. While no Ssp120 cargo interactions were identified, an *ssp120* strain was sensitive to calcium to a similar extent as *emp47* and *emp47 ssp120* strains, consistent with a role for Ssp120 in recognizing a cargo required for calcium homeostasis. Together, these results indicate Emp46/Emp47/Ssp120 form a conserved complex that may adapt cargo to COPII.

This study also demonstrated that an interaction between Rab5-family GEFs and retromer likely plays a role in retromer recruitment to endosomes. Both Muk1 and Vps9 were found to interact with retromer and the presence of at least one VPS9 domain-containing Rab5-family GEF was required for recruitment of retromer to endosomes. Furthermore, a third putative Rab5-family GEF named Vrl1 was identified that could recruit retromer in a *muk1 vps9* strain. The Rab5-family GEFs appear to act through Rab5-family GTPases to drive the endosomal recruitment of Vps34 and subsequent PI3P production. We propose that the retromer-GEF interaction results in local PI3P production, which allows efficient retromer recruitment. Together the experiments in

this study reveal the complexity of cargo adaptors and present a strategy for efficient recruitment.

4.2 Functional relevance of Ssp120 in the Emp46/Emp47 complex

Ssp120/Emp46/Emp47 were found to form a complex required for tolerance of high calcium concentrations. We hypothesize that Ssp120 may bind a subset of Emp46/Emp47 cargo, but this is currently difficult to test as the cargo bound by the complex have not been identified. The original study that found a role for Emp46/Emp47 in ER export captured radiolabeled secreted glycoproteins using concanavalin A (ConA) sepharose and ran the captured proteins on an SDS-PAGE gel (Sato and Nakano, 2002). Compared to the wild type strain, *emp46* and *emp47* strains lacked several bands, leading the authors to conclude the proteins are important for the secretion of a subset of glycoproteins. Repeating the experiment with an *ssp120* strain could identify glycoproteins that require Ssp120 for secretion, though the identity of the bands would be unknown. A stable isotope labeling by amino acids in cell culture (SILAC) mass spectrometry-based approach could identify the cargo. Here, either *emp47* or *ssp120* yeast would be grown in normal media whereas wild type yeast would be grown in the presence of heavy, ¹³C-labeled amino acids. After incorporation of the amino acid, the media derived from both light and heavy labeled cells would be combined. Secreted glycoproteins would then be captured by ConA sepharose, eluted and peptides with different abundances between the samples would be identified using mass spectrometry. This experiment may allow the identification of a comprehensive set of secreted glycoproteins transported by the Emp47-based complex. Alternatively, recent advances in automated microscopy and image analysis (Herzig *et al.*, 2012) have made it possible to screen for the cargo of membrane trafficking pathways by looking for

disruptions in the localization of GFP-tagged proteins upon deletion of a protein involved in the pathway. This approach could be used to identify Emp46/Emp47 and Ssp120 cargo.

It is striking that both Emp47 and its human homolog LMAN1 bind proteins with similar domains, Ssp120 and MCFD2 respectively. However, Ssp120 may have a different function. Ssp120 contains two EF-hand calcium binding domains that, unlike the MCFD2 and LMAN1 interaction (Wigren *et al.*, 2010), are not necessary for binding to Emp47. Thus, an alternate hypothesis for the function of Ssp120 is that it uses its EF-hands to buffer calcium, directly contributing to calcium homeostasis. Interestingly, a BLAST search suggests that another possible human homolog of Ssp120 is nucleobindin, a luminal Golgi resident that appears to be the major Ca^{2+} binding protein at the Golgi (Lin *et al.*, 1998). If Ssp120 interacts with calcium to a similar extent, it may play an important role in calcium homeostasis. Future experiments should probe Ssp120 calcium binding in Golgi fractions by $^{45}\text{Ca}^{2+}$ overlay. In addition, the ability of overexpressed Emp47 and Ssp120 to rescue growth on media with high calcium concentrations should be tested to determine if Emp47/Ssp120 are directly responsible for calcium homeostasis. Furthermore, the calcium sensitivity of Ssp120 EF-hand calcium binding mutants should be tested.

4.3 Rab regulators in retromer recruitment

This study found that retromer physically interacts with the Rab5-family GEFs Muk1 and Vps9, and that these GEFs are required for normal retromer recruitment. However, the details of these interactions remain to be elucidated. Both the cross-linking co-immunoprecipitation and iMYTH experiments do not exclude the possibility of an indirect interaction between the GEFs and

retromer. To show a direct interaction, *E. coli* could be used to express maltose binding protein (MBP)-tagged GEFs and FLAG tagged retromer CSC, and the ability of MBP-GEFs to pull down FLAG-CSC could be probed. The difficulty with this approach is that the subunits of the CSC must be expressed together to fold properly, which requires a complicated construct such as that used in Tabuchi *et al.* (Tabuchi *et al.*, 2010). Another approach is to delete retromer subunits in the retromer-Cub iMYTH strains to test which are required for the interaction. Preliminary iMYTH results suggest that the GEFs may contact retromer through more than one subunit, including Vps29. Interestingly, the human Rab5 GEF VARP binds Vps29, suggesting conservation of the retromer-GEF interaction (Hesketh *et al.*, 2014). Once the subunit(s) that mediate the interaction are identified, a mutational analysis can be carried out to find the specific GEF-binding site on the retromer subunit(s). Studying the resultant strains that express a form of retromer unable to interact with the Rab5-family GEFs will allow us to assess the function of the interactions without the confounding factors associated with deletion of the GEFs.

Based on microscopy of Vps34-GFP (Figure 3.6 D), both Rab5-family GTPases and GEFs appear to be required for the endosomal localization of Vps34-GFP. As VPS34 is a Rab5 effector in humans (Christoforidis *et al.*, 1999), it is not surprising that the Rab5-family GTPases localize yeast Vps34. A co-immunoprecipitation would provide further evidence that Vps34 is a yeast Rab5-family GTPase effector. The mislocalization of Vps34-GFP in a *muk1 vps9* strain, combined with the inability of a constitutively active Rab5 GTPase, Vps21(Q66L) to localize retromer in a *muk1 vps9* strain, strongly suggests the GEFs localize the Rab5 GTPases. This result agrees with findings that GEFs play a critical role in localizing the Rab Ypt7 (Cabrera and Ungermann, 2013) and human Rab5 (Blümer *et al.*, 2013), but contrasts the need for the human

GDF Yip3 in Rab9 recruitment to endosomes (Sivars *et al.*, 2003). Some yeast Ypt-interacting proteins (YIPs) likely act as GDFs (Pfeffer and Aivazian, 2004) though only one, Yip1, is essential and it has been assigned a role in COPII trafficking (Heidtman *et al.*, 2003). To confirm that GDFs are not required for recruitment of Rab5-family GTPases, the localization of GFP-tagged Rabs could be assessed in YIP deletions. Furthermore, a knock-sideways approach similar to that used by Blümer *et al.* (Blümer *et al.*, 2013) could be taken. Here, a heterodimerization system would be used to pull Rab5-family GEFs to the mitochondria and probe their ability to recruit GFP-tagged Rab5-family GTPases independent of other endosomal factors, which would not be present on the mitochondrial membrane.

It is interesting to consider why retromer is not recruited to the vacuole in a *muk1 vps9* background even though Vps34-GFP localizes to the vacuolar limiting membrane and produces PI3P (Figure 3.6 C). The local PI3P synthesis model suggests that retromer is not recruited because the Rab5-family GEFs are needed to generate the high degree of local PI3P enrichment required for retromer tubule formation. Therefore, when Vps34 is recruited to the vacuolar membrane in the absence of the GEFs, likely through a Atg14-dependent autophagic pathway (Kihara *et al.*, 2001), it may not be producing a high enough concentration of PI3P to drive retromer recruitment. Furthermore, when an active form of Vps21 was overexpressed in strains lacking the GEFs, Vps26 recruitment to the vacuolar rim was enhanced, even though we did not observe enhanced puncta formation. These observations suggest that if enough PI3P is present at the vacuole, retromer may be recruited there. Consistent with this observation, a retromer-based trafficking pathway from the vacuole has recently been identified (Arlt *et al.*, 2015). Other factors may also contribute to the lack of Vps26 recruitment to the vacuole in a *muk1 vps9* strain.

For example, tubule formation is believed to involve ordered assembly of BAR domains at areas of high membrane curvature, and it's possible that the lipid composition of the vacuolar membrane in the absence of Rab5-family GEFs does not allow sufficient membrane curvature.

The results of this study provide further evidence that Rabs and their regulators are involved in retromer recruitment. In humans, retromer interacts with the Rab5 GEF VARP (Hesketh *et al.*, 2014), the Rab5 effector Rabankyrin-5 (Zhang *et al.*, 2012), Rab7 (Rojas *et al.*, 2008) and a putative Rab7 GAP TBC1D5 (Seaman *et al.*, 2009). Thus, retromer interacts with Rab regulators at various stages of endosomal maturation. What is the advantage of these interactions? To some extent the indirect interactions with Rab5 and the direct interaction with Rab7 (Rojas *et al.*, 2008) could facilitate the observed peak in retromer recruitment at the Rab transition (van Weering *et al.*, 2012b). It would also be interesting to know if any interaction sites on retromer are obscured when it forms tubules, which could drive spatial segregation. For example, perhaps Rab7 is involved in CSC recruitment to the base of a tubule, but once the CSC enters the tubule TBC1D5 activates the Rab so it can cycle off the tubule. Also, the retromer-GEF interaction may remove the GEFs from endosomes, allowing a Rab conversion. Studies probing the localization of Rabs and Rab regulators in retromer tubules should be able to identify any spatial segregation.

The interactions between retromer and Rab5-family GEFs identified in this study may provide insight into etiology of some diseases. The VPS35 D620N mutation has been linked to a rare autosomal dominant form of late onset Parkinson disease (Vilariño-Güell *et al.*, 2011). Currently there is debate in the field about the effect of the mutation. Some groups have found it disrupts the association of the actin nucleating Wiskott-Aldrich syndrome protein and scar homolog

(WASH) complex, preventing efficient retromer tubule scission (McGough *et al.*, 2014; Zavodszky *et al.*, 2014), whereas another group found that WASH and retromer still interact and colocalize (Follett *et al.*, 2014). The D620N mutation is near the VPS35-VPS29 interaction interface and the Rab5 GEF VARP binds VPS29 (Hesketh *et al.*, 2014). Therefore, another possible effect of the D620N mutation is that it disrupts retromer-GEF interactions causing defects in specific retromer functions. This hypothesis could be tested by pulldown experiments with wild type and mutant retromer. If interactions between retromer and other human Rab5 GEFs are identified, they could provide further insights into disease. In particular, alsin is a Rab5 GEF whose dysfunction has been linked to amyotrophic lateral sclerosis (ALS), but has a poorly defined function at endosomes (Chandran *et al.*, 2007). It would be interesting to test if alsin can interact with retromer and if mutant alsin disrupts retromer function. As mutations in both alsin and strumpellin, a component of the WASH complex, are linked to hereditary spastic paraplegia (HSP) (Harbour *et al.*, 2010), it is tempting to speculate that they may each cause a specific disruption of retromer function.

4.4 Vrl1 as a putative Rab5-family GEF

This study identified Vrl1 as a new VPS9-domain containing protein present in some *Saccharomyces cerevisiae* strains and other related fungi. Furthermore, Vrl1 was able to rescue the high temperature growth and retromer localization defects of a *muk1 vps9* strain in a manner dependent on a predicted key catalytic residue, D373, identified by homology with Rab5-family GEFs. Together, these results strongly suggest Vrl1 is a new yeast Rab5-family GEF. However, *in vitro* studies are required to confirm that Vrl1 has Rab5-family GEF activity. One such assay is based on loading purified Rab GTPases with the fluorescent GDP analogue Mant-GDP

(Davies *et al.*, 2005). Loaded Mant-GDP can be detected by Fluorescence Resonance Energy Transfer (FRET) with a tryptophan residue in the Rab. If Vrl1 is a Rab5-family GEF, in the presence of GTP it should preferentially catalyze the replacement of Mant-GDP with GTP on Rab5-family GTPases.

The three yeast VPS9 domain-containing proteins have both overlapping and unique functions. Specifically, while the proteins were generally redundant, only Vps9 appeared to be critical for CPY sorting (Figure 3.2 C). Recently, Shideler *et al.* found that the function of Vps9 in vacuolar protein sorting is dependent on its ubiquitin-binding CUE domain and that a Muk1-CUE domain fusion can rescue vacuolar protein sorting in a *vps9* strain (Shideler *et al.*, 2015). This stresses the importance of other domains in directing the VPS9-domain GEF activity. It will be important to identify the interaction that recruits Muk1 to endosomes. Furthermore, it is worth testing if Muk1, Vps9 and Vrl1 are in distinct locations, as one possible explanation for the existence of three yeast Rab5-family GEFs is that they can direct Rab5-family GTPases to different locations in order to perform unique functions.

Given the extensive conserved regions in Vrl1 outside of its VPS9 domain, it is interesting to speculate on what unique functions it may have. It has a similar organization to human VARP, which mediates a retromer-dependent endosome to plasma membrane trafficking pathway that has not been identified in yeast (Hesketh *et al.*, 2014). A tempting hypothesis is that Vrl1 drives a similar pathway in yeast. This would require an interaction with retromer, which we were unable to detect, though this was likely due to the low level of Vrl1 expression and the detection limits of our assays. Evidence for such a pathway would include increased surface levels of a

subset of plasma membrane proteins in lab strains expressing Vrl1, as they would be more rapidly recycled from endosomes. In particular, nutrient transporters might be affected as GLUT1 has been identified as cargo in humans (Hesketh *et al.*, 2014). The absence of Vrl1 specifically in lab strains suggests that its expression may result in a phenotype that was selected against when isolating those strains, such as flocculation. One hypothesis following this reasoning is that Vrl1 pathway maintains the surface levels of the lectins involved in flocculation (Goossens and Willaert, 2010). Here, expression of Vrl1 in lab strains should increase flocculation and deletion of *VRL1* in other strains should reduce flocculation. In the human endosome-to-plasma membrane pathway VARP links the v-SNARE VAMP7 to retromer-derived vesicles (Hesketh *et al.*, 2014). Therefore, yeast two-hybrid assays or dihydrofolate reductase protein complementation assays should be used to identify Vrl1 interactors, in particular SNAREs. Collectively, the above experiments will probe the existence of a yeast endosome-to-plasma membrane pathway.

4.5 Conclusions and future prospects

This study identified a novel subunit of a cargo selective adaptor and proposed a new GEF-dependent mechanism for the recruitment of a membrane trafficking complex. The discovery that Ssp120 forms a stable complex with the cargo adaptor Emp46/Emp47 suggests an evolutionary origin for the human LMAN1/MCFD2 cargo adaptor. Furthermore, future studies of the complex may provide insights into calcium homeostasis. Our finding that Rab5-family GEFs interact with retromer, and are required for its recruitment, demonstrates the important role compartment identity can play in the recruitment of membrane trafficking complexes. As the interaction between retromer and VARP (Hesketh *et al.*, 2014) suggests that retromer-GEF

interactions are conserved in humans, it will be important to assess if disruptions of these interactions contribute to disease.

Future work should focus on the functional characterization of mammalian retromer interactions in an effort to understand the contributions of retromer to endosome integrity and disease. In particular VPS29 and C-terminal end of VPS35, which it interacts with, are emerging as important interaction interfaces. For example, on VPS29 there is a hydrophobic patch that has been shown to interact with the membrane-deforming sorting nexins (Swarbrick *et al.*, 2011), the putative Rab7 GAP TBC1D5 (Harbour *et al.*, 2010) and the Rab GEF VARP (Hesketh *et al.*, 2014). Interestingly, preliminary iMYTH-based experiments suggest that Muk1 also interacts with yeast Vps29 indicating that the retromer-GEF interaction site may be conserved. The convergence of so many interactions on a relatively small region of retromer could allow spatial and temporal control of the complex by allowing a given binding partner to exclude other interactions. In particular, the interactions with VARP and TBC1D5, which are likely mutually exclusive as they are disrupted by the same point mutation (Swarbrick *et al.*, 2011; Hesketh *et al.*, 2014), could play roles in retromer recruitment and fission respectively as discussed earlier. Furthermore, interactions between retromer and the Rab regulators could be involved in maintaining endosome size by linking membrane removal through retromer-driven vesicle formation to Rab5-driven fusion with endosomes. It may be that disruption of these interactions leads to a loss of endosomal integrity that could play a role in diseases linked to retromer. Thorough investigation of retromer interactions will shed light on the mechanisms behind several neurological diseases including Parkinson disease, amyotrophic lateral sclerosis and hereditary spastic paraplegia.

References

- Aguilar, P. S. *et al.* (2010). A plasma-membrane E-MAP reveals links of the eisosome with sphingolipid metabolism and endosomal trafficking. *Nat. Struct. Mol. Biol.* *17*, 901–908.
- Angers, C. G., and Merz, A. J. (2009). HOPS Interacts with Apl5 at the Vacuole Membrane and Is Required for Consumption of AP-3 Transport Vesicles. *Mol. Cell. Biol.* *20*, 4563–4574.
- Antonny, B., Vanni, S., Shindou, H., and Ferreira, T. (2015). From zero to six double bonds: phospholipid unsaturation and organelle function. *Trends Cell Biol.* *25*, 427–436.
- Arlt, H., Reggiori, F., and Ungermann, C. (2015). Retromer and the dynamin Vps1 cooperate in the retrieval of transmembrane proteins from vacuoles. *J. Cell Sci.* *128*, 645–645.
- Attar, N., and Cullen, P. J. (2010). The retromer complex. *Adv. Enzyme Regul.* *50*, 216–236.
- Babu, M. *et al.* (2012). Interaction landscape of membrane-protein complexes in *Saccharomyces cerevisiae*. *Nature* *489*, 585–589.
- Babu, M., Krogan, N. J., Awrey, D. E., Emili, A., and Greenblatt, J. F. (2009). Yeast Functional Genomics and Proteomics. *Methods Mol. Biol.* *548*, 187–208.
- Backer, J. M. (2008). The regulation and function of Class III PI3Ks: novel roles for Vps34. *Biochem. J.* *410*, 1–17.
- Balaji, K., Mooser, C., Janson, C. M., Bliss, J. M., Hojjat, H., and Colicelli, J. (2012). RIN1 orchestrates the activation of RAB5 GTPases and ABL tyrosine kinases to determine the fate of EGFR. *J. Cell Sci.* *125*, 5887–5896.
- Balderhaar, H., Arlt, H., Ostrowicz, C., Brocker, C., Sundermann, F., Brandt, R., Babst, M., and Ungermann, C. (2010). The Rab GTPase Ypt7 is linked to retromer-mediated receptor recycling and fusion at the yeast late endosome. *J. Cell Sci.* *123*, 4085–4094.
- Bao, L., Redondo, C., Findlay, J. B. C., Walker, J. H., and Ponnambalam, S. (2009). Deciphering soluble and membrane protein function using yeast systems (Review). *Mol. Membr. Biol.* *26*, 127–135.
- Barlowe, C., Enfertn, C., and Schekman, R. (1993). Purification and Characterization of SARlp, a Small GTP-binding Protein Required for Transport Vesicle Formation from the Endoplasmic Reticulum. *J. Biol. Chem.* *268*, 873–879.

- Barlowe, C., Or, L., Yeung, T., Salama, N., Rexach, M. F., Ravazzola, M., Amherdt, M., and Schekman, R. (1994). COPII : A Membrane Coat Formed by Set Proteins That Drive Vesicle Budding from the Endoplasmic Reticulum. *Cell* 77, 895–907.
- Barlowe, C., and Schekman, R. (1993). SEC12 encodes a guanine-nucleotide-exchange factor essential for transport vesicle budding from the ER. *Nature* 365, 347–349.
- Belden, W. J., and Barlowe, C. (2001). Role of erv29 in Collecting Soluble Secretory Proteins into ER-Derived Transport Vesicles. *Science* (80-.). 294, 1528–1531.
- Bi, X., Corpina, R. A., and Goldberg, J. (2002). Structure of the Sec23/24–Sar1 pre-budding complex of the COPII vesicle coat. *Nature*, 271–277.
- Bi, X., Mancias, J. D., and Goldberg, J. (2007). Insights into COPII coat nucleation from the structure of Sec23.Sar1 complexed with the active fragment of Sec31. *Dev. Cell* 13, 635–645.
- Blümer, J., Rey, J., Dehmelt, L., Mazel, T., Wu, Y.-W., Bastiaens, P., Goody, R. S., and Itzen, A. (2013). RabGEFs are a major determinant for specific Rab membrane targeting. *J. Cell Biol.* 200, 287–300.
- Bonifacino, J., and Hurley, J. (2008). Retromer. *Curr. Opin. Cell Biol.* 20, 427–436.
- Bonifacino, J., and Rojas, R. (2006). Retrograde transport from endosomes to the trans-Golgi network. *Nat. Rev. Mol. Cell Biol.* 7, 568–579.
- Boyadjiev, S. a *et al.* (2006). Cranio-lenticulo-sutural dysplasia is caused by a SEC23A mutation leading to abnormal endoplasmic-reticulum-to-Golgi trafficking. *Nat. Genet.* 38, 1192–1197.
- Braun, V., Wong, A., Landekic, M., Hong, W., Grinstein, S., and Brumell, J. (2010). Sorting nexin 3 (SNX3) is a component of a tubular endosomal network induced by Salmonella and involved in maturation of the Salmonella-containing vacuole. *Cell. Microbiol.* 12, 1352–1367.
- Brett, C. L., Plemel, R. L., Lobingier, B. T., Lobinger, B. T., Vignali, M., Fields, S., and Merz, A. J. (2008). Efficient termination of vacuolar Rab GTPase signaling requires coordinated action by a GAP and a protein kinase. *J. Cell Biol.* 182, 1141–1151.
- Brigance, W. T., Barlowe, C., and Graham, T. R. (2000). Organization of the yeast Golgi complex into at least four functionally distinct compartments. *Mol. Biol. Cell* 11, 171–182.
- Bröcker, C., Kuhlee, A., Gatsogiannis, C., Balderhaar, H. J. K., Hönscher, C., Engelbrecht-Vandré, S., Ungermann, C., and Raunser, S. (2012). Molecular architecture of the multisubunit homotypic fusion and vacuole protein sorting (HOPS) tethering complex. *Proc. Natl. Acad. Sci. U. S. A.* 109, 1991–1996.

- Burd, C., and Cullen, P. J. (2014). Retromer: A Master Conductor of Endosome Sorting. *Cold Spring Harb. Perspect. Biol.* *6*, 1–13.
- Burda, P., Padilla, S. M., Sarkar, S., and Emr, S. D. (2002). Retromer function in endosome-to-Golgi retrograde transport is regulated by the yeast Vps34 PtdIns 3-kinase. *J. Cell Sci.* *115*, 3889–3900.
- Burgo, A., Proux-Gillardeaux, V., Sotirakis, E., Bun, P., Casano, A., Verraes, A., Liem, R. K. H., Formstecher, E., Coppey-Moisan, M., and Galli, T. (2012). A Molecular Network for the Transport of the TI-VAMP/VAMP7 Vesicles from Cell Center to Periphery. *Dev. Cell* *23*, 166–180.
- Burgo, A., Sotirakis, E., Simmler, M.-C., Verraes, A., Chamot, C., Simpson, J. C., Lanzetti, L., Proux-Gillardeaux, V., and Galli, T. (2009). Role of Varp, a Rab21 exchange factor and TI-VAMP/VAMP7 partner, in neurite growth. *EMBO Rep.* *10*, 1117–1124.
- Burri, L., and Lithgow, T. (2004). A Complete Set of SNAREs in Yeast. *Traffic* *5*, 45–52.
- Burston, H., Maldonado-Baez, L., Davey, M., Montpetit, B., Schluter, C., Wendland, B., and Conibear, E. (2009). Regulators of yeast endocytosis identified by systematic quantitative analysis. *J. Cell Biol.* *185*, 1097–1110.
- Cabrera, M., Arlt, H., Epp, N., Lachmann, J., Griffith, J., Perz, A., Reggiori, F., and Ungermann, C. (2013). Functional separation of endosomal fusion factors and the class C core vacuole/endosome tethering (CORVET) complex in endosome biogenesis. *J. Biol. Chem.* *288*, 5166–5175.
- Cabrera, M., and Ungermann, C. (2013). Guanine Nucleotide Exchange Factors (GEFs) Have a Critical but Not Exclusive Role in Organelle Localization of Rab GTPases. *J. Biol. Chem.* *288*, 28704–28712.
- Cai, Y. *et al.* (2008). The structural basis for activation of the Rab Ypt1p by the TRAPP membrane-tethering complexes. *Cell* *133*, 1202–1213.
- Carney, D. S., Davies, B. A., and Horazdovsky, B. F. (2006). Vps9 domain-containing proteins: activators of Rab5 GTPases from yeast to neurons. *Trends Cell Biol.* *16*, 27–35.
- Chandran, J., Ding, J., and Cai, H. (2007). Alsin and the Molecular Pathways of Amyotrophic Lateral Sclerosis. *Mol. Neurobiol.* *36*, 224–231.
- Chen, Y. A., and Scheller, R. H. (2001). SNARE-mediated membrane fusion. *Nat. Rev. Mol. Cell Biol.* *2*, 98–106.

Chi, R. J., Liu, J., West, M., Wang, J., Odorizzi, G., and Burd, C. G. (2014). Fission of SNX-BAR-coated endosomal retrograde transport carriers is promoted by the dynamin-related protein Vps1. *J. Cell Biol.* *204*, 793–806.

Christoforidis, S., Miaczynska, M., Ashman, K., Wilm, M., Zhao, L., Yip, S. C., Waterfield, M. D., Backer, J. M., and Zerial, M. (1999). Phosphatidylinositol-3-OH kinases are Rab5 effectors. *Nat. Cell Biol.* *1*, 249–252.

Collins, S. R. *et al.* (2007a). Functional dissection of protein complexes involved in yeast chromosome biology using a genetic interaction map. *Nature* *446*, 806–810.

Collins, S. R., Kemmeren, P., Zhao, X.-C., Greenblatt, J. F., Spencer, F., Holstege, F. C. P., Weissman, J. S., and Krogan, N. J. (2007b). Toward a comprehensive atlas of the physical interactome of *Saccharomyces cerevisiae*. *Mol. Cell. Proteomics* *6*, 439–450.

Conibear, E., and Stevens, T. (2002). Studying Yeast Vacuoles. *Methods Enzymol.* *351*, 408–432.

Conibear, E., and Stevens, T. H. (2000). Vps52p, Vps53p, and Vps54p Form a Novel Multisubunit Complex Required for Protein Sorting at the Yeast Late Golgi. *Mol. Biol. Cell* *11*, 305–323.

Čopič, A., Starr, T., and Schekman, R. (2007). Ent3p and Ent5p Exhibit Cargo-specific Functions in Trafficking Proteins between the Trans-Golgi Network and the Endosomes in Yeast. *Mol. Biol. Cell* *18*, 1803–1815.

Costaguta, G., Stefan, C. J., Bensen, E. S., Emr, S. D., and Payne, G. S. (2001). Yeast Gga coat proteins function with clathrin in Golgi to endosome transport. *Mol. Biol.* *12*, 1885–1896.

Costanzo, M. *et al.* (2010). The genetic landscape of a cell. *Science* (80-.). *327*, 425–432.

Cowles, C. R., Odorizzi, G., Payne, G. S., and Emr, S. D. (1997). The AP-3 Adaptor Complex Is Essential for Cargo-Selective Transport to the Yeast Vacuole. *Cell* *91*, 109–118.

Cozier, G. E., Carlton, J., McGregor, A. H., Gleeson, P. a, Teasdale, R. D., Mellor, H., and Cullen, P. J. (2002). The phox homology (PX) domain-dependent, 3-phosphoinositide-mediated association of sorting nexin-1 with an early sorting endosomal compartment is required for its ability to regulate epidermal growth factor receptor degradation. *J. Biol. Chem.* *277*, 48730–48736.

Cullen, P. J., and Korswagen, H. C. (2012). Sorting nexins provide diversity for retromer-dependent trafficking events. *Nat. Cell Biol.* *14*, 29–37.

Davies, B. a, Topp, J. D., Sfeir, A. J., Katzmann, D. J., Carney, D. S., Tall, G. G., Friedberg, A. S., Deng, L., Chen, Z., and Horazdovsky, B. F. (2003). Vps9p CUE domain ubiquitin binding is required for efficient endocytic protein traffic. *J. Biol. Chem.* *278*, 19826–19833.

Davies, B. A., Carney, D. S., and Horazdovsky, B. F. (2005). Ubiquitin regulation of the Rab5 family GEF Vps9p. *Methods Enzymol.* *403*, 561–583.

De, M., Abazeed, M. E., and Fuller, R. S. (2012). Direct binding of the Kex2p cytosolic tail to the VHS domain of yeast Gga2p facilitates TGN to prevacuolar compartment transport and is regulated by phosphorylation. *Mol. Biol. Cell* *24*, 495–509.

Delprato, A., and Lambright, D. (2007). Structural basis for Rab GTPase activation by VPS9 domain exchange factors. *Nat. Struct. Mol. Biol.* *14*, 406–412.

Demmel, L. *et al.* (2008). The clathrin adaptor Gga2p is a phosphatidylinositol 4-phosphate effector at the Golgi exit. *Mol. Biol. Cell* *19*, 1991–2002.

Denks, K., Vogt, A., Sachelaru, I., Petriman, N.-A., Kudva, R., and Koch, H.-G. (2014). The Sec translocon mediated protein transport in prokaryotes and eukaryotes. *Mol. Membr. Biol.* *31*, 58–84.

Donaldson, K. M., Yin, H., Gekakis, N., Supek, F., and Joazeiro, C. a P. (2003). Ubiquitin signals protein trafficking via interaction with a novel ubiquitin binding domain in the membrane fusion regulator, Vps9p. *Curr. Biol.* *13*, 258–262.

Enright, A. J., Dongen, S. Van, and Ouzounis, C. A. (2002). An efficient algorithm for large-scale detection of protein families. *Nucleic Acids Res.* *30*, 1575–1584.

Fjorback, A. W. *et al.* (2012). Retromer binds the FANSHY sorting motif in SorLA to regulate amyloid precursor protein sorting and processing. *J. Neurosci.* *32*, 1467–1480.

Flinn, R. J., and Backer, J. M. (2010). mTORC1 signals from late endosomes: Taking a TOR of the endocytic system. *Cell Cycle* *9*, 1869–1870.

Follett, J. *et al.* (2014). The Vps35 D620N Mutation Linked to Parkinson’s Disease Disrupts the Cargo Sorting Function of Retromer. *Traffic* *15*, 230–244.

Froissard, M., Belgareh-Touzé, N., Dias, M., Buisson, N., Camadro, J.-M., Haguenaer-Tsapis, R., and Lesuisse, E. (2007). Trafficking of siderophore transporters in *Saccharomyces cerevisiae* and intracellular fate of ferrioxamine B conjugates. *Traffic* *8*, 1601–1616.

Fromme, J. C., Ravazzola, M., Hamamoto, S., Al-Balwi, M., Eyaid, W., Boyadjiev, S. a, Cosson, P., Schekman, R., and Orci, L. (2007). The genetic basis of a craniofacial disease provides insight into COPII coat assembly. *Dev. Cell* *13*, 623–634.

- Garrett, M. D., Zahner, J. E., Cheney, C. M., and Novick, P. J. (1994). GDI1 encodes a GDP dissociation inhibitor that plays an essential role in the yeast secretory pathway. *EMBO J.* *13*, 1718–1728.
- Gary, J. D., Wurmser, A. E., Bonangelino, C. J., Weisman, L. S., and Emr, S. D. (1998). Fab1p Is Essential for PtdIns(3)P 5-Kinase Activity and the Maintenance of Vacuolar Size and Membrane Homeostasis. *J. Cell Biol.* *143*, 65–79.
- Gavin, A.-C. *et al.* (2006). Proteome survey reveals modularity of the yeast cell machinery. *Nature* *440*, 631–636.
- Gaynor, E. C., Graham, T. R., and Emr, S. D. (1998). COPI in ER/Golgi and intra-Golgi transport: do yeast COPI mutants point the way? *Biochim. Biophys. Acta* *1404*, 33–51.
- Gelperin, D. M. *et al.* (2005). Biochemical and genetic analysis of the yeast proteome with a movable ORF collection. 2816–2826.
- Gerke, V., Creutz, C. E., and Moss, S. E. (2005). Annexins: linking Ca²⁺ signalling to membrane dynamics. *Nat. Rev. Mol. Cell Biol.* *6*, 449–461.
- Ghaemmaghani, S., Huh, W.-K., Bower, K., Howson, R. W., Belle, A., Dephoure, N., O’Shea, E. K., and Weissman, J. S. (2003). Global analysis of protein expression in yeast. *Nature* *425*, 737–741.
- Giraud, C. G., and Maccioni, H. J. F. (2003). Endoplasmic Reticulum Export of Glycosyltransferases Depends on Interaction of a Cytoplasmic Dibasic Motif with Sar1. *Mol. Biol. Cell* *14*, 3753–3766.
- De Godoy, L. M. F., Olsen, J. V., Cox, J., Nielsen, M. L., Hubner, N. C., Fröhlich, F., Walther, T. C., and Mann, M. (2008). Comprehensive mass-spectrometry-based proteome quantification of haploid versus diploid yeast. *Nature* *455*, 1251–1254.
- Gomez, T. S., and Billadeau, D. D. (2009). A FAM21-containing WASH complex regulates retromer-dependent sorting. *Dev. Cell* *17*, 699–711.
- Goossens, K., and Willaert, R. (2010). Flocculation protein structure and cell-cell adhesion mechanism in *Saccharomyces cerevisiae*. *Biotechnol. Lett.* *32*, 1571–1585.
- Gough, J., Karplus, K., Hughey, R., and Chothia, C. (2001). Assignment of homology to genome sequences using a library of hidden Markov models that represent all proteins of known structure. *J. Mol. Biol.* *313*, 903–919.
- Gutsche, W. (1991). Mark D. Rose, Fred Winston and Philip Hieter, *Methods in Yeast Genetics*. *J. Basic Microbiol.* *31*, 399.

- Hammer, J. a, and Sellers, J. R. (2012). Walking to work: roles for class V myosins as cargo transporters. *Nat. Rev. Mol. Cell Biol.* *13*, 13–26.
- Harbour, M., Breusegem, S., Antrobus, R., Freeman, C., Reid, E., and Seaman, M. (2010). The cargo-selective retromer complex is a recruiting hub for protein complexes that regulate endosomal tubule dynamics. *J. Cell Sci.* *123*, 3703–3717.
- Harbour, M. E., Breusegem, S. Y., and Seaman, M. N. J. (2012). Recruitment of the endosomal WASH complex is mediated by the extended “tail” of Fam21 binding to the retromer protein Vps35. *Biochem. J.* *442*, 209–220.
- Harrison, M. S., Hung, C.-S., Liu, T., Christiano, R., Walther, T. C., and Burd, C. G. (2014). A mechanism for retromer endosomal coat complex assembly with cargo. *Proc. Natl. Acad. Sci. U. S. A.* *111*, 267–272.
- Harterink, M. *et al.* (2011). A SNX3-dependent retromer pathway mediates retrograde transport of the Wnt sorting receptor Wntless and is required for Wnt secretion. *Nat. Cell Biol.* *13*, 914–923.
- Heidtman, M., Chen, C. Z., Collins, R. N., and Barlowe, C. (2003). A role for Yip1p in COPII vesicle biogenesis. *J. Cell Biol.* *163*, 57–69.
- Helenius, A., and Aebi, M. (2004). Roles of N-linked glycans in the endoplasmic reticulum. *Annu. Rev. Biochem.* *73*, 1019–1049.
- Herzig, Y., Sharpe, H. J., Elbaz, Y., Munro, S., and Schuldiner, M. (2012). A systematic approach to pair secretory cargo receptors with their cargo suggests a mechanism for cargo selection by Erv14. *PLoS Biol.* *10*, e1001329.
- Hesketh, G. G. *et al.* (2014). VARP Is Recruited on to Endosomes by Direct Interaction with Retromer, Where Together They Function in Export to the Cell Surface. *Dev. Cell*, 1–16.
- Hettema, E. H., Lewis, M. J., Black, M. W., and Pelham, H. R. (2003). Retromer and the sorting nexins Snx4/41/42 mediate distinct retrieval pathways from yeast endosomes. *EMBO J.* *22*, 548–557.
- Hierro, A., Rojas, A., Rojas, R., Murthy, N., Effantin, G., Kajava, A., Steven, A., Bonifacino, J., and Hurley, J. (2007). Functional architecture of the retromer cargo-recognition complex. *Nature* *449*, 1063–1067.
- Horiuchi, H. *et al.* (1997). A novel Rab5 GDP/GTP exchange factor complexed to Rabaptin-5 links nucleotide exchange to effector recruitment and function. *Cell* *90*, 1149–1159.
- Hsu, V., Lee, S., and Yang, J. (2009). The evolving understanding of COPI vesicle formation. *Nat. Rev. Mol. Cell Biol.* *1*, 33–51.

- Huh, W. K., Falvo, J. V., Gerke, L. C., Carroll, A. S., Howson, R. W., Weissman, J. S., and O'Shea, E. K. (2003). Global analysis of protein localization in budding yeast. *Nature* *425*, 686–691.
- Huotari, J., and Helenius, A. (2011). Endosome maturation. *EMBO J.* *30*, 3481–3500.
- Hutagalung, A. H., and Novick, P. J. (2011). Role of Rab GTPases in Membrane Traffic and Cell Physiology. *Physiol. Rev.* *91*, 119–149.
- Jahn, R., and Scheller, R. H. (2006). SNAREs--engines for membrane fusion. *Nat. Rev. Mol. Cell Biol.* *7*, 631–643.
- James, P., Halladay, J., and Craig, E. A. (1996). Genomic Libraries and a Host Strain Designed for Highly Efficient Two-Hybrid selection in Yeast. *Genetics* *144*, 1425–1436.
- Janke, C. *et al.* (2004). A versatile toolbox for PCR-based tagging of yeast genes: new fluorescent proteins, more markers and promoter substitution cassettes. *Yeast* *21*, 947–962.
- Jensen, D., and Schekman, R. (2011). COPII-mediated vesicle formation at a glance. *J. Cell Sci.* *124*, 1–4.
- Jia, D., Gomez, T. S., Billadeau, D. D., and Rosen, M. K. (2012). Multiple repeat elements within the FAM21 tail link the WASH actin regulatory complex to the retromer. *Mol. Biol. Cell* *23*, 2352–2361.
- Jin, L., Pahuja, K. B., Wickliffe, K. E., Gorur, A., Baumgärtel, C., Schekman, R., and Rape, M. (2012). Ubiquitin-dependent regulation of COPII coat size and function. *Nature* *482*, 495–500.
- John Peter, A. T., Lachmann, J., Rana, M., Bunge, M., Cabrera, M., and Ungermann, C. (2013). The BLOC-1 complex promotes endosomal maturation by recruiting the Rab5 GTPase-activating protein Msb3. *J. Cell Biol.* *201*, 97–111.
- Jones, B. *et al.* (2003). Mutations in a Sar1 GTPase of COPII vesicles are associated with lipid absorption disorders. *Nat. Genet.* *34*, 29–31.
- Kaksonen, M., Toret, C. P., and Drubin, D. G. (2005). A modular design for the clathrin- and actin-mediated endocytosis machinery. *Cell* *123*, 305–320.
- Kihara, a, Noda, T., Ishihara, N., and Ohsumi, Y. (2001). Two distinct Vps34 phosphatidylinositol 3-kinase complexes function in autophagy and carboxypeptidase Y sorting in *Saccharomyces cerevisiae*. *J. Cell Biol.* *152*, 519–530.

- Koumandou, V. L., Klute, M. J., Herman, E. K., Nunez-Miguel, R., Dacks, J. B., and Field, M. C. (2011). Evolutionary reconstruction of the retromer complex and its function in *Trypanosoma brucei*. *J. Cell Sci.* *124*, 1496–1509.
- Krogan, N. J. *et al.* (2006). Global landscape of protein complexes in the yeast *Saccharomyces cerevisiae*. *Nature* *440*, 637–643.
- Kung, L. F. *et al.* (2012). Sec24p and Sec16p cooperate to regulate the GTP cycle of the COPII coat. *EMBO J.* *31*, 1014–1027.
- Lachmann, J., Barr, F. A., and Ungermann, C. (2012). The Msb3/Gyp3 GAP controls the activity of the Rab GTPases Vps21 and Ypt7 at endosomes and vacuoles. *Mol. Biol. Cell* *23*, 2516–2526.
- Lam, K., Davey, M., Sun, B., Roth, A., Davis, N., and Conibear, E. (2006). Palmitoylation by the DHHC protein Pfa4 regulates the ER exit of Chs3. *J. Cell Biol.* *174*, 19–25.
- Lee, M. C. S., Orci, L., Hamamoto, S., Futai, E., Ravazzola, M., and Schekman, R. (2005). Sar1p N-terminal helix initiates membrane curvature and completes the fission of a COPII vesicle. *Cell* *122*, 605–617.
- Lemmon, M. (2008). Membrane recognition by phospholipid-binding domains. *Nat. Rev. Mol. Cell Biol.* *9*, 99–111.
- Lewis, M., Nichols, B., Prescianotto-Baschong, C., Riezman, H., and Pelham, H. (2000). Specific retrieval of the exocytic SNARE Snc1p from early yeast endosomes. *Mol. Biol.* *11*, 23–38.
- Li, Z. *et al.* (2011). Systematic exploration of essential yeast gene function with temperature-sensitive mutants. *Nat. Biotechnol.* *29*, 361–367.
- Lin, P., Le-niculescu, H., Hofmeister, R., Mccaffery, J. M., Jin, M., Hennemann, H., Mcquistan, T., Vries, L. De, and Farquhar, M. G. (1998). The Mammalian Calcium-binding Protein, Nucleobindin (CALNUC), Is a Golgi Resident Protein. *J. Cell Biol.* *141*, 1515–1527.
- Liu, K., Surendhran, K., Nothwehr, S. F., and Graham, T. R. (2008). P4-ATPase Requirement for AP-1 / Clathrin Function in Protein Transport from the trans -Golgi Network and Early Endosomes. *Mol. Biol. Cell* *19*, 3526–3535.
- Liu, T. T., Gomez, T. S., Sackey, B. K., Billadeau, D. D., and Burd, C. G. (2012). Rab GTPase regulation of retromer-mediated cargo export during endosome maturation. *Mol. Biol. Cell* *23*, 2505–2515.
- Longtine, S. M., Pringle, and R. J. (1998). Additional Modules for Versatile and Economical PCR-based Gene Deletion and Modification in *Saccharomyces cerevisiae*. *Yeast* *14*, 953–961.

Lord, C., Bhandari, D., Menon, S., Ghassemian, M., Nycz, D., Hay, J., Ghosh, P., and Ferro-Novick, S. (2011). Sequential interactions with Sec23 control the direction of vesicle traffic. *Nature* 473, 181–186.

Lord, C., Ferro-novick, S., and Miller, E. A. (2013). The Highly Conserved COPII Coat Complex Sorts Cargo from the Endoplasmic Reticulum and Targets It to the Golgi. *Cold Spring Harb. Perspect. Biol.* 5, 1–13.

Losev, E., Reinke, C. a, Jellen, J., Strongin, D. E., Bevis, B. J., and Glick, B. S. (2006). Golgi maturation visualized in living yeast. *Nature* 441, 1002–1006.

Lucin, K. M. *et al.* (2013). Microglial beclin 1 regulates retromer trafficking and phagocytosis and is impaired in Alzheimer’s disease. *Neuron* 79, 873–886.

Lynch-Day, M., Bhandari, D., Menon, S., Huang, J., Cai, H., Bartholomew, C., Brumell, J., Ferro-Novick, S., and Klionsky, D. (2010). Trs85 directs a Ypt1 GEF, TRAPPIII, to the phagophore to promote autophagy. *Proc. Natl. Acad. Sci.* 107, 7811–7816.

Ma, W., and Goldberg, J. (2013). Rules for the recognition of dilysine retrieval motifs by coatomer. *EMBO J.* 32, 926–937.

Macleod, D. *et al.* (2013). RAB7L1 Interacts with LRRK2 to Modify Intraneuronal Protein Sorting and Parkinson’s Disease Risk. *Neuron* 77, 425–439.

Mamo, A., Jules, F., Dumaresq-Doiron, K., Costantino, S., and Lefrancois, S. (2012). The role of ceroid lipofuscinosis neuronal protein 5 (CLN5) in endosomal sorting. *Mol. Cell. Biol.* 32, 1855–1866.

Markgraf, D. F., Ahnert, F., Arlt, H., Mari, M., Peplowska, K., Epp, N., Griffith, J., Reggiori, F., and Ungermann, C. (2009). The CORVET subunit Vps8 cooperates with the Rab5 homolog Vps21 to induce clustering of late endosomal compartments. *Mol. Biol. Cell* 20, 5276–5289.

Mayer, A., Wickner, W., and Haas, A. (1996). Sec18p (NSF)-Driven Release of Sec17p (alpha-SNAP) Can Precede Docking and Fusion of Yeast Vacuoles. *Cell* 85, 83–94.

McGough, I., and Cullen, P. (2011). Recent Advances in Retromer Biology. *Traffic* 12, 963–971.

McGough, I. J. *et al.* (2014). Retromer binding to FAM21 and the WASH complex is perturbed by the Parkinson disease-linked VPS35(D620N) mutation. *Curr. Biol.* 24, 1670–1676.

Mecozzi, V. J., Berman, D. E., Simoes, S., Vetanovetz, C., Awal, M. R., Patel, V. M., Schneider, R. T., Petsko, G. a, Ringe, D., and Small, S. a (2014). Pharmacological chaperones stabilize retromer to limit APP processing. *Nat. Chem. Biol.* 10, 443–449.

Van Meer, G., Voelker, D. R., and Feigenson, G. W. (2008). Membrane lipids: where they are and how they behave. *Nat. Rev. Mol. Cell Biol.* *9*, 112–124.

Mewes, H. W., Frishman, D., Mayer, K. F. X., Münsterkötter, M., Noubibou, O., Pagel, P., Rattei, T., Oesterheld, M., Ruepp, a, and Stümpflen, V. (2006). MIPS: analysis and annotation of proteins from whole genomes in 2005. *Nucleic Acids Res.* *34*, D169–72.

Miller, E. A., Beilharz, T. H., Malkus, P. N., Lee, M. C. S., Hamamoto, S., Orci, L., and Schekman, R. (2003). Multiple Cargo Binding Sites on the COPII Subunit Sec24p Ensure Capture of Diverse Membrane Proteins into Transport Vesicles. *Cell* *114*, 497–509.

Miller, J., Lo, R., Ben-Hur, A., Desmarais, C., Stagljar, I., Noble, W., and Fields, S. (2005). Large-scale identification of yeast integral membrane protein interactions. *Proc.* *102*, 12123–12128.

Miura, E. *et al.* (2014). VPS35 dysfunction impairs lysosomal degradation of α -synuclein and exacerbates neurotoxicity in a *Drosophila* model of Parkinson's disease. *Neurobiol. Dis.* *71*, 1–13.

Muñiz, M., Nuoffer, C., Hauri, H., and Riezman, H. (2000). The Emp24 Complex Recruits a Specific Cargo Molecule into Endoplasmic Reticulum–derived Vesicles. *J. Cell Biol.* *148*, 925–930.

Munro, S. (2001). What can yeast tell us about N-linked glycosylation in the Golgi apparatus? *FEBS Lett.* *498*, 223–227.

Nakatsu, F., and Ohno, H. (2003). Adaptor Protein Complexes as the Key Regulators of Protein Sorting in the Post-Golgi Network Identification of AP complexes Recognition of sorting signals by AP complexes. *Cell Struct. Funct.* *28*, 419–429.

Newman, A. P., Shim, J., and Ferro-novick, S. (1990). BET1, BOSI, and SEC22 Are Members of a Group of Interacting Yeast Genes Required for Transport from the Endoplasmic Reticulum to the Golgi Complex. *Mol. Cell. Biol.* *10*, 3405–3414.

Nickerson, D. P., Russell, M. R. G., Lo, S.-Y., Chapin, H. C., Milnes, J., and Merz, A. J. (2012). Msb3/Gyp3 GAP selectively opposes Rab5 signaling at endolysosomal organelles. *Traffic* *13*, 1411–1428.

Nordmann, M., Cabrera, M., Perz, A., Bröcker, C., Ostrowicz, C., Engelbrecht-Vandré, S., and Ungermann, C. (2010). The Mon1-Ccz1 complex is the GEF of the late endosomal Rab7 homolog Ypt7. *Curr. Biol.* *20*, 1654–1659.

Nothwehr, S. F., Bruinsma, P., and Strawn, L. A. (1999). Distinct domains within Vps35p mediate the retrieval of two different cargo proteins from the yeast prevacuolar/endosomal compartment. *Mol. Biol. Cell* *10*, 875–890.

- Nothwehr, S. F., Ha, S. A., and Bruinsma, P. (2000). Sorting of yeast membrane proteins into an endosome-to-Golgi pathway involves direct interaction of their cytosolic domains with Vps35p. *J. Cell Biol.* *151*, 297–310.
- Novick, P., Ferro, S., and Schekman, R. (1981). Order of Events in the Yeast Secretory Pathway. *Cell* *25*, 461–469.
- Novick, P., Field, C., and Schekman, R. (1980). Identification of 23 Complementation Groups Required for Post-translational Events in the Yeast Secretory Pathway. *Cell* *21*, 205–215.
- Nyfeler, B., Zhang, B., Ginsburg, D., Kaufman, R., and Hauri, H. (2006). Cargo Selectivity of the ERGIC-53/MCFD2 Transport Receptor Complex. *Traffic* *7*, 1473–1481.
- Odorizzi, G., Babst, M., and Emr, S. D. (2000). Phosphoinositide signaling and the regulation of membrane trafficking in yeast. *Trends Biochem. Sci.* *25*, 229–235.
- Ohbayashi, N., Yatsu, A., Tamura, K., and Fukuda, M. (2012). The Rab21-GEF activity of Varp, but not its Rab32/38 effector function, is required for dendrite formation in melanocytes. *Mol. Biol. Cell* *23*, 669–678.
- Orlean, P., and Menon, A. K. (2007). Thematic review series: lipid posttranslational modifications. GPI anchoring of protein in yeast and mammalian cells, or: how we learned to stop worrying and love glycospholipids. *J. Lipid Res.* *48*, 993–1011.
- Ortiz, D., Medkova, M., Walch-solimena, C., and Novick, P. (2002). Ypt32 recruits the Sec4p guanine nucleotide exchange factor, Sec2p, to secretory vesicles; evidence for a Rab cascade in yeast. *J. Cell Biol.* *157*, 1005–1015.
- Ostlund, G., Schmitt, T., Forslund, K., Köstler, T., Messina, D. N., Roopra, S., Frings, O., and Sonnhammer, E. L. L. (2010). InParanoid 7: new algorithms and tools for eukaryotic orthology analysis. *Nucleic Acids Res.* *38*, D196–203.
- Owen, D. J., and Evans, P. R. (1998). A Structural Explanation for the Recognition of Tyrosine-Based Endocytotic Signals. *Science* (80-.). *282*, 1327–1333.
- Page, L. J., Sowerby, P. J., Lui, W. W. Y., and Robinson, M. S. (1999). γ -Synergisin: An EH Domain – containing Protein that Interacts with γ -Adaptin. *J. Cell Biol.* *146*, 993–1004.
- Di Paolo, G., and De Camilli, P. (2006). Phosphoinositides in cell regulation and membrane dynamics. *Nature* *443*, 651–657.
- Paulsel, A. L., Merz, A. J., and Nickerson, D. P. (2013). Vps9 family protein Muk1 is the second Rab5 guanosine nucleotide exchange factor in budding yeast. *J. Biol. Chem.* *288*, 18162–18171.

- Paumi, C. M., Menendez, J., Arnoldo, A., Engels, K., Iyer, K. R., Thaminy, S., Georgiev, O., Barral, Y., Michaelis, S., and Stagljar, I. (2007). Mapping Protein-Protein Interactions for the Yeast ABC Transporter Ycf1p by Integrated Split-Ubiquitin Membrane Yeast Two-Hybrid Analysis. *Mol. Cell* 26, 15–25.
- Peplowska, K., Markgraf, D. F., Ostrowicz, C. W., Bange, G., and Ungermann, C. (2007). The CORVET tethering complex interacts with the yeast Rab5 homolog Vps21 and is involved in endo-lysosomal biogenesis. *Dev. Cell* 12, 739–750.
- Peter, B. J., Kent, H. M., Mills, I. G., Vallis, Y., Butler, P. J. G., Evans, P. R., and McMahon, H. T. (2004). BAR domains as sensors of membrane curvature: the amphiphysin BAR structure. *Science* 303, 495–499.
- Pfeffer, S., and Aivazian, D. (2004). Targeting Rab GTPases to distinct membrane compartments. *Nat. Rev. Mol. Cell Biol.* 5, 886–896.
- Pieper, U. *et al.* (2011). ModBase, a database of annotated comparative protein structure models, and associated resources. *Nucleic Acids Res.* 39, D465–74.
- Pomorski, T., and Menon, A. K. (2006). Lipid flippases and their biological functions. *Cell. Mol. Life Sci.* 63, 2908–2921.
- Powers, J., and Barlowe, C. (2002). Erv14p Directs a Transmembrane Secretory Protein into COPII-coated Transport Vesicles. *Mol. Biol. Cell* 13, 880–891.
- Pu, S., Vlasblom, J., Emili, A., Greenblatt, J., and Wodak, S. J. (2007). Identifying functional modules in the physical interactome of *Saccharomyces cerevisiae*. *Proteomics* 7, 944–960.
- Pu, S., Wong, J., Turner, B., Cho, E., and Wodak, S. (2009). Up-to-date catalogues of yeast protein complexes. *Nucleic Acids Res.* 37, 825–831.
- Pucadyil, T. J., and Schmid, S. L. (2009). Conserved Functions of Membrane Active GTPases in Coated Vesicle Formation. *Science* (80-.). 325, 1217–1221.
- Rana, M., Lachmann, J., and Ungermann, C. (2015). Identification of a Rab GAP cascade that controls recycling of the Rab5 GTPase Vps21 from the vacuole. *Mol. Biol. Cell* 26.
- Rapoport, I., Chen, Y. C., Cupers, P., Shoelson, S. E., and Kirchhausen, T. (1998). Dileucine-based sorting signals bind to the β chain of AP-1 at a site distinct and regulated differently from the tyrosine-based motif-binding site. *EMBO J.* 17, 2148–2155.
- Reguly, T. *et al.* (2006). Comprehensive curation and analysis of global interaction networks in *Saccharomyces cerevisiae*. *J. Biol.* 5, 1–27.

- Renard, H.-F., Demaegd, D., Guerriat, B., and Morsomme, P. (2010). Efficient ER exit and vacuole targeting of yeast Sna2p require two tyrosine-based sorting motifs. *Traffic* *11*, 931–946.
- Rink, J., Ghigo, E., Kalaidzidis, Y., and Zerial, M. (2005). Rab conversion as a mechanism of progression from early to late endosomes. *Cell* *122*, 735–749.
- Roberg, K. J., Crotwell, M., Espenshade, P., Gimeno, R., and Kaiser, C. A. (1999). LST1 Is a SEC24 Homologue Used for Selective Export of the Plasma Membrane ATPase from the Endoplasmic Reticulum. *J. Cell Biol.* *145*, 659–672.
- Rojas, R., van Vlijmen, T., Mardones, G. a, Prabhu, Y., Rojas, A. L., Mohammed, S., Heck, A. J. R., Raposo, G., van der Sluijs, P., and Bonifacino, J. S. (2008). Regulation of retromer recruitment to endosomes by sequential action of Rab5 and Rab7. *J. Cell Biol.* *183*, 513–526.
- Rotin, D., Staub, O., and Haguener-Tsapis, R. (2000). Ubiquitination and Endocytosis of Plasma Membrane Proteins: Role of Nedd4/Rsp5p Family of Ubiquitin-Protein Ligases. *J. Membr. Biol.* *176*, 1–17.
- Sato, K., and Nakano, A. (2002). Emp47p and Its Close Homolog Emp46p Have a Tyrosine-containing Endoplasmic Reticulum Exit Signal and Function in Glycoprotein Secretion in *Saccharomyces cerevisiae*. *Mol. Biol. Cell*, 1–15.
- Sato, K., and Nakano, A. (2003). Oligomerization of a Cargo Receptor Directs Protein Sorting into COPII-coated Transport Vesicles. *Mol. Biol. Cell*, 1–9.
- Sato, K., and Nakano, A. (2007). Mechanisms of COPII vesicle formation and protein sorting. *FEBS Lett.* *581*, 2076–2082.
- Schäfer, I. B., Hesketh, G. G., Bright, N. a, Gray, S. R., Pryor, P. R., Evans, P. R., Luzio, J. P., and Owen, D. J. (2012). The binding of Varp to VAMP7 traps VAMP7 in a closed, fusogenically inactive conformation. *Nat. Struct. Mol. Biol.* *19*, 1300–1309.
- Schmidt, O., and Teis, D. (2012). The ESCRT machinery. *Curr. Biol.* *22*, R116–20.
- Scholz, O., Thiel, a, Hillen, W., and Niederweis, M. (2000). Quantitative analysis of gene expression with an improved green fluorescent protein. *Eur. J. Biochem.* *267*, 1565–1570.
- Schuldiner, M. *et al.* (2005). Exploration of the function and organization of the yeast early secretory pathway through an epistatic miniarray profile. *Cell* *123*, 507–519.
- Schwarz, K. *et al.* (2009). Mutations affecting the secretory COPII coat component SEC23B cause congenital dyserythropoietic anemia type II. *Nat. Genet.* *41*, 936–940.
- Seaman, M. (2007). Identification of a novel conserved sorting motif required for retromer-mediated endosome-to-TGN retrieval. *J. Cell Sci.* *120*, 2378–2389.

- Seaman, M. N. (2012). The retromer complex - endosomal protein recycling and beyond. *J. Cell Sci.* *125*, 4693–4702.
- Seaman, M. N. J. (2004). Cargo-selective endosomal sorting for retrieval to the Golgi requires retromer. *J. Cell Biol.* *165*, 111–122.
- Seaman, M. N. J. (2005). Recycle your receptors with retromer. *Trends Cell Biol.* *15*, 68–75.
- Seaman, M. N. J., Harbour, M. E., Tattersall, D., Read, E., and Bright, N. (2009). Membrane recruitment of the cargo-selective retromer subcomplex is catalysed by the small GTPase Rab7 and inhibited by the Rab-GAP TBC1D5. *J. Cell Sci.* *122*, 2371–2382.
- Seaman, M. N., McCaffery, J. M., and Emr, S. D. (1998). A membrane coat complex essential for endosome-to-Golgi retrograde transport in yeast. *J. Cell Biol.* *142*, 665–681.
- Sheff, M., and Thorn, K. (2004). Optimized cassettes for fluorescent protein tagging in *Saccharomyces cerevisiae*. *Yeast* *21*, 661–670.
- Shi, Y., Stefan, C., Rue, S., Teis, D., and Emr, S. (2011). Two novel WD40 domain-containing proteins, Ere1 and Ere2, function in the retromer-mediated endosomal recycling pathway. *Mol. Biol. Cell* *22*, 4093–4107.
- Shideler, T., Nickerson, D. P., Merz, A. J., and Odorizzi, G. (2015). Ubiquitin binding by the CUE domain promotes endosomal localization of the Rab5 GEF Vps9. *Mol. Biol. Cell* *9*, 1–35.
- Sidhu, R. S., Mathewes, S., and Bollon, A. P. (1991). Selection of secretory protein-encoding genes by fusion with PHO5 in *Saccharomyces cerevisiae*. *Gene* *107*, 111–118.
- Singer-Krüger, B., Stenmark, H., Düsterhöft, a, Philippsen, P., Yoo, J. S., Gallwitz, D., and Zerial, M. (1994). Role of three rab5-like GTPases, Ypt51p, Ypt52p, and Ypt53p, in the endocytic and vacuolar protein sorting pathways of yeast. *J. Cell Biol.* *125*, 283–298.
- Siniosoglou, S., Peak-Chew, S. Y., and Pelham, H. R. (2000). Ric1p and Rgp1p form a complex that catalyses nucleotide exchange on Ypt6p. *EMBO J.* *19*, 4885–4894.
- Sivars, U., Aivazian, D., and Pfeffer, S. R. (2003). Yip3 catalyses the dissociation of endosomal Rab-GDI complexes. *Nature* *425*, 856–859.
- Small, S. a, Kent, K., Pierce, A., Leung, C., Kang, M. S., Okada, H., Honig, L., Vonsattel, J.-P., and Kim, T.-W. (2005). Model-guided microarray implicates the retromer complex in Alzheimer's disease. *Ann. Neurol.* *58*, 909–919.

- Small, S., and Petsko, G. (2015). Retromer in Alzheimer disease, Parkinson disease and other neurological disorders. *Nat. Rev. Neurosci.* *16*, 126–132.
- Snider, J., Kittanakom, S., Damjanovic, D., Curak, J., Wong, V., and Stagljar, I. (2010). Detecting interactions with membrane proteins using a membrane two-hybrid assay in yeast. *Nat. Protoc.* *5*, 1281–1293.
- Stagg, S. M., Gürkan, C., Fowler, D. M., LaPointe, P., Foss, T. R., Potter, C. S., Carragher, B., and Balch, W. E. (2006). Structure of the Sec13/31 COPII coat cage. *Nature* *439*, 234–238.
- Stanley, P. (2011). Golgi glycosylation. *Cold Spring Harb. Perspect. Biol.* *3*, a005199.
- Steinberg, F., Gallon, M., Winfield, M., Thomas, E. C., Bell, A. J., Heesom, K. J., Tavaré, J. M., and Cullen, P. J. (2013). A global analysis of SNX27-retromer assembly and cargo specificity reveals a function in glucose and metal ion transport. *Nat. Cell Biol.* *15*, 461–471.
- Stenmark, H. (2009). Rab GTPases as coordinators of vesicle traffic. *Nat. Rev. Mol. Cell Biol.* *10*, 513–525.
- Stenmark, H., and Olkkonen, V. M. (2001). The Rab GTPase family. *Genome Biol.* *2*, 3007.1–7.
- Stepp, J. D., Pellicena-palle, A., Hamilton, S., Kirchhausen, T., and Lemmon, S. K. (1995). A Late Golgi Sorting Function for *Saccharomyces cerevisiae* Apm1p, but not for Apm2p, a Second Yeast Clathrin AP Medium Chain-related Protein. *Mol. Biol. Cell* *6*, 41–58.
- Strochlic, T. I., Schmiedekamp, B. C., Lee, J., Katzmann, D. J., and Burd, C. (2008). Opposing activities of the Snx3-retromer complex and ESCRT proteins mediate regulated cargo sorting at a common endosome. *Mol. Biol. Cell* *19*, 4694–4706.
- Strochlic, T., Setty, T., Sitaram, A., and Burd, C. (2007). Grd19/Snx3p functions as a cargo-specific adapter for retromer-dependent endocytic recycling. *J. Cell Biol.* *177*, 115–125.
- Stroupe, C., and Brunger, a T. (2000). Crystal structures of a Rab protein in its inactive and active conformations. *J. Mol. Biol.* *304*, 585–598.
- Stroupe, C., Collins, K. M., Fratti, R. a, and Wickner, W. (2006). Purification of active HOPS complex reveals its affinities for phosphoinositides and the SNARE Vam7p. *EMBO J.* *25*, 1579–1589.
- Swarbrick, J. D., Shaw, D. J., Chhabra, S., Ghai, R., Valkov, E., Norwood, S. J., Seaman, M. N. J., and Collins, B. M. (2011). VPS29 is not an active metallo-phosphatase but is a rigid scaffold required for retromer interaction with accessory proteins. *PLoS One* *6*, e20420.
- Sztul, E., and Lupashin, V. (2009). Role of vesicle tethering factors in the ER-Golgi membrane traffic. *FEBS Lett.* *583*, 3770–3783.

- Tabuchi, M., Yanatori, I., Kawai, Y., and Kishi, F. (2010). Retromer-mediated direct sorting is required for proper endosomal recycling of the mammalian iron transporter DMT1. *J. Cell Sci.* *123*, 756–766.
- Tamura, K., Ohbayashi, N., Ishibashi, K., and Fukuda, M. (2011). Structure-function analysis of VPS9-ankyrin-repeat protein (Varp) in the trafficking of tyrosinase-related protein 1 in melanocytes. *J. Biol. Chem.* *286*, 7507–7521.
- Tarassov, K., Messier, V., Landry, C. R., Radinovic, S., Serna Molina, M. M., Shames, I., Malitskaya, Y., Vogel, J., Bussey, H., and Michnick, S. W. (2008). An in vivo map of the yeast protein interactome. *Science* (80-.). *320*, 1465–1470.
- Temkin, P., Lauffer, B., Jäger, S., Cimermancic, P., Krogan, N. J., and Zastrow, M. (2011). SNX27 mediates retromer tubule entry and endosome-to-plasma membrane trafficking of signalling receptors. *Nat. Cell Biol.* *13*, 717–723.
- Trahey, M., and Hay, J. C. (2010). Transport vesicle uncoating: it's later than you think. *F1000 Biol. Rep.* *2*, 1–6.
- Traub, L. M. (2009). Tickets to ride: selecting cargo for clathrin-regulated internalization. *Nat. Rev. Mol. Cell Biol.* *10*, 583–596.
- Turner, B., Razick, S., Turinsky, A. L., Vlasblom, J., Crowdy, E. K., Cho, E., Morrison, K., Donaldson, I. M., and Wodak, S. J. (2010). iRefWeb: interactive analysis of consolidated protein interaction data and their supporting evidence. *Database* *2010*, 1–15.
- Valdivia, R., Baggott, D., Chuang, J., and Schekman, R. (2002). The Yeast Clathrin Adaptor Protein Complex 1 Is Required for the Efficient Retention of a Subset of Late Golgi Membrane Proteins. *Dev. Cell* *2*, 283–294.
- Valdivia, R. H., and Schekman, R. (2003). The yeasts Rho1p and Pkc1p regulate the transport of chitin synthase III (Chs3p) from internal stores to the plasma membrane. *Proc. Natl. Acad. Sci.* *100*, 10287–10292.
- Valdmanis, P. N. *et al.* (2007). Mutations in the KIAA0196 Gene at the SPG8 Locus Cause Hereditary Spastic Paraplegia. *Am. J. Hum. Genet.* *80*, 152–161.
- Vilariño-Güell, C. *et al.* (2011). VPS35 Mutations in Parkinson Disease. *Am. J. Hum. Genet.* *89*, 162–167.
- Wang, C.-W., Hamamoto, S., Orci, L., and Schekman, R. (2006). Exomer: A coat complex for transport of select membrane proteins from the trans-Golgi network to the plasma membrane in yeast. *J. Cell Biol.* *174*, 973–983.

Wang, X. *et al.* (2013). Loss of sorting nexin 27 contributes to excitatory synaptic dysfunction by modulating glutamate receptor recycling in Down's syndrome. *Nat. Med.* *19*, 473–480.

Wassmer, T. *et al.* (2009). The retromer coat complex coordinates endosomal sorting and dynein-mediated transport, with carrier recognition by the trans-Golgi network. *Dev. Cell* *17*, 110–122.

Van Weering, J. R. T., Sessions, R. B., Traer, C. J., Kloer, D. P., Bhatia, V. K., Stamou, D., Carlsson, S. R., Hurley, J. H., and Cullen, P. J. (2012a). Molecular basis for SNX-BAR-mediated assembly of distinct endosomal sorting tubules. *EMBO J.* *31*, 4466–4480.

Van Weering, J. R. T., Verkade, P., and Cullen, P. J. (2012b). SNX-BAR-Mediated Endosome Tubulation is Co-ordinated with Endosome Maturation. *Traffic* *13*, 94–107.

Wigren, E., Bourhis, J., Kursula, I., Guy, J. E., and Lindqvist, Y. (2010). Crystal structure of the LMAN1-CRD/MCFD2 transport receptor complex provides insight into combined deficiency of factor V and factor VIII. *FEBS Lett.* *584*, 878–882.

Witter, D. J., and Poulter, C. D. (1996). Yeast Geranylgeranyltransferase Type-II: Steady State Kinetic Studies of the Recombinant Enzyme. *Biochemistry* *35*, 10454–10463.

Wurmser, A. E., Sato, T. K., Emr, S. D., and Vam, V. (2000). New Component of the Vacuolar Class C-Vps Complex Couples Nucleotide Exchange on the Ypt7 GTPase to SNARE-dependent Docking and Fusion. *J. Cell Biol.* *151*, 551–562.

Xu, C., and Ng, D. T. W. (2015). O-mannosylation: The other glycan player of ER quality control. *Semin. Cell Dev. Biol.*, 1–6.

Xu, Y., Seet, L. F., Hanson, B., and Hong, W. (2001). The Phox homology (PX) domain, a new player in phosphoinositide signalling. *Biochem. J.* *360*, 513–530.

Yu, H. *et al.* (2008). High-Quality Binary Protein Interaction Map of the Yeast Interactome Network. *Science* (80-.). *322*, 104–111.

Yu, J. W., and Lemmon, M. a (2001). All phox homology (PX) domains from *Saccharomyces cerevisiae* specifically recognize phosphatidylinositol 3-phosphate. *J. Biol. Chem.* *276*, 44179–44184.

Zavodszky, E., Seaman, M. N. J., Moreau, K., Jimenez-Sanchez, M., Breusegem, S. Y., Harbour, M. E., and Rubinsztein, D. C. (2014). Mutation in VPS35 associated with Parkinson's disease impairs WASH complex association and inhibits autophagy. *Nat. Commun.* *5*, 3828.

Zhang, B. (2009). Recent developments in the understanding of the combined deficiency of FV and FVIII. *Br. J. Haematol.* *145*, 15–23.

Zhang, J., Reiling, C., Reinecke, J., Prislán, I., Marky, L. A., Sorgen, P. L., Naslavasky, N., and Caplan, S. (2012). Rabankyrin-5 interacts with EHD1 and Vps26 to regulate endocytic trafficking and retromer function. *Traffic* *13*, 745–757.

Zhang, X., He, X., Fu, X.-Y., and Chang, Z. (2006). Varp is a Rab21 guanine nucleotide exchange factor and regulates endosome dynamics. *J. Cell Sci.* *119*, 1053–1062.

Zhang, Z., Zhang, T., Wang, S., Gong, Z., Tang, C., Chen, J., and Ding, J. (2014). Molecular mechanism for Rabex-5 GEF activation by Rabaptin-5. *Elife*, e02687.

Appendices

Appendix A Online supplementary material for chapter 2

Supplementary material for chapter 2 including text, tables 1-13 and figures 1-7 can be found online by following the link below.

<http://www.nature.com/nature/journal/v489/n7417/full/nature11354.html> - [supplementary-information](#)

Appendix B Supplementary material for chapter 3

Table B.1 Yeast strains used in chapter 3

Strain ID	Genotype	Source or Reference
BY4741	<i>MATa his3Δ1; leu2Δ0; met15Δ0; ura3Δ0</i>	O'shea Lab
Vps5-TAP	<i>BY4741 VPS5-TAP::HIS3</i>	Yeast Tap-tagged fusion library (Ghaemmaghami <i>et al.</i> , 2003)
Vps17-TAP	<i>BY4741 VPS17-TAP::HIS3</i>	Yeast Tap-tagged fusion library
Vps26-TAP	<i>BY4741 VPS26-TAP::HIS3</i>	Yeast Tap-tagged fusion library
Vps29-TAP	<i>BY4741 VPS29-TAP::HIS3</i>	Yeast Tap-tagged fusion library
Vps35-TAP	<i>BY4741 VPS35-TAP::HIS3</i>	Yeast Tap-tagged fusion library
BBY203	<i>BY4741 VPS35-GFP::KAN</i>	This Study
BBY204	<i>BY4741 NatNT2::ADHI-3HA-VPS9</i>	This Study
BBY207	<i>BY4741 NatNT2::ADHI-3HA-VPS9 VPS35-GFP::KAN</i>	This Study
BBY208	<i>BY4741 NatNT2::ADHI-3HA-MUK1 VPS35-GFP::KAN</i>	This Study
CUY4412	<i>MATa VPS26-GFP::KANMX4 his3D200 leu2D0 lys2D0 met15D0 ura3D0</i>	Balderhaar <i>et al.</i> 2010
BBY210	<i>CUY4412 muk1Δ::NAT</i>	This Study
BBY211	<i>CUY4412 vps9Δ::HIS3</i>	This Study
BBY212	<i>CUY4412 muk1Δ::NATR vps9Δ::HIS3</i>	This Study
BBY177	<i>BY4741 muk1Δ::KANR</i>	This Study
BBY201	<i>BY4741 vps9Δ::HIS3</i>	This Study
BBY182	<i>BY4741 muk1Δ::KANR vps9Δ::HIS3</i>	This Study
BBY422	<i>BY4741 NatNT2::ADHI-3HA-YML003W</i>	This Study
MDY956	<i>CUY4412 vps21Δ::NAT</i>	This Study

Strain ID	Genotype	Source or Reference
BBY312	<i>CUY4412 vps21Δ::NAT ypt52Δ::HPH</i>	This Study
NMY51	<i>his3Δ200 trp1-901 leu2-3,112 LYS2::(lexAop)4-HIS3 ura3::(lexAop)8-lacZ ade2::(lexAop)8-ADE2 GAL4</i>	Snider <i>et al.</i> 2010
AO445	<i>NMY51 VPS5-Cub-LexA-VP16-KANMX</i>	This Study
AO447	<i>NMY51 VPS35-Cub-LexA-VP16-KANMX</i>	This Study
AO464	<i>NMY51 VPS26-Cub-LexA-VP16-KANMX</i>	This Study
AO468	<i>NMY51 Artificial Bait-Cub-LexA-VP16-KANMX</i>	Snider <i>et al.</i> 2010
BBY327	<i>BY4741 VPS26-tDimer2::URA NatNT2::ADHpr-yeGFP-MUK1</i>	This Study
BBY216	<i>BY4741 NatNT2::ADHpr-yeGFP-VPS9</i>	This Study
BBY322	<i>BY4741 NatNT2::ADHpr-yeGFP-VPS9 vps35Δ::HPH</i>	This Study
BBY217	<i>BY4741 NatNT2::ADHpr-yeGFP-MUK1</i>	This Study
BBY324	<i>BY4741 NatNT2::ADHpr-yeGFP-MUK1 vps35Δ::HPH</i>	This Study
BBY413	<i>BY4741 VPS34-GFP+::NAT</i>	This Study
BBY414	<i>BY4741 muk1Δ::KANR VPS34-GFP+::NAT</i>	This Study
BBY420	<i>BY4741 vps9Δ::HIS3 VPS34-GFP+::NAT</i>	This Study
BBY421	<i>BY4741 muk1Δ::KANR vps9Δ::HIS3 VPS34-GFP+::NAT</i>	This Study
BBY416	<i>BY4741 vps21Δ::NATR ypt52Δ::HPH VPS34-GFP+::HIS3</i>	This Study

Table B.2 Plasmids used in chapter 3

LC#	Plasmid ID	Description	Source or Reference
-	pMuk1-HA	<i>pGAL1pr-MUK1-HA::URA3</i>	MORF collection (Gelperin <i>et al.</i> , 2005)
1069	pCS11	<i>pSNF7-RFP::LEU2(CEN)</i>	Conibear Lab
1407	pRS415	<i>pLEU2(CEN)</i>	ATCC#87520
698	pRS416	<i>pURA3(CEN)</i>	ATCC#87521
596	pTS48	<i>pVPS9::URA3(2μ)</i>	Stevens Lab
2070	pMUK1(2μ)	<i>pMUK1::LEU2(2μ)</i>	MoBY ORF collection (Ho <i>et al.</i> 2006)

LC#	Plasmid ID	Description	Source or Reference
2324	pMD120	<i>pMUK1pr-3HA-MUK1::URA3(CEN)</i>	This Study (Conibear Lab)
2468	pBB12	<i>pMUK1pr-3HA-MUK1(D353A)::URA3(CEN)</i>	This Study (Conibear Lab)
2627	pBB33	<i>pADH1pr-3HA-MUK1::URA3(CEN)</i>	This Study (Conibear Lab)
2628	pBB34	<i>pADH1pr-3HA-MUK1(D353A)::URA3(CEN)</i>	This Study (Conibear Lab)
2325	pMD121	<i>pMUK1pr-GFP-MUK1::URA3(CEN)</i>	This Study (Conibear Lab)
2458	pMT1	<i>pADH1pr-GFP-MUK1::URA3(CEN)</i>	This Study (Conibear Lab)
2470	pBB14	<i>pADH1pr-GFP-MUK1(D353A)::URA3(CEN)</i>	This Study (Conibear Lab)
2467	pMT2	<i>pADH1pr-GFP-MUK1(503-612)::URA3(CEN)</i>	This Study (Conibear Lab)
2501	pBB15	<i>pADH1pr-GFP-MUK1(1-575)::URA(CEN)</i>	This Study (Conibear Lab)
2556	pBB23	<i>pADH1pr-VRL1::URA3(CEN)</i>	This Study (Conibear Lab)
2616	pBB28	<i>pVRL1pr-3HA-VRL1::URA3(CEN)</i>	This Study (Conibear Lab)
2620	pBB32	<i>pVRL1pr-3HA-VRL1(D373A)::URA3(CEN)</i>	This Study (Conibear Lab)
2555	pBB22	<i>pADH1pr-GFP-VRL1::URA3(CEN)</i>	This Study (Conibear Lab)
2175	pAO538	<i>pCYC1pr-NubG-HA-MUK1(1-417t)::TRP1(2μ)</i>	This Study (Stagljar Lab)
2178	pAO542	<i>pCYC1pr-NubG-HA-MUK1(74-417t)::TRP1(2μ)</i>	This Study (Stagljar Lab)
2180	pAO531	<i>pCYC1pr-NubG-HA-MUK1(D353A)::TRP1(2μ)</i>	This Study (Stagljar Lab)
2181	pAO470	<i>pCYC1pr-NubG-HA-MUK1::TRP1(2μ)</i>	This Study (Stagljar Lab)
2266	pBB9	<i>pCYC1pr-NubG-HA-VPS9::TRP1(2μ)</i>	This Study (Conibear Lab)
2559	pBB24	<i>pCYC1pr-NubG-HA-VRL1::TRP1(2μ)</i>	This Study (Conibear Lab)
2080	pPR3N-NubG-Rho1	<i>pCYC1pr-NubG-HA-RHO1::TRP1(2μ)</i>	Stagljar Lab
2081	pPR3N-NubI-Rho1	<i>pCYC1pr-NubI-RHO1::TRP1(2μ)</i>	Stagljar Lab
2527	pBB21	<i>pGFP-FYVE(EEA1)::LEU2(2μ)</i>	This Study (Conibear Lab)
599	pSRG92	<i>p-myc-VPS21::URA3(2μ)</i>	Stevens Lab
600	pSRG93	<i>p-myc-VPS21(Q66L)::URA3(2μ)</i>	Stevens Lab

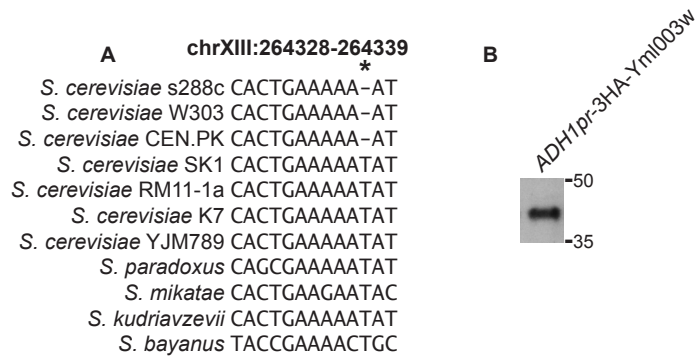
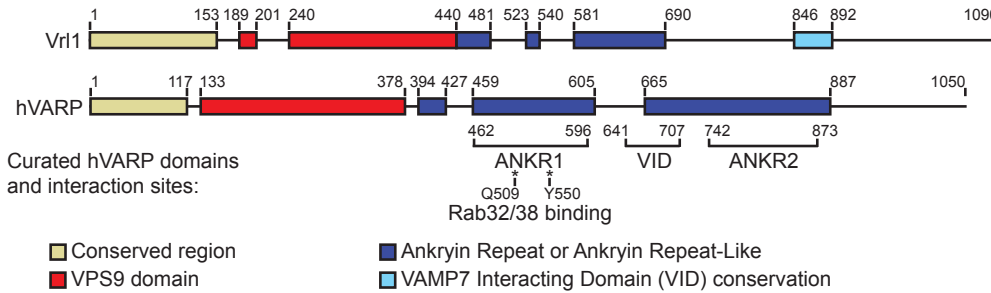


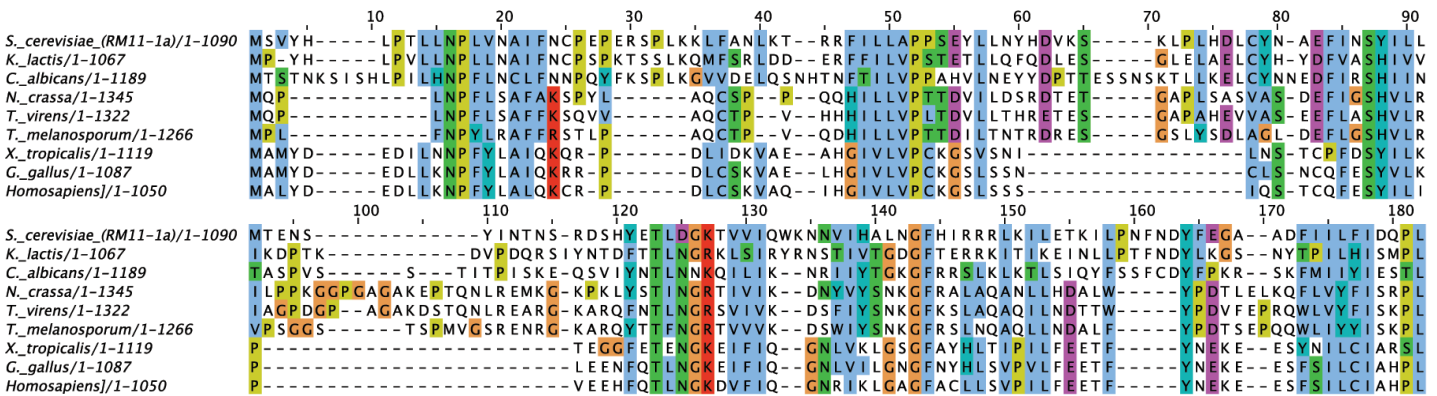
Figure B.1 There is a deletion present in lab *Saccharomyces cerevisiae* strains in the gene *YML003W* that is absent from other *S. cerevisiae* and truncates the normal gene product.

(A) An alignment of *YML003W* in laboratory/wild *S. cerevisiae* strains and other related fungi. **(B)** Cells expressing *ADH1pr-3HA-Yml003w* were lysed, resolved by 10% SDS-PAGE and immunoblotted with anti-HA. Expected size of the protein expressed from the truncated ORF was roughly 40 kDa. HA, hemagglutinin.

A



B. N-terminal Conservation



C. VAMP7 Interacting Domain

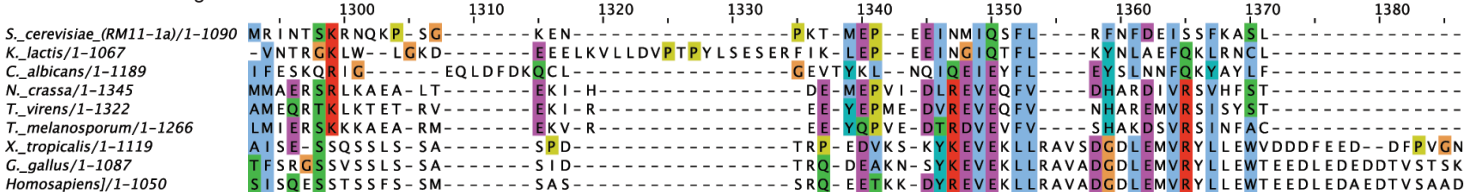


Figure B.2 Conservation of the hVARP N-terminal domain and the VAMP7-interacting domain.

(A) Schematic of Vrl1 and hVARP with curated domains (Tamura *et al.*, 2011) including Ankyrin repeat domains (ANKR), the VAMP7 interacting domain (VID) and key Rab32/38-interacting residues. (B) An alignment of the N-terminus of hVARP/Vrl1 shows broad conservation. (C) Partial conservation of the VAMP7-interacting domain.

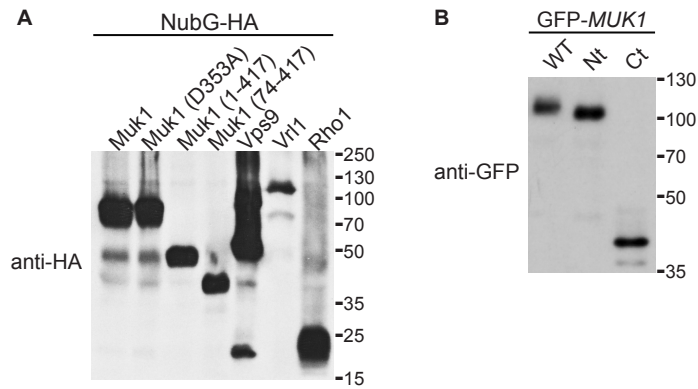


Figure B.3 All NubG iMYTH and GFP-*MUK1* vectors were expressed.

(A) iMYTH strains expressing different Nub-HA-tagged GEFs were lysed and immunoblotted with anti-HA to determine relative expression levels. **(B)** By immunoblotting with anti-HA, strains with *ADH1pr*-GFP-Muk1 vectors were found to express GFP-Muk1 at similar levels. HA, hemagglutinin.